ADVANCED HEALTHCARE MATERIALS
www.advhealthmat.de

Organ-On-A-Chip Platforms: A Convergence of Advanced Materials, Cells, and Microscale Technologies

*Samad Ahadian, Robert Civitarese, Dawn Bannerman, Mohammad Hossein Mohammadi, Rick Lu, Erika Wang, Locke Davenport-Huyer, Ben Lai, Boyang Zhang, Yimu Zhao, Serena Mandla, Anastasia Korolj, and Milica Radisic**

Significant advances in biomaterials, stem cell biology, and microscale technologies have enabled the fabrication of biologically relevant tissues and organs. Such tissues and organs, referred to as organ-on-a-chip (OOC) platforms, have emerged as a powerful tool in tissue analysis and disease modeling for biological and pharmacological applications. A variety of biomaterials are used in tissue fabrication providing multiple biological, structural, and mechanical cues in the regulation of cell behavior and tissue morphogenesis. Cells derived from humans enable the fabrication of personalized OOC platforms. Microscale technologies are specifically helpful in providing physiological microenvironments for tissues and organs. In this review, biomaterials, cells, and microscale technologies are described as essential components to construct OOC platforms. The latest developments in OOC platforms (e.g., liver, skeletal muscle, cardiac, cancer, lung, skin, bone, and brain) are then discussed as functional tools in simulating human physiology and metabolism. Future perspectives and major challenges in the development of OOC platforms toward accelerating clinical studies of drug discovery are finally highlighted.

1. Introduction

Extensive preclinical examination and validation of potential therapeutic compounds are required prior to their clinical evaluation and approval. This process is time-consuming (approximately ten years), extremely costly (approximately two billion dollars), and has low efficiency (<20%).[1] Some drug candidates have shown preclinical success, while they were ineffective and sometimes deadly in the clinic. For example, encainide and flecainide as class I antiarrhythmic agents showed a great promise at suppressing irregular cardiac pacing in preclinical trials in 1980,[2] whereas a subsequent cardiac arrhythmia suppression trial in 1991 proved that the risk of a fatal cardiac event was 2.5 times higher for patients taking encainide and flecainide.[3] Research and development costs in drug development still continue to increase with the total cost up to $2.5 billion for every drug approval.[4] However, despite this increasing investment in drug development and discovery, the number of drugs approved by the Food and Drug Administration (FDA) has decreased over the last couple of decades.[5]

One of the main reasons for high cost and low efficiency of conventional drug development process is the lack of physiologically relevant preclinical models capable of predicting human responses to new drugs.[6] Animal models have been provided a living system with possible assessment of drug efficacy on target site and nontarget organ toxicity. However, the use of animal models is associated with high cost, ethical concerns, and low throughput.[7] Clear imaging of the animal body is limited, hindering visual transportation of therapeutic agents in tissues and organs. Moreover, results from animal models are often inconsistent with human trials mainly because of physiological or pathophysiological differences between animals and humans.[8] Therefore, more accurate and reliable human tissue models are needed for preclinical drug screening to improve the efficiency and success rate of clinical trials.

Tissue engineering (TE) aims to recreate functional tissues and organs outside the body. Engineered tissues have been developed to restore and replace diseased or damaged native tissues. In fact, TE has aimed to solve the organ shortage problem, which has kept many people waiting for donor organs. Before the mid-1980s, the word TE was used in the literature to indicate the surgical manipulation of tissues and organs or in more general cases when biomaterials or prosthetic devices were used.[9] The current definition of TE was introduced in 1987 as "the application of the principles and methods of engineering and life sciences toward the fundamental understanding of structure–function relationships in normal and pathologic mammalian tissue and the development of biological substitutes to

Dr. S. Ahadian, R. Civitarese, D. Bannerman, M. H. Mohammadi, R. Lu, E. Wang, L. Davenport-Huyer, B. Lai, Dr. B. Zhang, A. Korolj, Prof. M. Radisic
Institute of Biomaterials and Biomedical Engineering
University of Toronto
Toronto, M5S 3G9 Ontario, Canada
E-mail: m.radisic@utoronto.ca
D. Bannerman, M. H. Mohammadi, L. Davenport-Huyer, Dr. B. Zhang, Y. Zhao, S. Mandla, A. Korolj, Prof. M. Radisic
Department of Chemical Engineering and Applied Chemistry
University of Toronto
Toronto, M5S 3G9 Ontario, Canada

DOI: 10.1002/adhm.201700506

restore, maintain, or improve function."[10] Following a major contribution of Langer and Vacanti to the TE field,[11] many researchers in the world pursued the TE toward production of functional tissues as a therapeutic solution.

In general, a tissue can be constructed by culturing suitable cells on a scaffold that provides structural support and integrity for the tissue. Scaffolds aim to recapitulate the composition, structure, and function of the extracellular matrix (ECM) that the cells are normally surrounded by in vivo. Growth factors and other supplements are also required to regulate cell behavior and function. Using microscale technologies, tissue engineers are able to make complex tissues.[12,13] Among the first engineered tissues and organs were skin, cartilage, bone, blood vessel, and bladder,[14] and later cardiac[15] and muscle tissues.[16] Engineered tissue products can either be prepared fully functional in vitro and then be implanted (e.g., cardiac patches[17]) or use the host tissue for further maturation and function (e.g., chondrocytes encapsulated in biomaterials[18]). Recent studies have focused on using artificial tissues and organs as the human-cell based models in drug screening and discovery.[19] However, the early stages of drug development are still based on in vitro cellular models as discussed below.

In this review, we briefly explain cellular and tissue models used in drug discovery and prediction. We then describe biomaterials, cells, physiochemical parameters, and microscale technologies as essential components to construct organ-on-a-chip (OOC) platforms. We also discuss sensory systems to monitor real-time physiological changes in cells and tissues. Following that, this review describes currently developed tissues and OOC platforms (e.g., liver, skeletal muscle, cardiac, cancer, lung, skin, bone, and brain) as functional tools in simulating the human physiology and metabolism. Finally, we highlight future perspectives and major challenges in the development of OOC platforms toward accelerating clinical studies of drug discovery.

Samad Ahadian is a research fellow at the University of Toronto, Canada. He received his Ph.D. in materials science from the Tohoku University, Japan in 2011. He then worked as postdoctoral research associate under the supervision of Prof. Ali Khademhosseini (MIT and Harvard Medical School) at the Tohoku University from 2011 to 2014. In 2014, he was promoted to Assistant Professor at the Tohoku University and worked there until July 2015. He then moved to Canada and worked as a research fellow in the laboratory of Prof. Milica Radisic. He is currently a Biomaterials Scientist at Covalon Technologies Ltd., Canada. His research interests include muscle tissue engineering, nanobiomaterials, hydrogels, cardiac tissue regeneration, and antimicrobial biomedical devices and materials.

Milica Radisic is a professor at the University of Toronto and Canada Research Chair in Functional Cardiovascular Tissue Engineering. She obtained Ph.D. from the MIT in 2004. She is a Fellow of the Canadian Academy of Engineering and a Fellow of the American Institute for Medical and Biological Engineering. Dr. Radisic received is a member of the Royal Society of Canada. Her research interests include biomaterials and development of tissue models for drug testing. She is a co-founder of a start-up company TARA Biosystems focused on the use of engineered tissues in drug development.

1.1. In Vitro Cellular Models

In vitro 2D cellular models are extensively used in preclinical evaluation of drug candidates.[20] They are helpful tools in drug screening to provide a controlled and simplified milieu to observe and examine cellular activity in response to a potential drug candidate. For example, Foster et al. used the A549 cell line as a 2D pulmonary epithelial model to study drug metabolism.[21] However, 2D models are often not suitable for drug screening. For example, Anthérieu et al. used HepaRG cell model (first human hepatocyte-like cells) for the study of toxicity and drug metabolism; however, human hepatocyte cell lines have negligible amounts of metabolites compared to human primary hepatocytes and thus they are not suitable for drug metabolism studies.[22] The major limitation of 2D cellular models is that they are often comprised of a single cell type with some complimentary cells and as a result these models do not replicate the complex structure and function of cells in tissues in the human body.[23] They often suffer from cell immaturity, limited lifespan, and functional development, which make it difficult to extrapolate the cell response to the native tissue function.[24] In addition, the simplicity of in vitro cellular models is particularly a major drawback in studying metabolite activity of drugs on nontarget tissues, complex drug metabolism, and inflammatory responses. Therefore, more sophisticated human tissue models are beginning to emerge to provide more physiologically relevant models in drug analysis and discovery.

1.2. Need for Human Tissue Models

In general, development of physiologically relevant and functional tissue models using human cell sources has recently emerged as a hot research topic in regenerative medicine. Making human tissues on a chip facilitates measurement of tissue activity and function in a reliable, reproducible, real-time, and preferably high-throughput manner for pharmaceutical applications.[25] Human tissue models can be scaled based on organ size in the body. Therefore, drug toxicity or

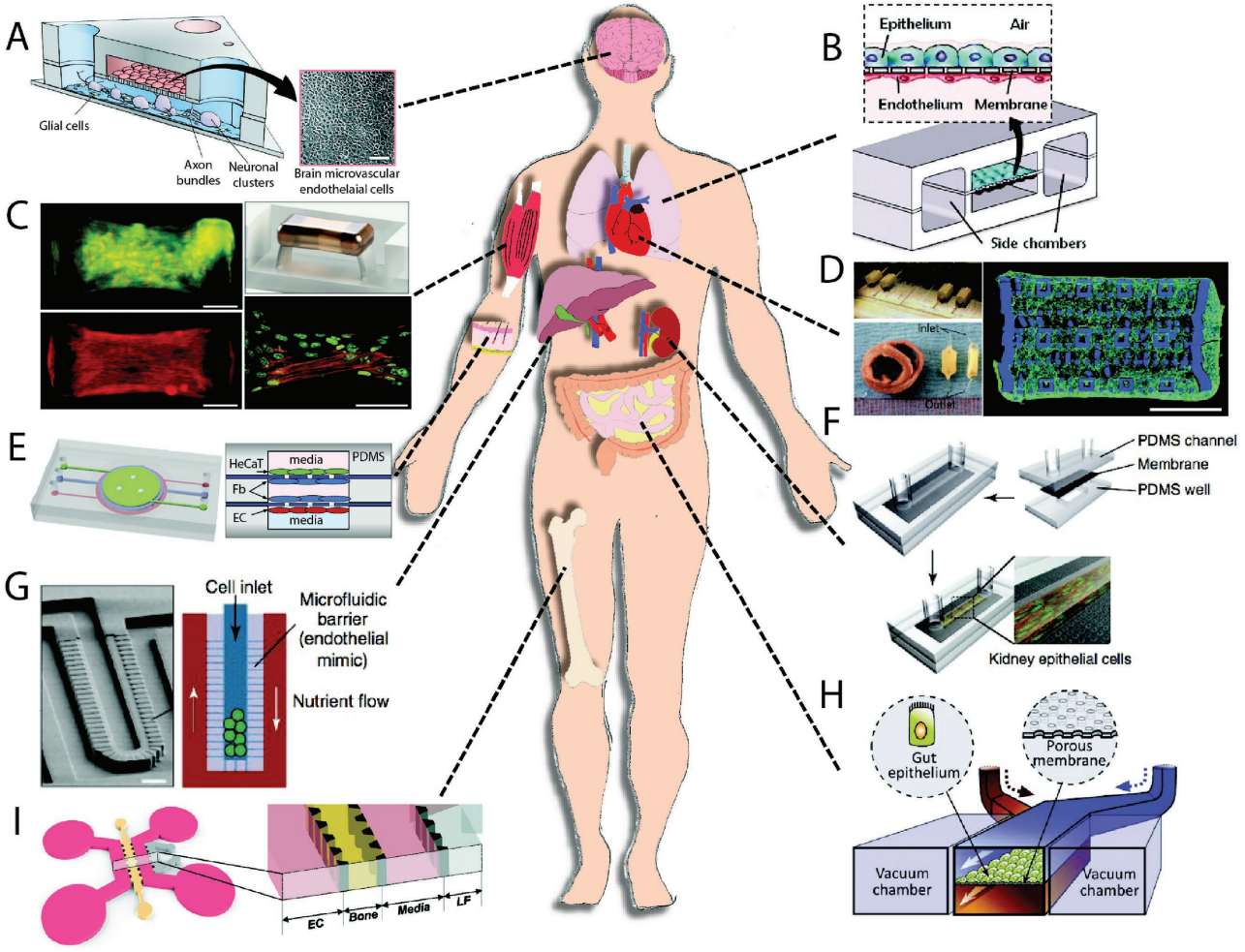

Figure 1. Different OOC models with their corresponding organs in the body. A) Cross-section of a brain-on-a-chip platform demonstrating a layer of human neuronal and glial cells, which interact through a membrane containing perforations and a monolayer of human BMECs (scale bar, 250 µm).[31] Reproduced with permission.[31] Copyright 2016, Royal Society of Chemistry. B) A microengineered lung-on-a-chip that mimics lung microarchitecture and induced cyclic mechanical distortion of the alveolar–capillary interface.[32] Reproduced with permission.[33] Copyright 2012, American Association for the Advancement of Science. C) A skeletal muscle microtissue and representative immunofluoresence imaging demonstrating skeletal muscle alignment (F-actin in red) (scale bars, 100 µm).[34] Reproduced with permission.[34] Copyright 2012, Royal Society of Chemistry. D) Thick AngioChip cardiac tissues placed face up and side up beside a slice of an adult rat heart and immunostaining of F-actin (green) of the cross-section of the thick multilayer human AngioChip cardiac tissue (scale bar, 1 mm).[35] Reproduced with permission.[35] Copyright 2016, Nature Publishing Group. E) Skin-on-a-chip device filled with fluid of three different colors comprising of three PDMS layers and two polyethylene terephthalate porous membranes, which allow for stacking of multiple cell types present in the skin.[36] Reproduced with permission.[36] Copyright 2016, Nature Publishing Group. F) A microfluidic kidney-on-a-chip model that incorporates stacked PDMS layers with microchannels and a PDMS well separated by a porous polyester material, which allows physiologically relevant 3D kidney microarchitecture.[37] Reproduced with permission.[37] Copyright 2009, Royal Society of Chemistry. G) A liver-on-a-chip mimicking hepatic microarchitecture containing a permeable endothelial barrier between hepatocytes and the liver sinusoid (scale bar, 50 µm).[38] Reproduced with permission.[39] Copyright 2007, John Wiley & Sons. H) A gut-on-a-chip device containing a flexible porous ECM-coated membrane lined by gut epithelial cells in the middle and vacuum chambers on both sides to mimic intestinal peristalsis.[40] Reproduced with permission.[40] Copyright 2012, Royal Society of Chemistry. I) A bone-on-a-chip microfluidic model consisting of four parallel channels separated by 100 µm gaps via microposts allowing for paracrine communication between ECs and stromal cells (connective tissue) during vessel formation.[41] Reproduced with permission.[41] Copyright 2015, Royal Society of Chemistry.

effectiveness using human tissue models can be extrapolated to the whole human body using metabolite concentrations in the model and knowing physiological ratios of blood surrogate to the cells.[25] Moreover, human tissue models are more cost-effective compared to animal models and combinations of different drug candidates can be tested in the tissue models in parallel.[26] Therefore, the total cost of drug screening is substantially decreased using tissue models and has less ethical concerns compared to drug testing using animals. Additionally, an important advantage of human tissue models is that they can operate under either nonphysiological or physiological conditions. Drug screening process should be done under physiological conditions; however, drug monitoring under nonphysiologic conditions is also advantageous.

Results from OOC platforms (**Figure 1**) can be also combined with pharmacokinetic mathematical models.[27] These

mathematical models are based on our knowledge of metabolic pathways and can be used to enhance our understanding of human metabolism.[28] Human tissue models can also be constructed with patient biopsy samples, providing a novel path to individualized medicine.[29] In addition, gene-editing technologies enable us to precisely introduce disease-causing mutations to the cells.[30] As a result, therapeutic strategies can be personalized with lower risks and higher impact for patients compared to traditional and widely used therapeutic solutions.

2. Materials in Organ-On-A-Chip Platforms

In this section, we categorized these materials into two general sections: materials used in chips and biomaterials used in tissue fabrication. Polydimethylsiloxane (PDMS) has been widely used as the chip material. Biomaterials in OOC platforms are often biodegradable and have porous structures derived from synthetic materials (e.g., polyglycolide and polylactide), natural materials (e.g., fibrin and collagen), or hybrid natural–synthetic materials.[42] They have selective interactions with cells and other biological moieties in vivo.[43] There are still opportunities and challenges in the fabrication and characterization of biomaterials, particularly for those used in OOC platforms. In this section, we review properties of materials used in chips and biological tissues. Future perspectives in material design and fabrication are also discussed.

2.1. Chip Materials and Their Fabrication

OOC devices rely on a material support for tissue attachment and organization. Furthermore, they serve as structure of device channels and features, providing the basis for device construction. Unique properties of each material dictate its application in a specific device. Many OOC devices that have reached the commercial space rely on a process of replica molding, where a microfabricated design is developed using soft lithography and replicas are generated using PDMS.[44]

PDMS is a synthetic polymeric elastomer based on silicone, with silicone–oxygen linkages. Widely available through commercial sources, it is sold as an un-crosslinked gel with a corresponding crosslinking solution. Combination of these fluids activates the material, allowing it to be poured onto a master mold as a liquid to conform to intricate features, and then undergoes crosslinking to generate a solid chip device. Following production of a master mold, the solution is poured over the features and cured at high temperatures (or room temperature for prolonged period), and peeled away from the design.[45] The obtained mold can then be capped with a glass slide or a second PDMS block through plasma oxidation methods or through pressure application to form noncovalent bonds.[46] PDMS prototypes in this phase can both serve as on chip devices, or support further fabrication by serving as a mold for a secondary material type.[35,47] Microchannel cross-sections of straight lines and rectangles, are easy to fabricate but they have little resemblance to complicated branching structures in the body that involve tortuous microchannels with a round cross-section.[48] The elasticity of PDMS is tunable, allowing for optimization of the material properties as per the specific tissue application within the device.

PDMS has quickly become the most prevalent substrate for biological microfabricated devices as a result of its low cost, low cytotoxicity, and ease of processing.[49] PDMS is transparent, allowing for on-chip imaging, and multiple layer deposition.[50] With these characteristics, laboratories are able to produce on-chip devices at a relatively low cost in comparison to previous methods that relied on thermoplastics, such as poly(methyl methacrylate) and polycarbonate.[51] The latter approach facilitates more rapid prototyping of designs and reduces the fabrication cost.[52] Despite the many favorable properties of PDMS, it has significant limitations, specifically regarding the integration of biological components of OOC platforms. First of all, and of significant importance, is the hydrophobic nature of the material, limiting cell attachment without surface modification.[53] Surface treatment is often conducted using methods such as oxygen plasma treatment, but these are not completely effective and often yield devices with hydrophobic surfaces limiting attachment.[51] Further issues occur when considering the material permeability, as PDMS devices have a high ability to adsorb small hydrophobic molecules.[54] The latter issue can have a significant effect on solution concentration of bioactive molecules. The concentration can further be changed through water evaporation attributed to high gas permeability of PDMS devices.[50] PDMS also does not degrade, which limits its applicability in certain contexts. For these reasons, other biomaterials are often incorporated into OOC platforms to enable cell culture.

2.2. Biomaterials in Tissue Engineering

In the context of TE, biomaterials serve as an artificial ECM for cells and should function similarly to the native ECM. The biomaterial scaffold should reproduce as closely as possible the in vivo microenvironment that exists in the specific native tissue and should encourage the assembly of cells into a multicellular structure, eventually forming a functional tissue.[55]

The ideal biomaterial for TE technology must possess several main characteristics. The material must remain intact long enough to allow cells to organize, communicate with one another, and recruit new cells. However, it must not stay long enough to disrupt the coupling of cells that is required for the formation of functional tissue. At some point, the ideal scaffold material will be replaced with the ECM proteins secreted by cells. Second, the biomaterial must possess the adequate mechanical strength to support the cells. Third, the material must have an appropriate porosity. The pore size and scaffold interconnectivity are important factors that affect cell trafficking and impact the material integrity. In addition to the aforementioned properties, biomaterials also need to be biocompatible and noncytotoxic to the cells.[56]

In the following section, biomaterials for TE in OOC systems will be discussed (**Table 1**). Biomaterials for this application can fit into two main categories: natural biomaterials and synthetic biomaterials. For each section, main examples will be introduced and examples of current OOC technology that utilizes these materials will be presented.

Table 1. Different biomaterials used in OOC platforms.

Natural biomaterials	Strengths	Weaknesses	OOC models
Collagen	• Biocompatible • Low antigenicity/immunogenicity • Degraded enzymatically • Contains cell adhesive domains • Can be formed into specific geometries[57,58] • Major component of native ECM • Cells able to remodel and contract gel matrix[59,60] • Culture media, proteins, and growth factors can be transported across collagen gel[60–62] • Orientation of collagen fibers can be achieved[63] • Cells can penetrate, remodel, and contract gel matrix[59,60,62]	• Chemical crosslinking used for increased stability[64] • Without mechanical support, collagen-based cell models remain intact for short time[59,65]	• Cardiac[59,66] • Hepatic[62,67,68] • Vascular[62,69] • Skeletal muscle[61] • Kidney[70] • Neuronal networks[63,71] • Tumor spheroids[72,73] • Microvessels[60,74] • Cancer cell migration[58]
Fibrin	• Biocompatible • Noninflammatory • Biodegradable • Gel formation at room temperature through enzymatic polymerization of fibrinogen by thrombin • Bioadhesive properties • Delivery of proteins and growth factors[75]	• Weak mechanical properties[76]	• Skeletal muscle[77] • Vascularized human tissue[78] • Fibrin clot formation in lung model[33]
HA	• Biocompatible • Natural ECM component • Structural component of tissue and joints • Degradable with hyaluronidase • Tunable elastic modulus capability[79]	• Weak mechanical properties[32]	• Cancer metastasis[79] • Barrier tissue[80]
Chitosan	• Biocompatible • Biodegradable • Similar in structure to glycosaminoglycans • Flexible and porous[81] • Minimal foreign-body response[82]	• Mechanical weakness[83] • Instability[83]	• Vascular[84]
Alginate	• Biocompatible • Degradable • Immediate gelation upon exposure to divalent cations • Use as sacrificial material and gel dissolves culture medium[85,86]	• Uncontrollable degradation • Limited protein adsorption[87] • Lack of cell binding[87,88]	• Cardiac[85] • Tumor spheroids[73,89] • Hepatocyte spheroids[90] • Liver, tumor, marrow[88]
Gelatin	• Biocompatible • Biodegradable • Similar in composition to collagen • Contains cell adhesion sites • Less antigenic than collagen • Tunable and physiologically relevant elastic modulus[91]	• Chemical crosslinking for stability[92,93]	• Cardiac,[91] vascular[94] • Muscle[95]
Synthetic biomaterials	• Tunable mechanical properties • Tunable degradation properties • Less batch-to-batch variability than natural biomaterials • Chemical modification to incorporate bioactive molecules[96] • Polyesters degraded through hydrolysis • Moldable	• Lack of cell adhesion ligands prior to modification • Degradation products could have cytotoxic effects • Immune response must be evaluated	• Cardiac[97,98] • Hepatic[98]

2.2.1. Natural Biomaterials

Natural biomaterials include any material used for this application that is taken from a natural source. These biomaterials include the ECM components, such as collagen, elastin, proteoglycans, and hyaluronic acid (HA). The degradation of natural biomaterials often results in products that are nontoxic because they are found in the native ECM.

There are, however, several downsides to using natural biomaterials. First of all, because they come from natural sources, there is often significant batch-to-batch variation. They must be sterilized and purified as well, which can introduce challenges. Furthermore, it is possible for protein denaturation to occur through the steps of processing. Compared to synthetic materials, less control over chemical and physical properties and degradation rates exists.[99]

ECM derived natural biomaterials include collagen, fibrin, and HA. Other natural sources are plant, animal, or insect-derived, and examples of biomaterials from these sources include chitosan, gelatin, and alginate. In the following section, we will discuss each of these natural biomaterials and describe some examples of their use in OOC platforms.

Protein-Based Biomaterials—Collagen: Collagen is a widely used biomaterial in TE. Collagen types I–IV comprise a large component of the natural ECM and it is the main protein responsible for structure of most connective tissues.[100] Despite there being many different types of collagen, collagen consistently exists in a triple helix structure of peptide chains. Notably, collagen is biocompatible, has low antigenicity/immunogenicity, and can be enzymatically degraded. To enhance mechanical properties and stability of collagen, chemical crosslinking using a variety of chemicals, such as glutaraldehyde has been used.[101]

A favorable property of collagen is that it possesses cell-adhesive domains. This property makes collagen particularly useful for incorporation in OOC platforms to provide essential adhesion sites for cells. Countless OOC platforms rely on the incorporation of collagen gels within microchannels or microchambers to support cell growth. Examples include OOC models for heart tissue,[59,66] liver tissue,[67] vascular tissue,[69] skeletal muscle tissue,[61] kidney tissue,[70] neuronal networks,[63] and tumor spheroids,[72,73] among others. Furthermore, collagen has been used as a structural component of microfluidic and microfabricated devices for OOC systems. These include: the formation of biomimetic microvessels embedded within collagen hydrogels for the study of microenvironmental regulation of angiogenesis,[60] the use of microcontact printed collagen to create regions of cell adhesion in a microfabricated hepatocyte spheroid culture system,[68] and 3D collagen gels used to guide neural network formation by controlling the cultivable gel region through photothermal etching method (**Figure 2**A).[71] Specific geometries of collagen have also been demonstrated for use in OOC platforms, such as ultrathin collagen layers for assembly on top of cells in a microfluidic device[57] and collagen droplets used for fabricating 3D microtissues to study cell migration.[58]

Gelatin is a single-stranded protein and is extracted from collagen through partial hydrolysis. It closely resembles collagen in composition[105] but its advantages over collagen are its lower cost and the fact that it is less antigenic. It is highly biocompatible and biodegradable, and it can form gels easily. Gelatin has been used in TE for liver tissue[106] and cardiac tissue applications.[91]

Gelatin is used in numerous 3D tissue models as a hydrogel for cell seeding[107] and in the form of microbeads to act as microscaffolds for cell seeding.[108] It is also commonly combined with other natural biomaterials to support cell culture.[109] In work by McCain et al., gelatin hydrogels were used as muscular thin film (MTF) substrates for engineered cardiac tissues (Figure 2B).[91]

Another form of gelatin that has benefits in OOC technology is gelatin methacryloyl (GelMA),[110] which is produced through chemical modification of gelatin with methacrylic anhydride. GelMA hydrogels are advantageous because they can be polymerized with UV light and their mechanical properties can be tuned through changes in degree of methacrylation. GelMA has been used for cell culture or encapsulation in cardiac tissue models,[111] vascular tissue models,[94] and muscle tissue.[95]

Protein-Based Biomaterials—Fibrin: Fibrin is a fibrous protein, composed of fibrinogen monomers, resulting from the enzymatic polymerization of fibrinogen by thrombin,[112] the process involved in the clotting of blood. Its biomaterial utility includes formation of a gel at room temperature that is non-toxic and noninflammatory. It has been used as a scaffold for cell encapsulation,[113] as a delivery matrix for soluble factors such as proteins or growth factors,[114] as a bioadhesive glue,[115] and in the fabrication of various tissues.[114,116] In terms of OOC platforms, fibrin has been used as a component of artificial ECM. For example, alginate/gelatin/fibrin were used to achieve adipose derived stem cells (SCs) and hepatocyte attachment and growth in a 3D channel for analysis of fluid and cell behaviors.[109] An alternative use of fibrin in OOC models is to study the formation of fibrin clots. Huh et al. introduced fibrinogen and prothrombin into a fluid channel of a pulmonary edema lung-on-chip model to demonstrate the formation of fibrin clots that mimic natural fibrin clots.[117]

Protein-Based Biomaterials—Hyaluronic Acid: HA or hyaluronan is a glycosaminoglycan and hydrogel that makes up the ECM and is found in connective tissues as well as epithelial and neural tissues. It is also a structural component in tissues and joints where it improves biomechanical stability of the synovial fluid and vitreous humor.[118] Furthermore, it plays a significant role in cell proliferation and migration, inflammation, and wound healing.[119] HA can be degraded by hyaluronidase, which is produced by cells. High molecular weight of HA (>800 kDa) inhibits proinflammatory responses in the body.[120] HA can be chemically modified to enhance its hydrophobicity[121] and can be processed into fibers, microspheres, and membranes.[122] This biomaterial generally possesses weak mechanical properties,[123] however it can be crosslinked with other polymers, including poly(ethylene glycol) (PEG)[121] and polylactic acid (PLA)[124] to make these properties more favorable. The use of HA in OOC models is limited, but several examples include a system that used HA in thiolated form, along with thiolated gelatin and PEG diacrylate, as the hydrogel for tissue constructs in a metastasis-on-a-chip platform.[79]

Polysaccharide-Based Biomaterials—Chitosan: Chitosan, a linear polysaccharide, is a deacetylated derivative of chitin, which exists in crustacean shells. It is structurally similar to glycosaminoglycans, which makes it an interesting candidate for TE applications.[125] Other favorable properties include its biodegradability, biocompatibility, flexibility, and porosity.[126] Furthermore, chitosan-based systems can be developed to be responsive to light, pH, temperature, and ionic concentration.[127] Limitations include its weak mechanical properties and instability.[83] Chitosan is highly crystalline and is easily processed into many different forms including gels, nanofibers, beads, nano- and microparticles, and sponges.[83]

Chiu et al. demonstrated the use of chitosan in an OOC platform forming a vascular network in cardiac tissue. Collagen–chitosan hydrogel with sustained release of angiogenic and cardioprotective peptide thymosin β4, was used on micropatterned substrates to allow capillary outgrowth from an explanted vein and artery, as well as to support cardiac tissue

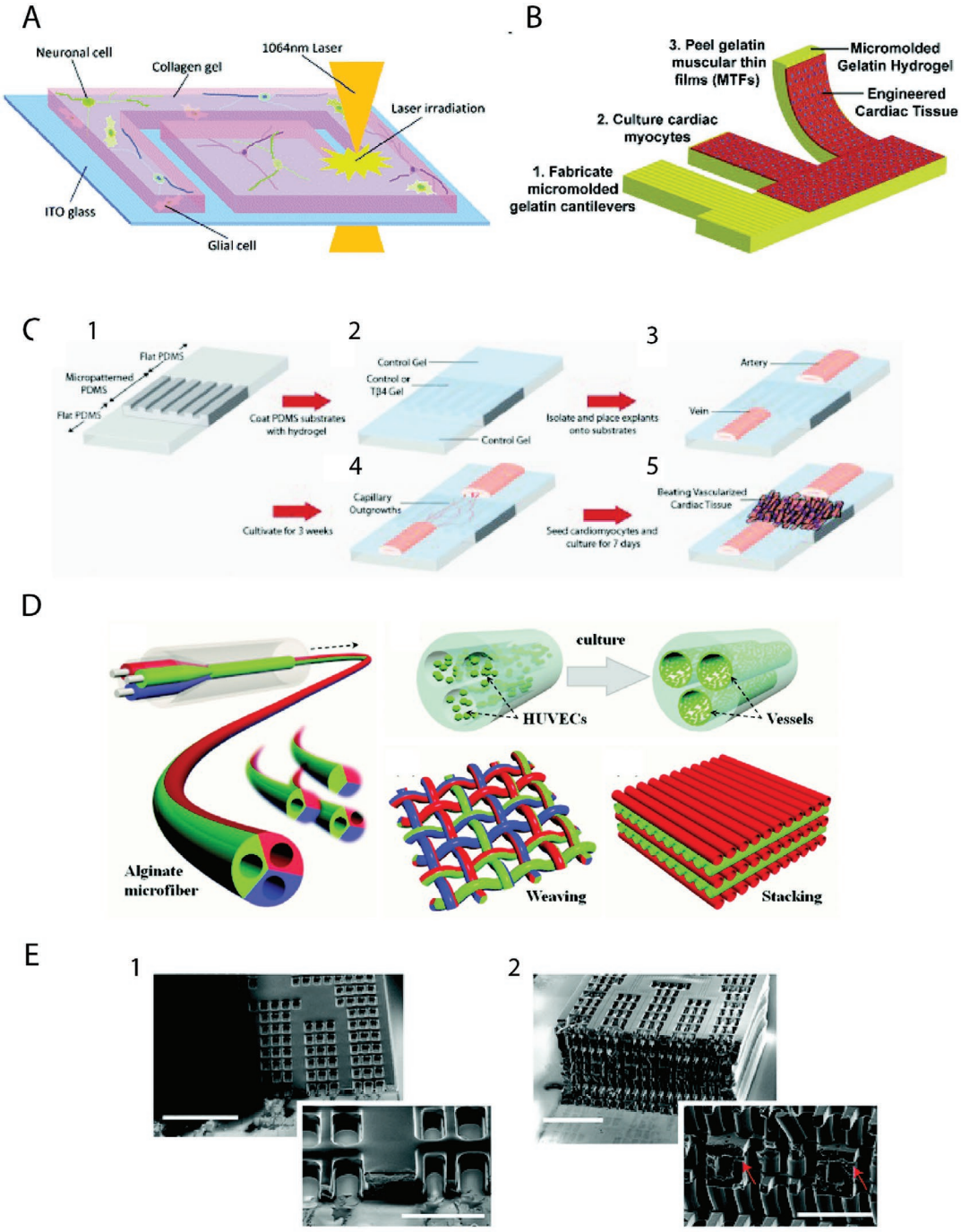

Figure 2. Biomaterials fabricated for various scaffolding applications. A) Cell-laden collagen gel being patterned with photothermal etching, to fabricate a platform with desired spatial conformation, cell number, cell type, and orientation during growth.[63] Reproduced with permission.[63] Copyright 2013, Royal Society of Chemistry. B) Flexible MTF cantilevers made of micromolded gelatin, for culture of contractile cardiac tissues.[91] Reproduced with permission.[91] Copyright 2014, Elsevier. C) Collagen–chitosan with encapsulated T β4 used as a hydrogel for 3D capillary outgrowths from arteries and veins. (1) PDMS substrates fabricated with soft lithography technique were used as a platform that was (2) coated with hydrogel, (3) with two additional microchannels to represent artery and vein, and (4) cultivated for two weeks with hepatocyte growth factor (HGF) or VEGF or for three weeks without growth factors, during which time capillary outgrowths could form. Then, (5) CMs were seeded and cultured for an additional 7 days to form a vascularized cardiac tissue.[102] Reproduced with permission.[103] Copyright 2012, National Academy of Science. D) Alginate microfibers seeded with cells to generate vessel-like structures. Fibers could be woven and stacked to create various scaffolds.[104] Reproduced with permission.[104] Copyright 2016, American Chemical Society. E) POMAC has tunable elasticity and biodegradability, allowing it to be used for fabrication and molding of scaffold structures. Scanning electron microscope (SEM) images show the AngioChip, a tissue culture scaffold with built-in vasculature, which is made of POMAC tubes and porous scaffolding that may be built into various configurations. (1) Single layer, scale bar 1 mm and 300 µm for inset. (2) Multilayer, scale bar 1 mm and 400 µm for inset.[35] Reproduced with permission.[35] Copyright 2016, Nature Publishing Group.

culture surrounding the vasculature with improved functional properties (Figure 2C).[103]

Polysaccharide-Based Biomaterials—Alginate: Alginate is a polysaccharide block copolymer comprised of α-L-guluronic acid and β-D-mannuronic acid derived from algae and seaweed.[128] It is beneficial for many applications in TE as it has low cost, low toxicity, and is easily capable of gelation and chemical modification.[129] However, main drawbacks for applications involving cells include unpredictable degradation and lack of cell binding and interactions as a result of limited protein adsorption.[102] To overcome the cell attachment issue, alginate can be modified with peptides.[130]

One of the benefits of using alginate is immediate gelation upon exposure to divalent cations such as calcium (commonly in the form of calcium chloride solution), which can allow microfibers or specific structures to be formed.[102] Additional polymers were added to alginate to improve performance in cell culture (Figure 2D).[104] Alginate was used as a component of bioink for the bioprinting of a scaffold with human umbilical vein endothelial cells (HUVECs). Ionic crosslinking of the alginate component during the bioprinting process was achieved by exposing microfibers to a $CaCl_2$ solution, and additional crosslinking of another component was completed after printing using UV exposure with a photoinitiator. This microfibrous scaffold material was loaded onto a layer of PDMS, seeded with cardiomyocytes (CMs), and maintained in a microfluidic perfusion bioreactor.[85]

A common use of alginate is to form microbeads for cell encapsulation. Alessandri et al. demonstrated the production of hollow and elastic alginate shells for cell encapsulation of multicellular spheroids to mimic microtumors.[89] Chan et al. produced hepatocyte spheroids microencapsulated in alginate and alginate–collagen hydrogels using a microfluidic approach. Hepatocyte functions were improved when the alginate–collagen composite hydrogel was used.[90]

The use of alginate in other OOC platforms include 3D alginate hydrogels for cell encapsulation in a wide array of patterns fabricated using a visible-light induced electrodeposition approach[131] and the use of sodium alginate as a sacrificial material to rapidly make patterned vascular networks in a variety of ECM mimicking gels.[86] One study that used a microfluidic device as a pharmacokinetic–pharmacodynamic model mimicking multiple tissues (i.e., liver, tumor, and marrow) suggested that the metabolic function of cells in their study may be slower in alginate compared to Matrigel since alginate prevents cell attachment.[88]

2.2.2. Synthetic Biomaterials

Some of the drawbacks of naturally derived biomaterials can be addressed using synthetic biomaterials. One major advantage is that the chemical and physical properties of synthetics are more tunable than those of natural biomaterials. Mechanical properties and degradation rates of these polymers can be modified to suit the specific application. Molecular weight, concentration, and level of crosslinking are a few of the parameters that can be adjusted to tune these properties. Another favorable aspect of synthetic biomaterials is their reproducibility. Processes for their fabrication can be controlled such that batch-to-batch variability is minimal relative to naturally derived biomaterials.

A significant disadvantage of the use of synthetic biomaterials is that there are no cell adhesion ligands present on the surface. This characteristic can, however, be addressed through chemical modification of the surface with adhesion molecules such as laminin,[132] fibronectin,[133] and arginylglycylaspartic acid peptide sequences.[134] Additionally, bioactive molecules with other favorable properties can also be incorporated through covalent attachment, adsorption, or electrostatic interactions to provide desirable properties such as prosurvival or angiogenic properties.

In TE applications, work has primarily focused on the use of polyesters and synthetic hydrogels. Synthetic biomaterials have been studied extensively in TE applications, and have been reviewed thoroughly elsewhere.[56,135] Synthetic hydrogels provide many of the advantageous properties related to natural materials, but allow for tuning of mechanical properties as per tissue application. For example, polyethylene glycol is an inert, FDA approved biomaterial hydrogel that can be chemically functionalized as per application. Modifications include peptide attachment,[136] photo-crosslinkable moieties,[137] and combination with other natural materials.[138] Its utility for cells is related to its high-water content, which can be tuned along with its mechanical properties. It presents an advantageous synthetic alternative to natural materials in OOC.[138]

Recently, polyesters have been used as a flexible, moldable alternative in OOC devices. They are degraded mainly through hydrolysis as a result of nucleophilic attack of the ester linkage and degradation rates depend on water penetration.[139] Common polyesters include PLA, poly(lactic acid-*co*-glycolic acid) (PLGA), polyglycolic acid, poly(1,8-octanediol citrate), and poly(glycerol sebacate).[56] We have recently used polyesters in OOC technology including poly(octamethylene maleate (anhydride) citrate) (POMAC),[140] and poly(octamethylene maleate (anhydride) 1,2,4-butanetricarboxylate) (124 polymer).[47,97] These materials are moldable and elastic, and demonstrated utility in developing a biodegradable microvascularized scaffolds for OOC constructs (Figure 2E).[35]

2.2.3. Hybrid Biomaterials

Hybrid natural–synthetic biomaterials could have advantages of both natural and synthetic biomaterials. For example, these biomaterials offer a wide range of chemical and mechanical properties and can be synthesized in a controllable and reproducible approach. Degradation rate of these materials is also tunable. More importantly, natural component of hybrid natural–synthetic biomaterials provides cell affinity for hybrid biomaterials.[141] Some examples of hybrid biomaterials used in TE include PEG–fibrinogen,[142] PLA–chitosan–gelatin,[143] and chitosan–siloxane.[144]

3. Cell Sources for Tissue Engineering

The most critical consideration for in vitro models is the reproduction of a desired in vivo organ by selecting a suitable cell

type from an appropriate cell source.[145] While animals were the main source of cells for TE, they fail to mimic the human functionality and complexity.[146] Moreover, utilizing animal cells results in only a limited success in representing human disease.[147] The human cells utilized in TE, especially in OOC platforms, are primary cells, immortalized cell lines, SCs and their differentiated progeny (**Table 2**). These categories have their own strengths and weaknesses, which will be discussed in this section.

3.1. Primary Cells

Cells directly extracted from an organ or a tissue without any modification are defined as primary cells.[241] They are mature cells that are the most phenotypically similar to cells found in tissues in vivo.[242] These features have been used in drug screening applications. Primary cells have been used from different organs in various TE approaches such as skin,[243] liver,[244] cardiac,[245] fat,[238] and skeletal muscle.[246] However, these cells have a few disadvantages that may compel researchers to utilize other cell sources. Extraction and growth of adult cells from certain organs such as the brain are more challenging due to the postmitotic nature of these cells.[247] While primary cells have the most similar phenotype to that of in their native in vivo environment, their functionality (gene and protein expression) is altered after only few days in culture, as a result of the drastic changes in the cell microenvironment.[248] Moreover, primary cells are difficult to obtain and are challenging to maintain in culture for an extended period of time due to their finite lifespan.[202] Alongside with the fact that each extraction may reveal different responses from the same donor, derived primary cells can behave differently based on the sex, age, genetics, and the possible disease states of the donor.[249]

3.2. Immortalized Cell Lines

To make cells immortalized, they have to be prevented from reaching senescence, i.e., they have to survive and remain active indefinitely. Telomeres, known as the biological clock of the cell, become shorter after each replication.[250] The most common technique for immortalization is blocking or losing function of telomeres.[251] Cell lines can be obtained from either chemical or viral modification of primary cells.[242] These cell lines are safe and capable of achieving replicable results. However, since these cell lines have experienced genotypic and phenotypic drifting modification, they are not able to exhibit similar function as seen in the original tissue or organ.[252] Due to the facile handling and growth, immortalized cell lines have been widely utilized for OOC platforms.

3.3. Stem Cells

SCs are defined as cells capable of self-renewal and differentiation to various cell types. These cells can be collected from inner cell mass of developing blastocyst, fetuses, and adult organs.[241] SCs can be classified based on their capability to differentiate into different cell types into totipotent, pluripotent, and multipotent. According to their origin, they can be divided into embryonic stem cells (ESCs), adult SCs, and induced pluripotent stem cells (iPSCs), which will be described in more detail below.

3.3.1. Pluripotent Stem Cells

ESCs are pluripotent, capable of differentiation to all cell lineages in the body via the three embryonic germ layers; ectoderm, endoderm, and mesoderm. They can be maintained in cell culture and proliferate for indefinite periods of time. As a result, ESCs theoretically are an unlimited source of cells from a single donor. They are derived from the inner cell mass of developing blastocyst, resulting from the in vitro fertilizations. Despite all advantages of ESCs, they have major challenges that limit their usage in OOC platforms. For example, the use of human ESCs has long raised ethical concerns.[92] Differentiated progeny is required for use in OOC platforms. Despite significant advances in directed differentiation of many cell types (e.g., CMs[93]), it is still not possible to get all cell types in vitro at high yields starting from human ESCs and the resulting cells often have low functionally and structurally immature phenotype.

It is an antecedent opinion that cell differentiation is unidirectional and irreversible process has completely changed by the advent of reprograming of differentiated cells to human iPSCs. This major discovery was first reported by Takahashi and Yamanaka using retroviral vectors.[253] After one year, Thomson group published their method to reprogram human skin fibroblasts and generate human iPSCs utilizing lentiviral vectors.[254] Human iPSCs revealed their potential for differentiation into multiple cell types by applying different biological, mechanical, and electrical cues. As such, new cell lines were developed that retained human relevance and the capacity to differentiate into any cell that makes up the human body without the ethical issues associated with their use. Extracting somatic cells (e.g., blood cells,[255] testicular,[256] keratinocytes,[257] and pancreatic[258]) from patients and reprograming them to human iPSCs enable researchers to fabricate patient specific platforms for drug discovery and disease modeling purposes.[259,260] Some cell types can be directly reprogrammed into other lineages.[261] However, novel concerns such as patient privacy, low reprogramming output, viral vector utilization, genomic instability, alternation in differentiation potential depending on the donor, and oncogenic possibility still act as challenges for human iPSC utilization and reprogramming procedures.[262]

Human iPSCs are outstanding candidates for OOC platforms to reach their ultimate goal of personalized medicine (i.e., patient-on-a-chip). This cell source can recapitulate various diseases as well as be utilized as a sophisticated preclinical model with various age, sex, and other characteristics. Some studies established methods to fabricate OOC platforms applying human iPSCs. For instance, in a recent study, Giobbe et al. designed a microfluidic approach to differentiate human iPSCs to functional CMs and hepatocytes.[263] Moreover, Vunjak-Novakovic et al. reported the fabrication of a multi

Table 2. Different cell sources used in OOC platforms.

Organ model	Primary cells	Cell lines	Stem cells	Coculture
Liver	Primary rat hepatocytes[148–152]	HepG2[153]	Human iPSCs to hepatic cells and ECs[154]	Primary rat hepatocytes and 3T3-J2 fibroblasts[155,156]
	Primary human hepato-cyte[151,157,158]			Primary rat hepatocytes and 3T3 fibroblasts[159]
				Primary rat hepatocytes and hepatic stellate cells[160,161]
				Immortal hepatocyte cells, immortal hepatic stellate cells, and lung micro-vascular endothelial cells[162]
				Primary rat hepatocytes and primary rat adrenal medullary endothelial cells[163]
				Primary human hepatocytes, EA.hy926, LX-2, and U937 cell lines[164]
				Primary rat hepatocytes, primary rat adrenal medullary endothelial cells and bovine aortic endothelial cells[165]
				Primary rat hepatocytes and human hepatic stellate cell line[166]
Skin				Human keratinocytes, HS27 fibroblasts, and HUVECs[36]
				Normal human dermal fibroblasts, normal human epidermal keratinocytes, and HUVECs[167]
				Immortalized human keratinocytes and human leukemic monocyte lym-phoma cell line[168] EpiDermFT[169]
				Human fibroblasts and keratinocytes[170]
Vascular	Primary human dermal microvas-cular endothelial cells[171]	Hy926 human endothelial cell line[172]		HUVECs, normal human lung fibroblasts, human promyelocytic leukemia cells, and human glioblastoma multiforme cells[173]
	HUVECs[174–177]			HUVECs, human mesenchymal SCs, human ESCs differentiated to hepato-cyte, primary rat hepatocytes, fibroblasts, and CMs[98]
				Human breast carcinoma cell line and telomerase-immortalized human microvascular endothelial cell line[178]
				Primary human bone marrow-derived mesenchymal SCs, osteo-differenti-ated primary human bone marrow-derived mesenchymal SCs and primary human umbilical vein endothelial cells[179]
Cardiac	Primary rat cardiac ventricular myocytes[59,180–182]	H9c2 cell line[183]	Human iPSC derived CMs[182]	
			Human ESC-derived CMs[59]	
			Human iPSC derived CMs[184]	
			Barth syndrome iPSC derived CMs[185]	
Skeletal Muscle		C2C12[61,77,186–188]		Mouse neural SCs and C2C12[189]
Lung	Human alveolar basal epithelial[190]	Human non-small cell lung cancer cell line[191]		Human alveolar epithelial cells and human pulmonary microvascular ECs[192]
	Human alveolar epithelial cells[193]			Human pulmonary microvascular endothelial cells and alveolar epithelial cells[194]
	Primary human airway epithelial cells[195]			
Bone				Hematopoietic SCs, progenitors, and differentiated blood cells[196]
				Leukemic cells, human bone marrow stromal cells, and human osteoblasts[197]
				Hematopoietic SCs, progenitors, and myeloid cells[198]

Table 2. Continued.

Organ model	Primary cells	Cell lines	Stem cells	Coculture
Brain	Primary rat and mouse cortical and hippocampal dissociated neurons[199]	Immortalized human brain endothelial cell line[200,201]		Brain microvascular endothelial cells derived from human iPSC and rat primary astrocytes[202]
	Primary rat forebrain[203]	Caco-2 intestinal epithelial cells and human alveolar type II like lung epithelial cells[200,201]		
	Primary rat hippocampal/cortical neurons and astrocytes[204]	Mouse brain endothelial and C8D1A (astrocyte) cell lines[205–208]		
	Primary rat hippocampus and entorhinal cortex[209]	Mouse brain endothelial cell line[205–207]		
	Primary rat cortical neurons[210]	Rat brain endothelial cell line[205–207]		
	Mice dopaminergic neurons [211]	Brain endothelial cell line bEnd.3 and the glial cell line C6[212]		
	Primary human brain-derived microvascular endothelial cells, primary human pericytes and astrocytes[213,214]			
	Normal adult human brain microvascular ECs and human adult astrocytes[213,214]			
	Human brain microvascular endothelial cells and human brain pericytes[215]			
Eye	Human corneal epithelial cells and human primary keratocytes[216]			
Gut		Human intestinal epithelial cells[217,218]		
Spleen	Anaerobic bacteria isolated from rat cecal contents[219]			
Kidney	Primary human proximal tubular epithelial cells[220]	Human immortalized proximal tubule epithelial cells[221]		
	Normal human renal cortex of nephrectomies[222]			
Cancer/Tumor	Non-neoplastic human mammary epithelial cells[223]	The human monocytic cell line[224]		Bone marrow stromal cells and osteotropic prostate cancer cell line[225]

Table 2. Continued.

Organ model	Primary cells	Cell lines	Stem cells	Coculture
	Human mammary fibroblast cells[226]			Human fibrosarcoma HT108 and breast carcinoma MDA231 cell line[227]
	Human dermal microvascular cells[228,229]			Primary human bone marrow-derived mesenchymal SCs and osteo-differentiated (OD) primary human bone marrow-mesenchymal SCs[230]
				Human adult dermal microvascular endothelial cells, MTLn3 breast cancer cells, and U87MG glioblastoma cells[231]
Multiorgans				Hepatocellular carcinoma-derived cells (HepG2/C3A) and MDCK tubular epithelial cells[232,233]
				HepG2/C3A cells, human colon carcinoma Caco-2 cells, and mucus producing cells[234]
				Caco-2 TC7 cell line and HepG2 C3A cell lines[235]
				Human HepaRG cell line, human primary hepatic stellate cells, human juvenile prepuce[236]
				human juvenile prepuce, skin biopsies, and human dermal microvascular endothelial cells
				human hepatocyte cell line, HepaRG, primary human hepatic stellate cells, and freshly generated skin biopsies[237]
				A549, C3A, HK-2, and human subcutaneous preadipocyte[238]
				Human HepaRG cell line, human primary hepatic stellate cells, human proximal tubule cell line, and reconstructed human small intestinal barrier models in cell culture inserts (EpiIntestinal)[239]
				Rat lung type II epithelial cells, HepG2/C3A and 3T3-L1 cells[240]

OOC platform called HeLiVa, which contains the same source of human SCs to form vascular, cardiac, and liver tissues, rendering the idea of a patient-on-a-chip one step closer.[264]

4. Environmental Parameters Affecting Cell Behavior and Function

4.1. Structure

3D tissue structure is critical for the complex spatial and temporal control of cellular behavior and function.[265] The ECM is a complex network consisting of proteoglycans, proteins, and other soluble biomolecules[266] and provides biochemical context and structural support to cells.[266] The dynamic interaction between the ECM and cellular components closely regulates cell behavior by influencing differentiation, proliferation, and migration.[266,267]

Different organs have diverse composition and spatial organization of ECM to maintain specific tissue morphologies and function.[266] For example, the ECM network in the heart is composed of fibrillar collagens I and III, fibronectin, proteoglycans, and basement membrane proteins.[268] It orients the CMs to enable formation of aligned cardiac bundles with elastic support.[269] Structural organization of the microenvironment is not only tissue-specific, but also highly dynamic and constantly undergoes physiological and pathological remodeling.[266] For instance, within fibrotic tissue, fibroblasts often synthesize extracellular collagen fibers, which subsequently leads to altered matrix properties.[270] In cardiac tissues undergoing fibrosis, diastolic and systolic dysfunctions are often closely linked to collagen deposition and ECM remodeling.[271]

Conventional monolayer models cannot adequately mimic cellular microenvironments in the human organs due to oversimplification of the tissue structure.[265] Efforts to address the need for extracellular structure resulted in the development of 3D cell cultures in which cells are grown with structural support provided by scaffolds. In the past decade, there have been tremendous efforts to develop tailored scaffold biomaterials that mimic the ECM and provide cells with sophisticated structural cues to recapitulate the native microenvironment.[266]

4.2. Mechanical Properties

The extracellular environment is an essential mediator of cell function and provides not only biochemical but also mechanical cues to influence cell phenotype and behavior. Among various mechanical cues, matrix elasticity has a crucial role in the induction of cellular responses and fate including proliferation, differentiation, migration, adhesion, and maturation.[266] Mechanical properties determine the tissue's capacity to resist deformation induced by stress, such as compression, elongation, or shear force.[270] In neural tissue, stiffness of cell-supporting substrates has been shown to modulate crosstalk between neural cells and surrounding microenvironment and regulates excitatory synaptic transmission.[272] In skeletal muscles, in vitro differentiation of myoblasts is largely modulated

by signaling pathways of matrix elasticity.[273] Moreover, elasticity of the microenvironment has been shown to regulate SC differentiation and contribute to cancer formation.[266] It is generally thought that mechanical properties reproducing elasticity of the native tissue environment are most suitable for cultivation of specific tissues in vitro.

Hydrogels have widely been used to modify matrix mechanics and provide control of cell microenvironment.[274] Natural hydrogels have been widely used, but synthetic hydrogels contribute to a broader range of mechanical properties, and thus are becoming preferable in TE applications.[275] For example, stiffness of polyacrylamide hydrogel is tunable by changing the concentrations of its acrylamide monomer and the crosslinker *bis*-acrylamide.[276] PEG remains another widely used material because its mechanical properties can be systematically adjusted by precursor molecular weight and concentration.[277] Advances in the design of novel materials with varying crosslinking levels via light or heat exposure make it easier to modulate mechanical properties with user-defined inputs. Among a new class of polyester elastomers, elastic properties of 124 polymer can be adjusted using monomer ratio, UV light exposure, and porosity of the cured elastomer.[278]

4.3. Electromechanical Stimulation

Other than geometrical and mechanical cues, electromechanical signals from the extracellular environment play pivotal roles in regulating cellular activities.[279] Electrical and mechanical stimulation has significant influence on cell morphology, cytoskeletal fiber orientation, and gene expression, especially in electroactive tissues, such as neural, skeletal muscle, and cardiac tissues.[280] In cardiac TE, electrical stimulation is critical for the development of conductive and contractile properties of tissue constructs.[281] Application of electrical stimulation in neural TE is also important due to its significant role in nervous system signaling.[282] Electrical stimulation has improved nerve regeneration and neurite extension.[283] Likewise, in muscle TE, sarcomere assembly, myofiber maturation, and tissue contractile activity can be enhanced through the application of electrical stimulation.[284]

Protocols have been proposed to electrically stimulate tissue constructs with positive results on OOC platforms.[285–287] For example, the Biowire platform developed by our group combines architectural and electrical cues on wire-like structures that recapitulate the native cardiac bundles.[285] In skeletal muscle TE, a number of studies have demonstrated that bioreactors including electrical stimulus with selected pulse amplitude, pulse frequency, and work-to-rest ratio can accelerate the maturation of sarcomeric structure.[284,288]

Development of materials comprised of biocompatible polymers along with embedded conductive components has received extensive attention for electrical stimulation of tissues.[289] Commonly used conductive biomaterials in TE include carbon nanotubes (CNTs), graphene, metallic nanoparticles (NPs), and conductive polymers.[289] The unique combination of electronic and mechanical properties makes CNTs suitable for biosensors and TE scaffolds.[290] Ahadian et al. reported the use of CNTs in making electrically conductive and mechanically strong polymeric scaffolds for cardiac tissue regeneration.[291] Other nanobiomaterials, such as metallic NPs and graphene have also been utilized to prepare conductive polymer composites.[292,293] In recent years, conductive polymers have also emerged as a new class of attractive candidates for the construction of scaffolds for TE.[292] Polypyrrole, polyaniline, and polythiophene are the most widely used conductive polymers with electrical stimulation because of their excellent conductivity and stability in tissue culture.[292]

Besides electrical stimulation, mechanical stimulation has also been reported to have a significant role in tissue development, especially in regulating fiber orientation, sarcomere organization, and cell junction formation in different tissues.[294] A concerted effort has been made to develop TE platforms with mechanical cues. The most widely used approaches for applying mechanical stimulation are step-wise stretch and cyclical stretch of 3D engineered tissues.[280] Eschenhagen and co-workers were among the first to incorporate mechanical stretch into the design of 3D tissue bioreactors.[295] By applying uniaxial mechanical stretch, they generated engineered heart tissue with structural and functional features of a mature myocardium.[296]

In native tissues, multiple stimulations are applied concurrently and electromechanical signals are strongly coupled.[279] On TE platforms, the simultaneous application of electrical and mechanical stimulation has shown better results in replicating the native microenvironment of a human tissue.[287] In an effort to mimic high fidelity of engineered tissues, some bioreactor designs have been made to use mechanical and electrical stimulation in one OOC platform. Liao et al. were among the first group to apply intermittent cyclic stretch and electrical stimulation concurrently to tubular skeletal muscle constructs in a multimodal bioreactor.[294] The dual stimulated samples showed higher expression of myosin heavy chain proteins and excitability compared to unstimulated controls.[294] Overall, OOC platforms with electromechanical stimulation hold promise in providing the most biomimetic culture environment for TE.

4.4. Dynamic Microenvironment

In whole organs and tissues, adequate function is dependent on a diverse array of coordinated environmental factors, including mechanical, electrical, biochemical, and spatiotemporal cues.[29,147,297] The physiological relevance of engineered tissues must thus incorporate dynamic microenvironments; interactive and responsive biomaterials and engineered constructs that involve or adapt to changes in environmental stimuli. In the following paragraphs, various environmental factors, their role in influencing cellular processes and function, and ways of mimicking dynamic physiological microenvironments in vitro will be discussed.

4.4.1. Mechanical Stimulation

Cells and tissues in the body experience varied degree of mechanical forces, ranging from tensile to compressive forces.[298,299] However, careful consideration regarding the

duration, frequency, and amplitude of mechanical forces are important to mimic physiological mechanical forces experienced by different cells and tissues in the body. For instance, the response to flow by ECs, including changes in morphogenesis and sprout formation, was demonstrated to be dependent on the direction of the applied fluid shear stress.[300]

In addition to applied stimuli, cells naturally experience varied degrees of mechanical strain due to their interactions with the ECM proteins. The ECM components can also be modified prior to cell seeding, which can be tailored to reproduce cell–ECM dynamics. For example, matrix metalloproteinases, enzymes that degrade the ECM, can be covalently bound to ECM substrates, allowing for dynamic changes in the amount of ECM and mechanical strain experienced by cells by modifying the ECM degradation.[301]

Despite the benefits of mechanical strain, the amount of mechanical force required to induce physiological levels of cellular tension is difficult to discern. Accurately sensing mechanical forces experienced by cells is an important step forward for the design and implementation of appropriate physiological levels of mechanical strain. While, an ongoing challenge, microfluidic platforms have also been designed to provide detailed mechanical feedback, which can be used to tailor mechanical stimulation.[299] It was demonstrated that the addition of microposts on the bottom of microchannel devices enabled shear stress measurement of ECs.[302] This system allowed for label-free force sensing and a platform that could be used in most microfluidic devices. Despite this advancement, the use of microposts is still limited given inherent surface rigidity and limited ability to incorporate ECM substrates. Future devices that allow for normal cell interactions and that do not alter the mechanical environment experienced by cells are needed for widespread applicability.

4.4.2. Electrical Stimulation

Electrical conduction is an essential component of excitable tissues, such as neurons and muscles (skeletal, cardiac, and smooth muscle) with action potential (AP) generation and propagation essential for a range of cellular functions. Similar to mechanical forces, the degree and timing of electrical stimuli is an important consideration. In the heart, for example, electrical conduction from pacemaker cells in the sinoatrial node travels toward the apex of the heart and back up, with the rhythm precisely controlled to ensure stable ventricular myocyte contractility. As such, regulating the timing, amplitude, and frequency of stimulation is particularly critical for replicating in vivo processes.

Aside from manually adjusting the amount of electrical stimulation or using cyclic approaches, live recording of electrical cell activity may allow for more precise regulation of electrical stimuli. For instance, nanoelectronic scaffolds were developed using microfabrication that allowed for real-time monitoring of the local electrical activity within 3D CM constructs.[303] Another group demonstrated that using gold electrodes dispersed throughout an SU-8 mesh, it was possible to measure the electrical conductivity of ventricular myocytes in real time.[304] As a result, the authors were able to tune the degree of electrical stimulation to ensure synchronized ventricular myocyte contraction. Incorporation of electronic sensors into biodegradable and biocompatible elastomeric polymer-based approaches is needed to create more applicable dynamic electrical microenvironments. For example, other groups have developed 3D nanoelectronic arrays utilizing a series of 3D tissue-scaffold-mimicking structures and showed that these nanoelectronic scaffolds were similar in dimension and mechanical properties to conventionally used cardiac tissue scaffolds, such as PLGA electrospun fibers.[305]

4.4.3. Biochemical Stimulation

In living organs, cells exist in close contact with other cells and are surrounded by variations in the ECM proteins.[297,306] Microengineering approaches have allowed the creation of cell–cell and cell–ECM interfaces that mimic sophisticated 3D microarchitectures of living tissues and organs. For example, in the liver, hepatocytes (liver epithelial cells) are separated by surrounding sinusoids (type of blood vessel containing ECs). To recreate this endothelial–epithelial interface, a microfluidic device with microfabricated barriers was created that separated cultured hepatocytes from fluid flow.[39] Hepatocytes were demonstrated to form cord-like structures and functional bile canaliculi as a result of this engineered tissue interface.[39] Other studies have used more sophisticated methods to seed cells by recreating cell–ECM interfaces. For example, assembly of a microfluidic cornea in a layer-by-layer fashion was done by growing corneal epithelial cells on a sacrificial collagen membrane, which when degraded enzymatically allowed the seeding of corneal stromal cells after the epithelial cells deposited their own basement membrane.[307] It allowed for a cellular tissue construct that maintained a physiological interface and barrier.[307]

In addition to biological interactions, cellular homeostasis requires continual ion and nutrient exchange, waste removal, and hormonal flux. As an example, a microfluidic perfusion culture system was developed to increase the albumin diffusion in the isolated pancreatic islet cells, which resulted in an increase in cell density.[308] Multiple groups have developed microfluidic systems that incorporate better oxygen diffusion gradients and vascularized systems. For example, one group combined microfluidics and paper-based 3D cell cultures to control oxygen gradients in 3D cultures.[309] To do so, the authors utilized a combination of chromatography paper and an ECM hydrogel to create a thin and mechanically strong 3D fabrication system, such that the grown cells retained access to nutrients and oxygen and thus they were not limited by mass transport. Other important considerations include the regulation of pH, responses to oxidation–reduction reactions, and enzymatic regulation, which are reviewed elsewhere.[310]

4.4.4. Spatiotemporal Cues

The last parameter that is an important consideration for creating a physiological dynamic microenvironment is spatiotemporal cue. Cells have been shown to respond on both

the nano- and microscale, sensing surface properties and ultimately, resulting in phenotypic changes. Engineering tissues requires directing cell growth, orientation, relative positions, and interactions to reproduce in vivo tissue-level organization. Controlling the geometric shape or architecture of the microengineered construct used to grow cells can be used to guide the structural organization of engineered tissue constructs and results in better functional and structural properties, such as improved cellular alignment and orientation, 3D tissue-level organization, and coordinated cellular function, such as contractile properties.[311,312]

A more overlooked parameter is the timeframe in which cells are grown in tissue constructs and the suitable timing of the introduction and maintenance of environmental factors for appropriate tissue maturation.[313,314] For example, forming appropriate 3D cartilage tissue was dependent on time in culture, with a more mature tissue construct developed over time as cells produced sufficient matrix and began to coalesce together.[314] Cultivation of cells to achieve properties of native tissues is largely variable and dependent on the complexity and type of tissue. Further, the period of time certain environmental stimuli, such as mechanical strain, and factors, including growth factors and hormones, introduced into cell cultivation and later unintroduced, can have a profound effect on cell maturation.

4.5. Soluble Factors

In addition to dynamic microenvironments, the incorporation of soluble factors, including growth factors and peptides, into TE constructs has been shown to be beneficial for angiogenesis, cell survival, migration, proliferation, and differentiation, helping to overcome current limitations in the field (summarized in **Table 3**).[315] For instance, covalent immobilization of an Ang-1-derived peptide, QHREDGS, to a collagen–chitosan hydrogel backbone, was shown to improve CM survival.[316,317] However, the simple addition of soluble factors into cell culture media is limited due to lack of controlled regulation and systematic effects on cell behavior. To overcome this, chemical immobilization and physical encapsulation of soluble factors into various biomaterials have allowed for sustained controlled release of growth factors and peptides and can be dynamically regulated (e.g., in response to pH, temperature, enzymatic degradation).

5. Microscale Technologies for Organ-On-A-Chip Construction

5.1. Photolithography

Photolithography method involves applying UV light through a photomask onto a UV-sensitive material. This fabrication method results in a desired pattern in the material (**Figure 3**B). However, the pattern resolution is limited by the light diffraction and is thereby a function of light wavelength.[326] Cells can be directly cultured on the patterned materials. The patterned materials can also serve as a master for soft-lithography technique[326] (Figure 3B). Hydrogels can also be incorporated into photolithographically patterned materials to control spatial resolution, promote cell seeding, and incorporate a physiological ECM environment.[318]

5.2. Soft Lithography and Micromolding

Soft lithography involves microfabrication methods to generate soft, flexible, micropatterned structures (Figure 3B).[326] Using a master mold from photolithography, PDMS is shaped, heated, cured, and removed to generate a microfabricated structure. Multilayered soft-lithographic approaches have also been developed using 3D stamping techniques, in which separate structures are assembled onto one another.[326] Soft-lithography technique showed that the ECM molecules on a 2D surface have a similar role to 3D ECM constructs. Microfabricated and planar islands of ECM molecules can limit cell spreading and direct certain cell behaviors. Microfabrication using a combination of photolithography and soft-lithography techniques have resulted in various OOC models that mimic physiological tissue processes, including alveoli expansion,[328] kidney filtration,[37] and intestinal absorption.[40]

5.3. Microfluidics

Microfluidics is defined as the science and technology of fluid manipulation in small channels with at least one-dimension size less than 1 mm.[329] The widespread application of silicon-based microelectromechanical systems in the 1980s caused a rapid growth in the fabrication and development of silicon-based microfluidic systems.[330] Microfluidic systems have been implemented in engineering vascular,[331] bone,[332] liver,[333] cartilage,[334] and neural tissues.[335] Major applications of microfluidics in TE field include cell culture and making gradient biomaterials.[336] Microfluidic cell culture platforms are better able to mimic the dynamic cellular environment compared to static cell culture systems.[337] For example, Vladisavljević introduced a cell-laden hydrogel inside a microfluidic channel to create a lumen (**Figure 4**A).[338] Bischel et al. constructed a microfluidic plate system having 96 chambers. The flow between microfluidic chambers was provided using passive pressure without using external pumps (Figure 4B).[339] Trietsch et al. showed a coculture of skin tissue with hair follicles in a microfluidic Boyden chamber-like system (Figure 4C).[340] Wagner et al. demonstrated a perfused system of colorectal cancer spheroids and liver. Drug metabolism was studied using this system (Figure 4D).[237]

Microfluidic technology is a powerful technique to generate gradients of cytokines and biomaterials. Fluid flow in microfluidic channels is completely laminar without any turbulence due to the small size of channels. This characteristic can be used to sustain complex microfluidic gradients for a long time.[342] Microfluidic gradients have generally found diverse biomedical applications in studying immune response,[343] wound healing,[344] and cancer metastasis.[345] For instance, Han et al. fabricated a microfluidic system to study the migration of neutrophils induced by a gradient of two chemoattractants. The

Table 3. Soluble factors in TE. Ang, angiopoietin; BMP, bone morphogenetic protein; EGF, epidermal growth factor; FGF, fibroblast growth factor; HGF, hepatocyte growth factor; IGF, insulin-like growth factor; PDGF, platelet-derived growth factor; TGF, transforming growth factor; Tß4, thymosin-beta 4; VEGF, vascular endothelial growth factor.

Function	Factor	Cells	Tissue	Ref.
Proangiogenic	Ang-1	ECs	Blood vessels, heart, skeletal muscle, intestine	[316–321]
	Ang-2			
	VEGF			
	FGF-2			
	PDGF-AB			
	Tß4			
Cell survival	Tß4	ECs, CMs	Blood vessels, heart	[317–320]
	VEGF			
Cell proliferation	FGF-2	ECs, epithelial cells, osteoblasts, mesenchymal SCs, neural cells	Blood vessels, bone, skin, skeletal muscle, liver, nerve	[319,321–324]
	HGF			
	IGF-1			
	PDGF-AB			
	TGF-ß			
	TGF-α			
	EGF			
Cell migration	Tß4	ECs, epicardial cells, epithelial cells, osteoblasts, mesenchymal SCs	Blood vessels, bone, heart, skin, skeletal muscle, cartilage, nerve, liver	[319–321,323,325]
	FGF-2			
	TGF-ß			
	BMP-2			
	BMP-7			
	HGF			
	PDGF-AB			
	VEGF			
Cell differentiation	BMP-2	Osteoblasts, mesenchymal SCs, epithelial cells, ESCs	Bone, cartilage, skin, nerve	[319,323–325]
	BMP-7			
	HGF			
	EGF			
	FGF-2			
	TGF-ß			

results showed that the neutrophils had different responses to the chemoattractants and the migration speed has a correlation with the ECM stiffness.[346]

The integration of microfluidic technology can help to develop sophisticated microfluidic devices with many micromechanical compartments and thereby the device can automatically handle multiple tasks in a short time.[347] Integrated microfluidic systems play an important role in OOC devices, replicating the complexity and interconnectivity of organs in the body.[348] The incorporation of pumps, mixers, valves, and heaters in integrated microfluidic systems can facilitate the fluid manipulation with higher throughput than conventional fluidic systems.[349] However, an optimal design for microfluidic systems should have sufficient complexity to mimic the structure and function of organs and tissues, while having enough simplicity for the ease of operation and assessment.[350] End users with little background and expertise in engineering and system design should be able to operate microfluidic systems easily.[351]

5.4. Dielectrophoresis

Dielectrophoresis (DEP) force is exerted on dielectric particles in a nonuniform electric field. The electric field polarizes the particle, causing the particle to experience a repulsive or attractive force depending on the orientation of the dipole relative to the electric field. DEP has been commonly used for

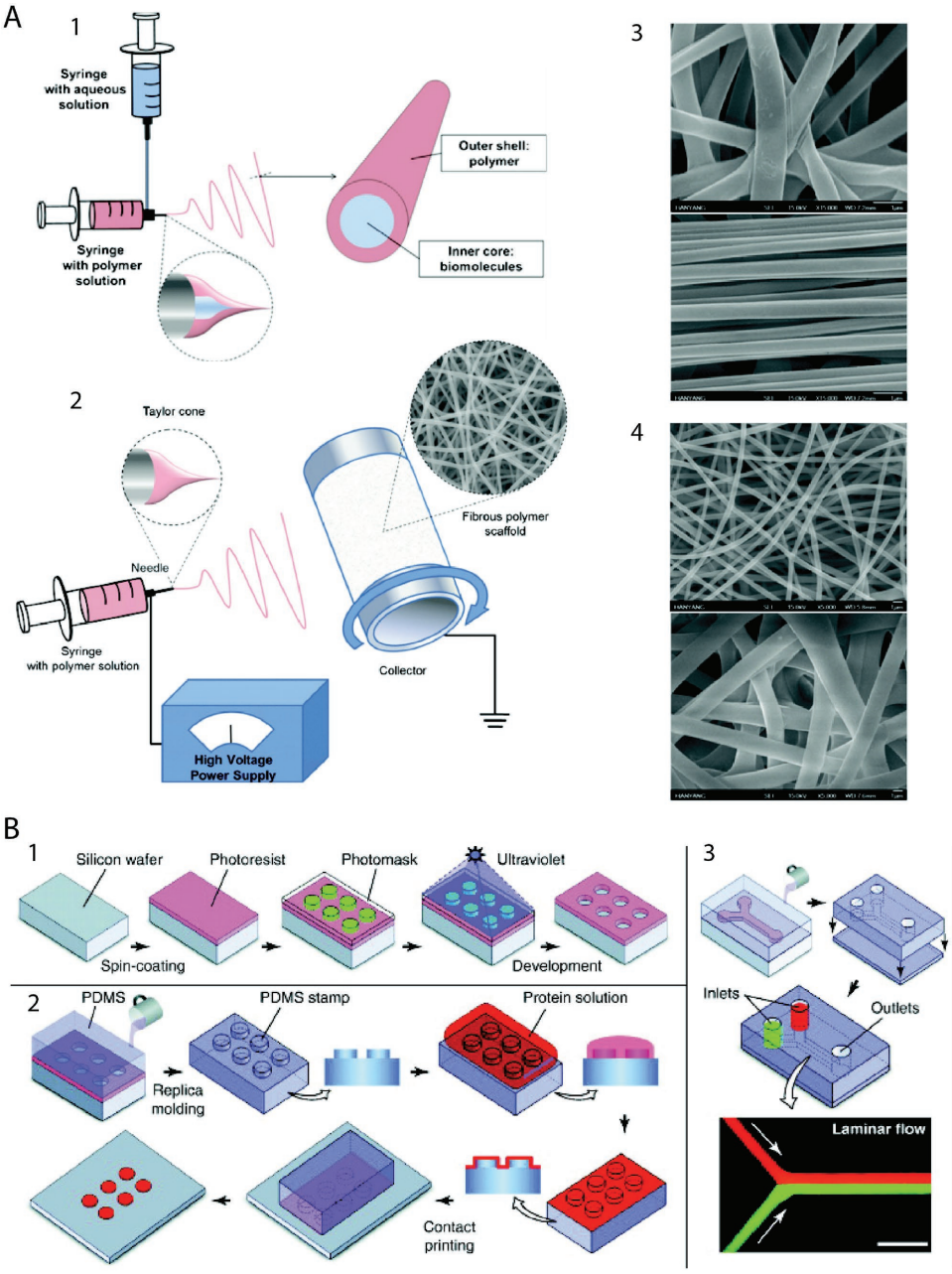

Figure 3. Principles of electrospinning and photolithography techniques. A) Electrospinning may be used to create various fibrous structures. (1) Core–shell structure with two different materials. (2) General setup for electrospinning consists of polymer solution ejected from a syringe that gets collected on a rotating drum, under an electric field. (3) Fibers may be randomly oriented or aligned, and (4) of various dimensions from nanoscale to microscale.[327] Reproduced with permission.[327] Copyright 2013, IOP Publishing Ltd. B) Photolithography. (1) Microscale patterns may be fabricated by selectively curing photoresist through a photomask and UV irradiation. The resulting microfabricated structures may be used in various applications. For example, it can serve as a mold for other more flexible and biocompatible materials to create (2) stamps or (3) microfluidic channels and devices (scale bar, 500 mm).[147] Reproduced with permission.[147] Copyright 2011, Elsevier.

manipulating biological entities, such as particle separation in microfluidic devices, cell electroporation, patterning, and isolation of live versus dead cells.[351] As DEP force is frequency-dependent, cells can be accurately manipulated via a specific frequency and thus form a desirable micropattern. In addition to frequency control, DEP can be customized by designing various microelectrode geometries, which can make complex cellular patterns. For example, in a liver-on-a-chip platform, microelectrodes were designed in a concentric fashion to make radial electric fields for patterning liver cells into hexagonal arrangement, similar to what is found in liver sinusoids (**Figure 5**).[352] However, DEP is limited as force is temporarily

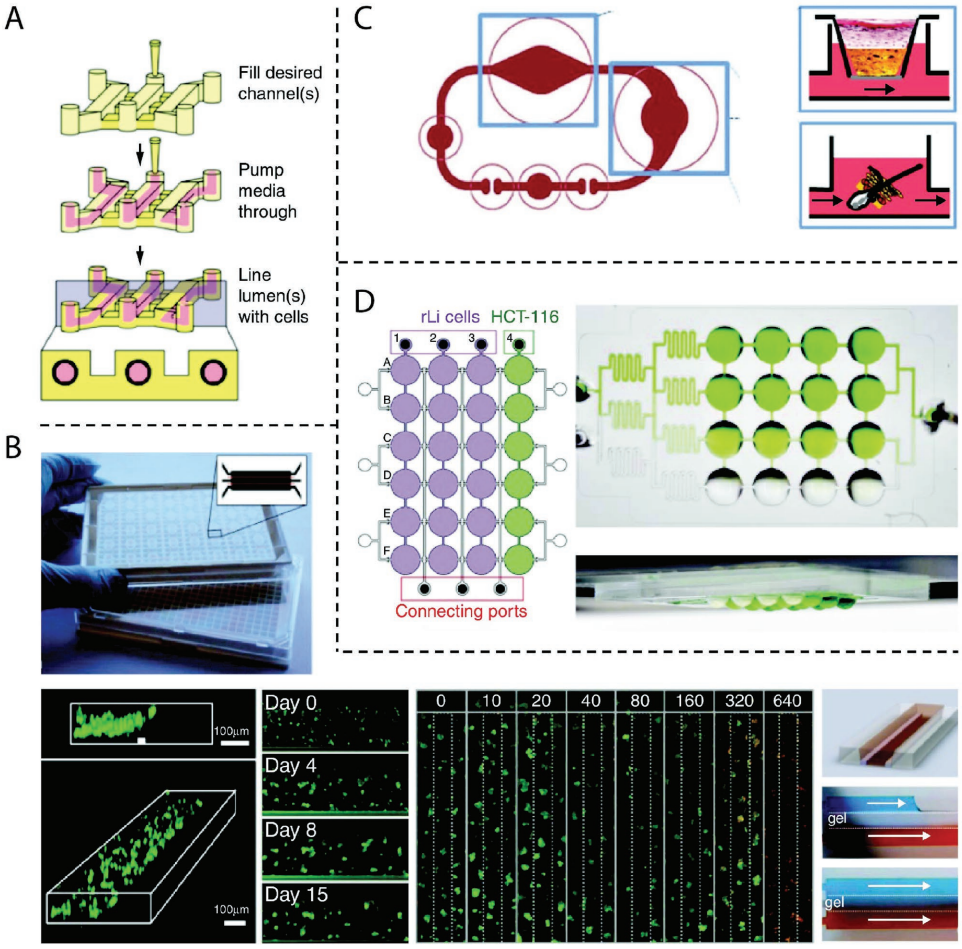

Figure 4. Microfluidic systems in TE. A) Cells encapsulated within a hydrogel may be delivered throughout a microfluidic device, using viscosity and pressure differences to control flow. B) Different conditions may be patterned in chambers of a 96 microfluidic culture plate. C) Hanging droplet system may be combined with flow and gradients in column and row format. D) Microfluidic channels connect multiple tissue chambers, allowing for continuous perfusion and paracrine signaling, that may be multiplexed and controlled with microfluidic valves.[341] Reproduced with permission.[341] Copyright 2015, Elsevier.

applied and as such cells can freely arrange after the stimulus is removed and is limited by small voltage in order to ensure biocompatibility.[353] As such, for long-term patterning, DEP should be combined with other immobilization techniques to ensure stable long-term culturing.[354]

5.5. Cell Sheet Technology

Cell sheet technology involves the layering of monolayers of cells that can be attached directly without the need for sutures, scaffolds, or mediators.[311] Cell sheeting allows for the creation of thick 3D tissues with different cell types that more appropriately mimic physiological tissues and organs.[356] For example, CMs can be layered along with ECs to promote vascularization to enhance cell survival in culture and upon implantation.[357] New cell sheet-stacking techniques have also combined microfabrication technology to promote vascularization by creating micropores between tissue layers. This technique was demonstrated to create a vascular network similar to microvessels in a multilayered tissue of neonatal human dermal fibroblasts with patterned endothelial cell sheets.[358] Along with horizontal layering of monolayers, it is also possible to use cell sheet technology to layer monolayers of cells in different planes. For example, using a tubular support, it was possible to create blood-vessel like structures using human smooth muscle cells and fibroblast cell sheets.[356] As a result, cell sheet technology is advantageous as cells can be grown on supporting membranes in a layer-by-layer fashion and cells can remain in close proximity to each other and to the ECM proteins.[311,359] This technology is also beneficial for growing dense tissues in a less time consuming and technically challenging manner and without the need for incorporating scaffolds, which present issues of biodegradability and biocompatibility.[311,359] However, cell sheet technology may not be able to control the temporal and spatial resolution of cell layering and is restricted in the construction of thick tissues and the formation of necrotic cores.[311,359]

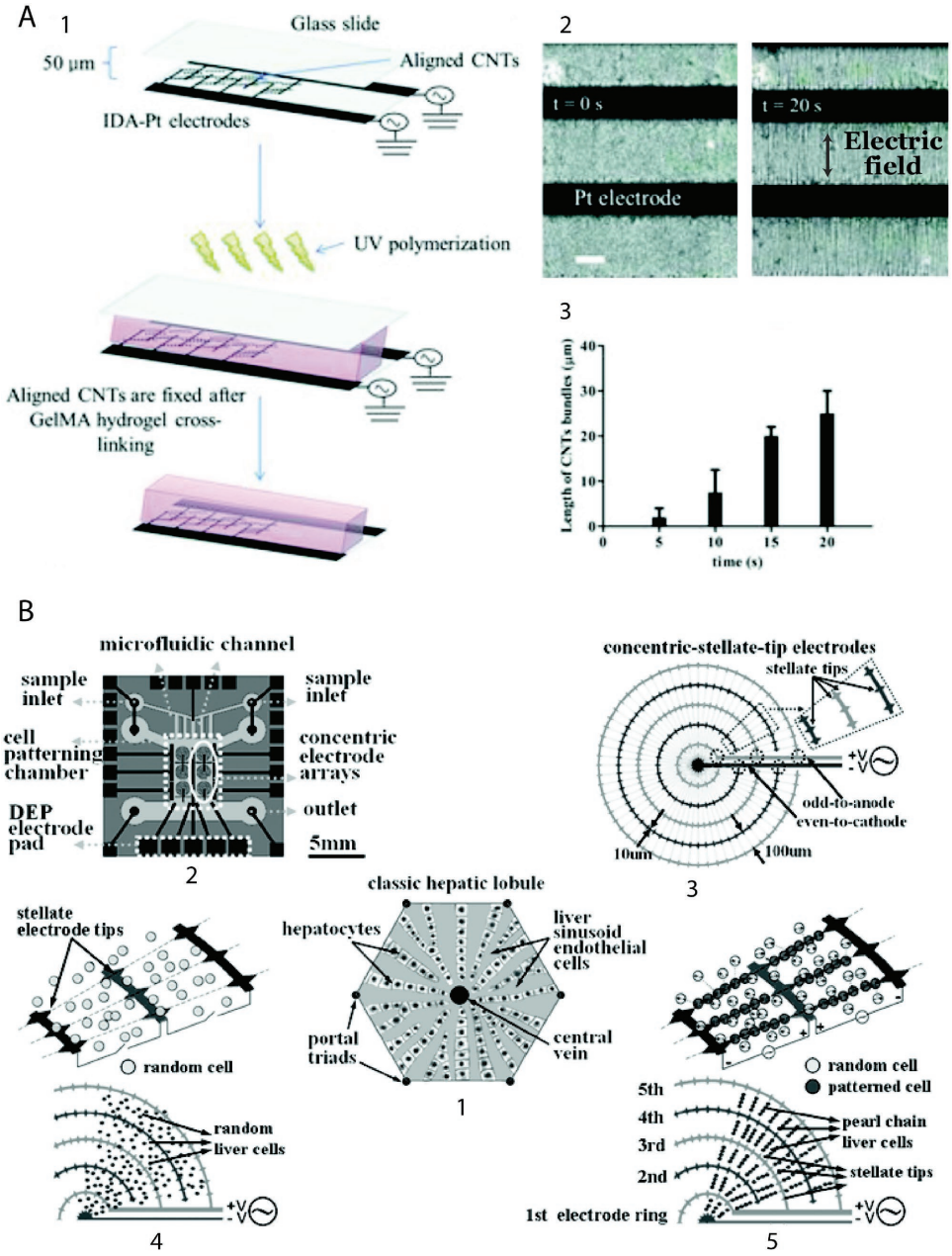

Figure 5. Applications of DEP in TE. A) (1) CNTs are aligned within GelMA hydrogel when DEP force is applied, showing (2) alignment (scale bar, 40 µm) and (3) increasing length of CNT bundles over time. CNT orientation may be fixed by curing the hydrogel.[188] Reproduced with permission.[188] Copyright 2013, John Wiley & Sons. B) Schematics describing concept and use of the microfluidic chip for patterning liver cells. Chip consists of concentric-stellate-tip array electrodes on a glass substrate with a PDMS cover. (1) Illustration of a single hepatic lobule. (2) Top view of the microfluidic chip. (3) View of one unit of the concentric-stellate-tip array electrodes. (4) Seeded liver cells are randomly distributed before applying DEP voltage, and (5) become snared and aligned when the DEP field is activated.[355] Reproduced with permission.[355] Copyright 2006, Royal Society of Chemistry.

5.6. Bioprinting

Bioprinting technology still remains in its infancy, however, advancing technology offers great promise for the spatial placement of cells and biomolecules and may be useful for fabricating 3D, macroscale designs.[360,361] Bioprinting consists of three main approaches: (1) laser-based writing,[362] (2) inkjet-based printing,[363] and (3) extrusion-based deposition.[364] In laser-based writing, which consists of a laser beam, a substrate, and a focusing system, cells are confined in a laser beam and deposited in a steady stream on nonabsorbing surfaces, including biological gels. As such, cells can be printed continuously and accurately without causing significant cell death. Laser-based writing can pattern cells with high resolution up to the micrometer scale and is advantageous over other bioprinting techniques as it

can be used with many materials and does not directly bring the live cells into contact with the substrate, improving cell survival.[362] This technique has been used to produce vascular networks with micrometer precision on biological gels in vitro.[12,360] However, the major drawback of laser-based writing is the slow printing speeds, making this process highly unsuitable for larger tissues or organ printing.[362] In inkjet printing, which consists of a reservoir tank, an orifice, and a print head, a pressure is created in the tank, which pushes the ink in the orifice and out to the printer head.[363] As a result, cell droplets are deposited on a surface, which provides the advantage of limiting contact of cells and materials on a surface. Other advantages of inkjet printing include controllable resolution, high printing speed, and relatively low material costs. However, inkjet printing is limited by low spatial resolution and cell perturbation as droplets are created through either thermal or mechanical means, which may affect cellular parameters. To form the actual tissue, crosslinking with potentially cytotoxic factors must be used, limiting the application to relatively low cell density and complexity. Finally, in extrusion printing, cells and materials are printed in a line-by-line fashion, representing an efficient and low cost method for cell seeding or encapsulation.[364] Extrusion printing allows for creation of large constructs; however, it has limited spatial resolution and requires a high viscosity for the biomaterial suspension. The incorporation of shear-thinning materials and temperature-dependent properties are emerging as potential solutions to improve resolution and the incorporation of a wide range of biomaterials used, though it is still a work in progress.

5.7. Electrospinning

Electrospinning utilizes electrostatic forces to make polymeric fibers.[362] The technique involves utilizing a high voltage source to induce charge into a polymer solution, which is injected through a capillary and then collected on a substrate with the opposite polarity (Figure 3A).[327,362] Processing parameters in an electrospinning apparatus can be adjusted to form fibers on micro- and nanometer scales. Electrospinning is useful for controlling fiber orientation and porosity/pore size, important for cell alignment and infiltration/migration.[365] Various processing and solution parameters can be adjusted for each specific application, providing an optimal combination of biomimetic and mechanical properties for tissue specific applications.[365] In addition, the high scaffold surface area produced by electrospinning is ideal for modification, such as the incorporation of bioactive molecules. However, one of the major disadvantages of electrospinning is the formation of small pore sizes, which limits the construction of 3D scaffolds in which cells can migrate or infiltrate into the scaffold, which is particularly relevant for ECs and creating vascularized tissues.[365] The number of polymers used in electrospinning is limited as well, in addition to the ability to control the structure and performance of nanofibers.[365] Finally, it remains a challenge to fabricate nanofibers with diameters less than 10 nm via electrospinning.[365]

6. Sensory Systems in Organ-On-A-Chip Platforms

With advances in the development of OOC platforms, it becomes important to develop an integrated sensor to monitor performance of tissues as well as extracellular environment in real time. There has been an effort to integrate sensors into OOC devices to monitor cell culture environment.[366] Most of the integrated sensors in OOC platforms are comprised of three components: (1) a detector element where analytes bind, (2) a transducing component that converts binding events to output signals, and (3) a signal processing device, which amplifies and converts output signals into appropriate reading.[38] Seamless integration of these components remains limited due to challenges in sample preparation, biocompatibility, and system integration. Additionally, tissues on OOC platforms are maintained in cell culture for several days or weeks, and many sensing components may suffer from biofouling and inconsistent functional reading. In this section, we give a fundamental introduction to existing OOC-based sensors. Among many available methods, optical and electrical methods are more popular due to their sensitivity, scalability, and miniaturization capabilities.

6.1. Optical Sensors

There has been an effort in the integration of optical sensors with OOC systems as they can be easily miniaturized, are highly sensitive, and exhibit near negligible consumption of analytes. In addition, optical sensors are less vulnerable to electrical or electrochemical interference caused by bioactive species in cell culture media. Optical detection methods cover a broad spectrum of sensing techniques, but most OOC optical sensors can be divided into three categories: absorbance,[367–369] fluorescence-intensity,[370–372] and surface plasmon based sensors[373,374] as described below.

Among the optical sensors, the simplest optical sensing technique is absorbance, in which the analyte concentration is correlated to light absorbance of a specific wavelength before and after the light passes through a sample.[367] At present, there are only a few examples of absorbance-based sensors in OOC platforms, which detect pH,[375] glucose,[368] Nicotinamide adenine dinucleotide,[368] and 6-hydroxydopamine.[369] A major limitation of this technique is decrease in sensitivity caused by the reduction of the optical length through the sample as described by the Beer–Lambert law. Additionally, background fluorescence often limits accurate absorbance measurement, as some components of culture media or scaffolds are a significant source of autofluorescence.[376] Therefore, most OOC optical sensors utilize optical fluorescence-intensity based schemes to measure analyte concentration.

Whereas some analytes are optically active, other analytes often use fluorescent or luminescent labels as a transducing element. Intensity-based measurement is particularly attractive for microfluidic cell culture as it has inherent compatibility with standard fluorescent microscopy and measurement methods are relatively straightforward. Intensity-based sensors typically require a suitable excitation source such as lamp-based excitation systems or lasers, filters to remove any extraneous lights,

and a photodetector to image emitted light from the sensor area. For analysis of small molecules, the fluorescent probe needs to be encapsulated in a host matrix such as polymer, silica, or sol–gel to prevent the interaction of probes with cells or proteins in the culture media, as well as to provide a constant barrier from other potential interferences. In the case of macromolecule detection, analysis is usually conducted through the formation of an antibody/antigen sandwich structure. However, because fluorescent intensity based sensor is generally used as a "yes" or "no" characterization rather than quantitative analysis, reverse luminescent quenching scheme is often used to address this concern. Currently, most luminescent-based sensors that have been integrated into OOC systems aim to monitor dissolved gases,[377,378] glucose,[379] and pH,[371,377] while sensing of other biomolecules is under development (e.g., cardiac markers).[380] For more detailed working principles and fabrications strategies, Grist et al.,[372] McDonagh et al.,[381] and Pfeiffer and Nagl[382] have published excellent reviews of integrating fluorescent/luminescent chemical sensors on microfluidic platforms. Other reviews have also covered selection strategies for fluorescent probes and host materials for oxygen,[372,383,384] pH,[385] and temperature.[386] However, intensity-based sensing has several disadvantages that can impact its reliability; susceptibility to photobleaching, intensity variation caused by inhomogeneous sensor layer thickness or illumination, dependence on detection optics, background fluorescence, and potential optical crosstalk for multisensory systems.

A tremendous effort has been invested to improve on the disadvantages of intensity-based sensing. Current trends suggest a movement from an "off-chip approach" to "on-chip approach," in which a wide range of optoelectronic technologies, such as waveguides, photodiodes, light emitting diodes, and fiber optics are directly coupled with microfluidic devices to minimize the number of optical components in OOC and increase its sensitivity.[387] Additionally, these miniaturized optical components can be easily integrated in microfluidic devices, making them as promising tools for chemical and biological sensing in OOC platforms.[388] Alternatively, analyte concentration can be monitored by fluorescent lifetime, in which the average time a luminophore remains in the excited state post excitation is measured.[389] Lifetime-based sensors are far superior and more robust when compared to intensity-based optical measurement as they yield improved contrast and suppression of background signals.[390] Attention is also paid to ratiometric Förster resonance energy transfer-based sensors.[391] This method uses the intensity ratio of an analyte sensitive fluorescent probe and reference probe to measure the analyte concentration. This method has utility in most of laboratory settings, and ratiometric measurement is independent of detection optics.[392]

Sensor technologies have also investigated the incorporation of NPs containing fluorescent indicator into host matrix.[383,393] The host matrix can be tuned using NPs, which are only permeable to target molecules and biocompatible matrix to minimize leaching of the probes. Utilizing NPs, dual or multisensory systems can be developed as they can act as a barrier to prevent crossing of two fluorescence signals. Therefore, OOC platforms with multisensory capability can be realized. Most examples of dual sensor platforms contain one oxygen sensor combined with a probe for another analyte, such as carbon dioxide,[394] pH,[395] and temperature.[396] Recently, chemiluminescents have generated much attention for analyte detection, as light is generated when they react with the analyte of interest. They eliminate the need for an external light source and emission filters, thus minimizing the background interference. Chemiluminescence-based sensing devices have successfully detected various analytes, such as tumor markers and other biological targets.[397] However, the drawback of this detection is the limited number of available chemiluminescent reagents.

Another light property that has been explored is surface plasmon resonance (SPR).[398] SPR is a surface sensitive approach that uses the excitation light coupled with a thin metallic surface, which is functionalized with probe molecules such as antibodies and aptamers. When photon energy matches that of the surface plasmon, the incident light energy is transferred into the surface plasmon. The SPR energy depends on the refractive index of the medium around the metal film, allowing the determination of analyte concentration from the shift in wavelength or resonance angle with binding of probe molecules and analyte molecules.[399] Recently developed miniaturized SPR platform for biosensing has applications in protein detection,[400] cancer marker detection,[373] and cell–matrix adhesion dynamics.[374]

6.2. Electrochemical Sensors

Electrochemical sensors have attracted wide attention in quantification of biological samples as the electrochemical measurements are based on the direct conversion of a biological event to an electrical signal. Electrochemical sensors are often comprised of three electrodes: a counter electrode, a reference electrode, and a working electrode. The reference electrode, commonly made of Ag/AgCl, maintains accurate potential to serve as a measurement reference for other electrodes. The working electrode is the transduction element in the biological reaction, where the redox reaction of interest occurs. In conjunction with a working electrode, the counter electrode is used to apply current to the working electrode through an electrolytic solution. The performance and sensitivity of electrodes in OOC can be affected by variety of parameters including electrode position,[401] electrode size,[402] biofouling,[403] and flow rate.[401] Therefore, the care needs to be taken in the placement of electrodes and materials.

Real-time monitoring of analyte concentration using an electrochemical method can be categorized based on the nature of its interaction with the target molecules. The most common strategy to measure analyte concentration is an affinity mechanism, in which binding between biorecognition element and analyte is measured. A biorecognition element can be immobilized on the electrode surfaces by covalent attachment, physical adsorption, or encapsulation in redox-active polymer layers or in sol–gel. Other reviews have discussed working principles and immobilization strategies for biorecognition elements including immunosensors,[380,404] nucleic biosensors,[405] and aptamer based biosensors.[406] Electrochemical biosensors also include catalytic biosensors, which are generally enzymatic based and form enzyme-linked immunosorbent assay-like sandwich setup where the secondary antibody is labeled with

redox initiating molecule. Binding of an analyte to the enzyme causes electron transfer across the double layer, which catalyzes a measurable reading. The analyte concentration can be obtained based on the number of electrons produced in the redox process by measuring the current.

The operating principle of electrochemical-based biosensors can be divided into three categories: amperometric, potentiometric, and conductometric measurements.[407] Amperometric sensors measure the current produced at the working electrode because of a redox reaction on the electrode surface, while a constant potential is applied between working electrode and counter electrode.[408,409] If a current is examined while electric potential changes with time, it is referred to as voltammetry. Potentiometric devices can be used to determine the analyte concentration based on the accumulation of a charge between working and the reference electrode when no voltage is present in an electrochemical cell.[405,409] These are most commonly integrated as ion sensitive field effect transistor devices to measure pH in solution.[410] In a recent example, a gate electrode was replaced with biochemically sensitive surface, and catalytic reactions affect accumulated charge carriers at the gate surface in proportion to the analyte concentration. In conductometric biosensors, binding of analyte molecule on a biorecognition element causes a change in impedance at the sensor surface, and the concentration of analyte can be determined based on the change in resistance or capacitance.

There has been an extensive effort to integrate electrochemical sensors in the OOC space, but only a handful utilize integrated electrochemical sensors to monitor dynamic changes in drug screening platforms, and even fewer have been presented that utilize parallel sensor arrays. Krommenhoek et al. developed a microchip to measure pH, temperature, and dissolved oxygen in yeast culture,[411] which could be easily translated into tissue models. Many methods have been also used to detect cell secretion molecules, including interleukin-6 (IL-6),[412] interferon-γ, tumor necrosis factor-α (TNF-α),[413] and transforming growth factor-β.[414] Numerous innovative strategies using nanotechnology[415] and magnetic beads[416] have opened new avenue for highly sensitive analyte detection. For example, Riahi et al. developed an automated microfluidic-based immunosensor to monitor biomarker secretions (transferrin and albumin) from primary hepatocyte spheroids.[417] Nanowires can be coupled with field effect transistors by linking a biorecognition element to their surface, generating a change in conductance with analyte binding. Utilizing this method, nanowire device arrays can be fabricated for multisensory, real-time sensing of biological species.[418]

Furthermore, electrochemical-based sensor technique integration into OOC platforms has been extended to transepithelial electrical resistance (TEER) sensors. TEER is a nondestructive, real-time, and label-free method to measure the integrity of tissue junction dynamics of endothelial and epithelial cells by monitoring Ohmic resistance or measuring impedance at a wide range of frequencies.[419] Impedance measurements can be used as a noninvasive method to quantify cell migration and proliferation, hallmarks of malignant tumor progression.[420]

Finally, there has been a significant research into measurement of cell electrophysiology in OOC platforms using neurons, CMs, muscle fibers, and pancreatic beta cells. Traditionally, the gold standard for studying ion channel activities is to use a patch clamping technique. However, conventional patch clamping technique using glass micropipettes is labor intensive, and the cellular components may lose their key biological activities due to the dilution of intracellular fluid with solution inside the recording electrode.[421] Most recently, Tian et al. and Feiner et al. demonstrated the concept of noninvasive coupling of nanoelectronics with tissue constructs to monitor extracellular electrical potential within their CMs to known drugs.[303,422]

7. Current Organ-On-A-Chip Platforms

7.1. Liver

The functional unit of the liver is the hepatic lobule. It is comprised of sinusoids and blood vessels lined with ECs. Hepatocytes and parenchymal liver cells form plate-like structures that surround these features. The microarchitecture of the liver is crucial to liver function.[423] Hepatocytes interact with mesenchymal cells, stellate cells, Küpffer cells, macrophages, and lymphocytes.[424] The liver can be considered one of the most critical organs on which to test new pharmaceuticals because it is involved in many metabolic and detoxification processes, and toxicity of the liver is often the cause of drug rejection.

A main feature of the liver is the perfusion of fluid. When compared to conventional cell culture, liver function can be enhanced in a microfluidic chip.[425] For instance, the creation of a perfusable liver biochip led to greater expression of key enzymes responsible for metabolism in liver cells when compared to growing these cells in plate cultures. An early design for liver-on-chip, developed by Powers et al., involved a silicon sheet scaffold with an array of channels and a microporous filter between them.[148] Upper and lower chambers, through which culture medium flowed, surrounded the scaffold. The fluid flow through the tissue in an individual channel was designed to mimic a single capillary bed. Spheroids of hepatocytes and nonparenchymal cells were used in the device.

Another system consisted of a PDMS microbioreactor with a perfusion circuit and a PDMS or polyester membrane that acted as a scaffold for cells.[149] The cellular aggregates demonstrated liver specific functions of albumin secretion and ammonium removal. One of the first commercially available liver-on-chip systems was the LiverChip.[150] This system used a pneumatic diaphragm micropump to regulate flow rates and shear forces, below a culture plate with wells. Each well, filled with cell culture medium, also contained a polystyrene or polycarbonate scaffold coated with collagen and placed on a PVDF filter and filter support. Hepatocytes or cocultures of hepatocytes and nonparenchymal cells were seeded on the scaffold and liver-specific functions were demonstrated.

There are other aspects of the liver besides parenchymal hepatocytes that have been mimicked, including the sinusoidal space and EC barrier.[151] Primary rat and human hepatocytes were used in the system and hepatotoxicity was tested using a liver toxicant. Another microfluidic chip system used DEP to assemble cells into structures resembling liver sinusoids.[157] Cell culture chambers were designed with integrated

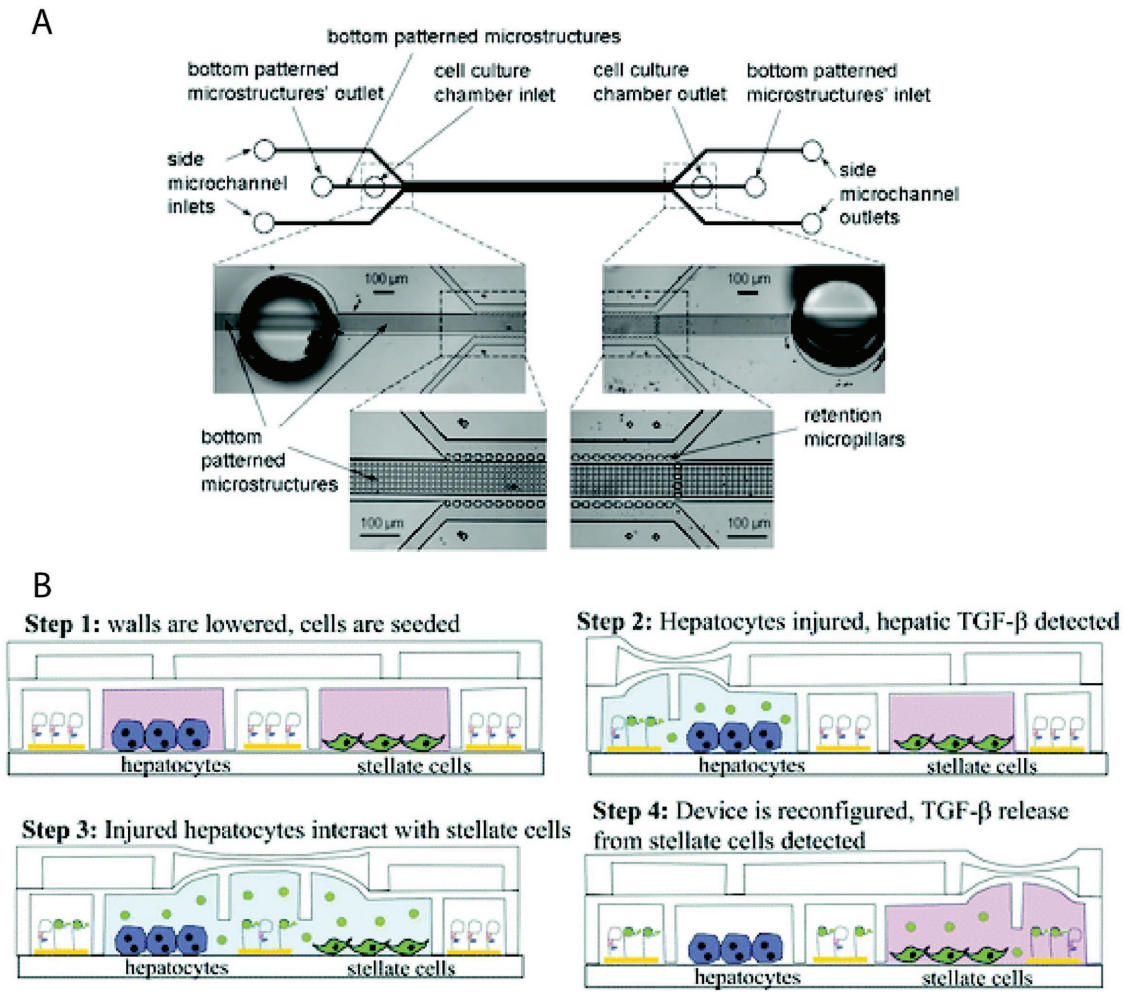

Figure 6. Liver-on-a-chip models. A) Perfusion-based microfluidic device for culture and study of hepatocytes, with two side microchannels separated by micropillars.[158] Reproduced with permission.[158] Copyright 2010, Royal Society of Chemistry. B) Liver-on-a-chip device with pneumatic operation uses two device layers to break up the communication between hepatocytes and stellate cells. (Step 1) Valves may be closed to allow for precoating and cell seeding. (Step 2) Unique culture media may be infused into hepatocyte chamber. (Step 3) Middle barrier may be raised to allow for communication between hepatocytes and stellate cells. (Step 4) Middle barrier may be closed again during monitoring.[166] Reproduced with permission.[166] Copyright 2015, Royal Society of Chemistry.

electrodes, and perfusion of culture media and test compounds occurred through the chambers.

Replication of the lobular structure of the liver has also been attempted. Ho et al. developed a system to mimic the hepatic lobule.[153] In other work, an extended bile canalicular structure was formed through the use of a PDMS device comprised of microfluidic channels (**Figure 6**A).[158] The formation of gap junctions was demonstrated, which promoted cell–cell interactions. Other approaches to create liver tissue aggregates include the use of nanofiber scaffolds to direct cell adhesion and migration.[152]

Coculture with cells other than hepatocytes is useful in the development of specific liver tissue. Coculture with fibroblasts is a widely used approach as well to enhance hepatocyte activity that results from cell–cell interactions. Kane et al. demonstrated rat hepatocytes in a coculture with 3T3-J2 fibroblasts under medium and oxygen perfusion in a microfluidic array.[155] In the work by Khetani and Bhatia, hepatocytes and 3T3 fibroblasts were seeded on micropatterned collagen in 24-well plates.[159] Another approach used a novel culture method and micropatterning technique to construct layered hepatocytes on fibroblast feeder layers.[156] Liver-specific functions of the hepatocytes, including intracellular albumin staining and albumin secretion, urea synthesis, and glycogen storage were enhanced as a result of increased heterotypic contact in the coculture system. Other platforms have reported improved hepatic function compared to hepatocytes alone, using coculture models of hepatoctyes with ECs,[154] with hepatic stellate cells (HSCs),[160] and both HSCs and ECs.[162] To investigate the paracrine effects of HSCs on hepatocytes, Lee et al. cultured hepatocytes and HSCs in a chip wherein the cell–cell contact was restricted.[161] They found the HSCs helped maintain hepatocyte spheroids and improved liver-specific functions.

Recently, several models have been developed that can be maintained over long term. Kang et al. developed a primary liver cell culture system with a coculture of hepatocytes and

ECs in both single and dual microchannel configurations, both with and without continuous perfusion.[163] The system was able to support the cell culture for at least 30 days. Another liver sinusoid model was developed using two microfluidic chambers separated by a porous membrane that could be maintained for 28 days.[164] Liver-on-chip systems that remain accurate over the long term could provide beneficial information on tissue responses to various molecules and conditions over time scales that are clinically relevant.

Furthermore, some disease or injury states have also been tested. Kang et al. used their system to analyze viral replication for hepatotropic hepatitis B virus.[165] Zhou et al. developed a system to model alcohol injury.[166] Their liver injury-on-a-chip system was made up of two chambers for seeding of hepatocytes and stellate cells, and three more chambers for miniature aptamer-modified electrodes to monitor liver cell signaling (Figure 6B). This system enabled the monitoring of paracrine crosstalk of a signaling molecule, transforming growth factor beta (TGF-β), which was secreted as a result of alcohol injury.

7.2. Skin

Skin is composed of epidermis (mainly formed with keratinocytes), dermis (mostly composed of fibroblasts, macrophages, and adipocytes), and hypodermis layers from outermost toward innermost, respectively.[426] Skin-equivalent models have existed for more than three decades.[427] Lack of vascularization and incapability for long-term culture remained a large barrier for drug testing and disease modeling.[428] Overcoming this problem, microfluidic-based platforms have been developed that incorporate previously engineered skin models to better simulate skin function in vitro.[429]

Identifying a suitable cell source that resembles the natural skin is a critical decision for developing a skin-on-chip platform. In addition, this source should be widely accessible, reproducible, and cost effective. Skin equivalent models are mainly composed of epidermis and dermis layers.[430] While some researchers utilized commercially available biopsies,[431] others cocultured human immortalized keratinocytes as an epidermis representative and another cell type for human immortalized dermis layer such as fibroblasts[167] or dendritic cells.[169] For instance, a skin-on-a-chip model that simulated inflammation and edema was developed.[36] Human keratinocytes (HaCaT), HS27 fibroblasts, and HUVECs were seeded on the upper, middle, and bottom layers, respectively (**Figure 7**A). Each layer was separated from one another with a polyester membrane. While immortalized human cell lines, human primary cells, and biopsies for skin-on-a-chip models have shown efficacy, iPSCs have emerged as a promising alternative cell source. For instance, functional keratinocytes derived from iPSCs showed similar gene and protein expressions to primary keratinocytes.[432]

In addition to using skin cells, other studies have utilized models incorporating vascularization and flow. Skin-on-a-chip platforms include continuous,[169] pulsatile,[168] and gravity flows.[36,170] Handling and operating gravity driven flow is simpler than pump driven flow; however, the flow rate is changing continually due to alterations in hydrostatic pressure over time. To circumvent this drawback, Abaci et al. reported a pumpless skin-on-a-chip setup (Figure 7B), where they placed the device on rocking platform.[170]

Epidermis layer is among the few tissues that have an air–liquid interface (ALI), in contrast with a liquid–liquid interface (LLI). A majority of studies applied LLI for in vitro research, while there are some studies that modeled ALI.[167] Ramadan and Ting developed a microfluidic human skin platform to model the epidermis and dermis layers. They applied both ALI and LLI conditions in their platform (Figure 7C).[169]

Disease modeling is one of the main targets of OOC platforms. There are numerous skin diseases including cancer, psoriasis, acne inflammation, and edema.[429] For instance, Wufuer et al. developed a microfluidic skin model for simulating inflammation and edema. They showed a dose-dependent increase in proinflammatory factors (IL-1β, IL-6, and IL-8) and mRNA expression levels with TNF-α. They tested Dex as a widely known drug for inflammation as a proof of concept and found that increasing Dex dose from 100×10^{-9} M to 10×10^{-6} M showed noticeable decrease in proinflammatory factors, revealing alleviation of inflammation (Figure 7D).[36] In another study, researchers utilized skin-on-a-chip platform to indicate toxic effects of doxorubicin on keratinocyte differentiation and proliferation.[170]

7.3. Vascular

The function of the vasculature is to transport blood and nutrients throughout the body. The human vasculature is made up of arterioles, arteries, venules, veins, and capillaries. ECs and vascular smooth muscle cells comprise the human vasculature, with ECs lining the vessel lumen. Developing tissue systems that mimic specific vascular networks is challenging because flow exerts transmural pressure, pulsatile wall shear stress, and cyclic mechanical stretching to cells.[433]

The use of microfluidic systems to mimic vascular structures is an intuitive approach because fluid flow at the scale of microvasculature can be replicated. Studying the transport and effects of drug molecules on vasculature is of particular importance because in order to reach the target tissue, they must travel through vascular networks and pass through the endothelial barrier. Furthermore, when developing multi-organ-on-chip models, incorporating the connecting vasculature becomes critical.

The effect of particles, such as drug carriers on the vascular system has been investigated in basic microfluidic systems. A microfluidic PDMS system was used to study the localization of microspheres and NPs in the blood using a monolayer of HUVECs.[174] The particles were composed of polystyrene and conjugated with ligands. It was found that microspheres of 2 µm better localized and adhered to the vessel wall compared to nanospheres. Kim et al. demonstrated the effect of NP dose on platelet adhesion and aggregation.[172] Using synthetic microvascular networks in microchannels, it was also demonstrated that rod-shaped polystyrene NPs have higher specific accumulation compared to spherical ones.[434]

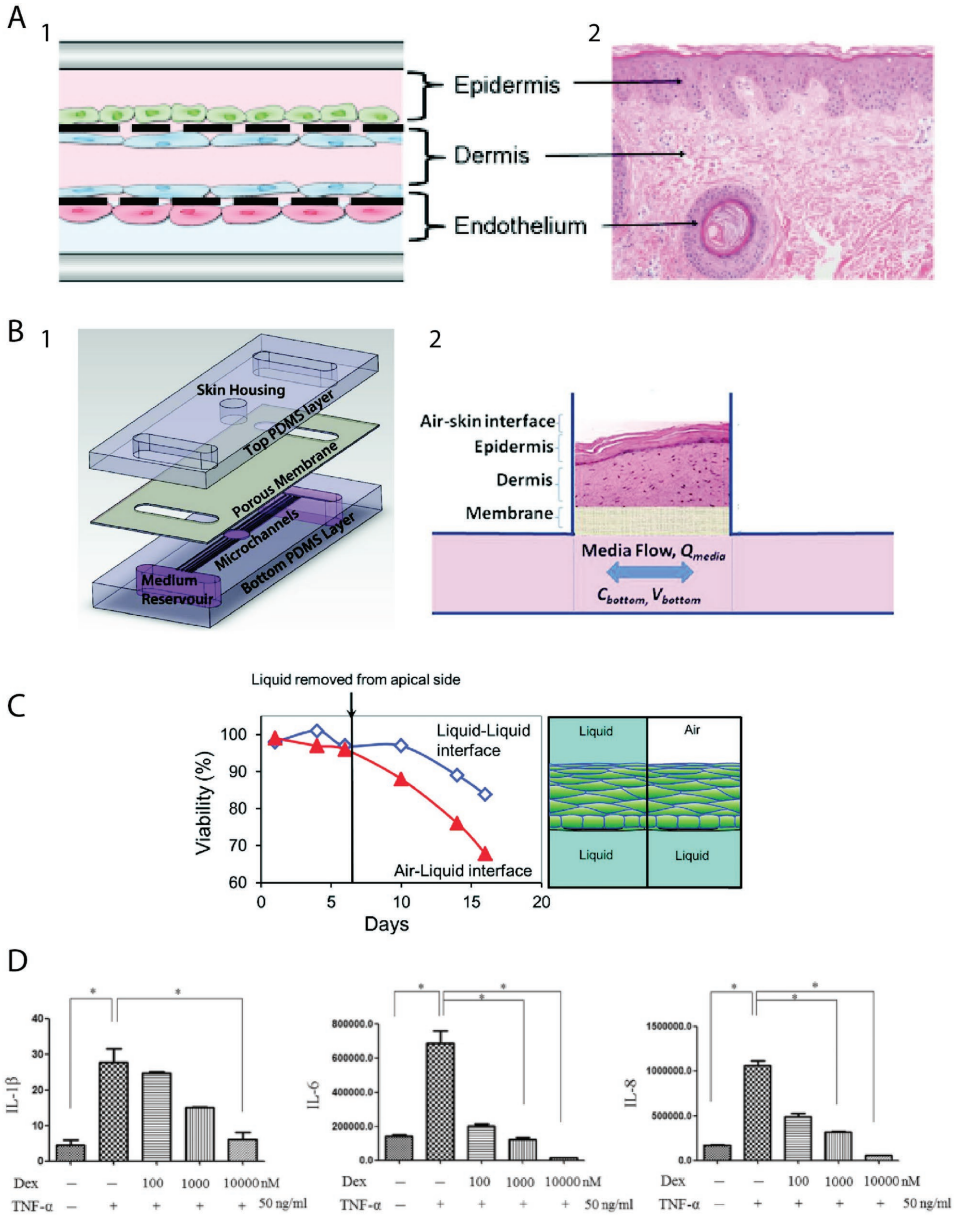

Figure 7. Skin-on-a-chip models. A) (1) Schematic of three layers for skin-on-chip platform made by soft lithography technique. (2) Histological skin showing skin cellular organization stained by hematoxylin and eosin.[36] Reproduced with permission.[36] Copyright 2016, Nature Publishing Group. B) (1) Schematic of pumpless skin-on-chip platform for drug testing application. (2) Schematic side view from skin housing showing a media perfusion.[170] Reproduced with permission.[170] Copyright 2015, Royal Society of Chemistry. C) Comparing ALI and LLI viability over 17 days.[169] Reproduced with permission.[169] Copyright 2016, Royal Society of Chemistry. D) Levels of IL-1β1b, IL-6, and IL-8 released from HUVECs inside culture medium.[36] Reproduced with permission.[36] Copyright 2016, Nature Publishing Group.

Models that mimic shear stress in the vasculature have also been developed. Korin et al. used a PDMS microfluidic system to study shear-activated nanotherapeutics coated with tissue plasminogen activator to break down aggregates in areas of high shear stress and dissolve blood clots.[435] The incorporation of a peristaltic micropump allowed pulsatile shear stress to be modeled in a microchannel system with branching down to 40 µm diameter vessels.[171] Another microfluidic system was able to mimic physiologically relevant flow with uniform or gradient shear stress and assess the accumulation and binding of targeted NPs to a monolayer of HUVECs.[175]

Models that mimic the geometry or structure of vasculature have also been developed. A bifurcating synthetic vascular network was designed and adhesion profile of particles functionalized with various coatings was studied. The particle adhesion was significantly affected by geometric features as well as the particle surface chemistry.[176] Morgan et al. designed a system resulting in fully enclosed, perfusable, endothelialized

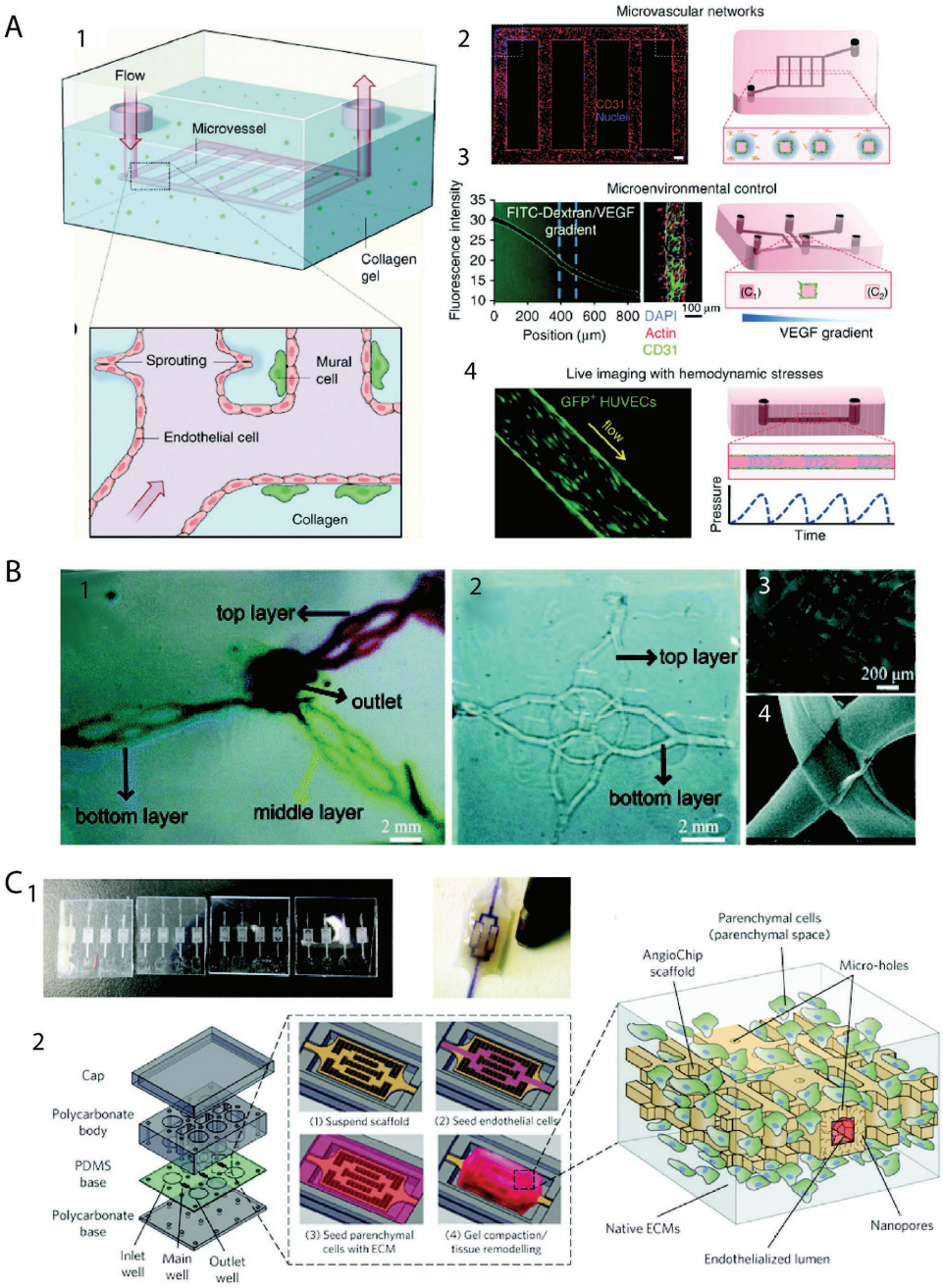

Figure 8. Vasculature-on-a-chip models. A) (1) Schematic of the microfluidic network coated to confluence with endothelial cells within the collagen constructs, pericyte interactions, and concept of angiogenic sprouting from the network. (2) Endothelial cells show viability and confluence. (3) Cell sprouting occurs with the use of biochemical gradients. (4) Effects of hemodynamic forces may also be studied using the microfluidic network system.[177] Reproduced with permission.[177] Copyright 2013, Nature Publishing Group. B) 3D microfluidic networks in gelatin are created with layering techniques. (1) Three layer configuration. (2) Two-layer interconnected configuration, (3) microscope, and (4) SEM images showing junctions between two layers (scale bar, 100 μm).[86] Reproduced with permission.[86] Copyright 2014, Royal Society of Chemistry. C) (1) AngioChip scaffolds patterned on glass slides, compared to the size of a ballpoint pen tip. (2) AngioChips are cultured in a custom bioreactor with separate media compartments to allow for seeding of both vascular cells and parenchymal cells.[35] Reproduced with permission.[35] Copyright 2016, Nature Publishing Group.

microvessels of various geometries in a type I collagen hydrogel (**Figure 8**A).[177]

Multilayer, interconnected 3D vascular networks were formed in hydrogels by using a crosslinked sodium alginate as a sacrificial material.[86] The size and morphology of the channels could be controlled. Furthermore, HUVECs adhered and proliferated to form an endothelial layer lining on the channels; barrier function and response to shear stress were demonstrated (Figure 8B). Kim et al. developed a microfluidic-based platform that modeled natural cellular programs, such as

vasculogenesis and angiogenesis.[173] Cocultures of HUVECs with pericytes, stromal fibroblasts, or cancer cells and a fibrin matrix with type I collagen were used. The ability to grow perfusable microvascular networks with similar architecture, barrier function, and biochemical markers to that of in vivo vasculature was demonstrated. Zhang et al. developed a novel system called AngioChip, which is a perfusable 3D microchannel network scaffold that mimics vascularized tissues.[98] This scaffold was coated with ECs and contained nanopores and microholes as well as an open-vessel lumen (Figure 8C). This system was used to distribute drugs through the vasculature and immediate blood perfusion was established following direct surgical anastomosis to femoral vessels in rats.

Vasculature-on-a-chip systems are useful in modeling and studying disease, as well as testing therapeutics. Microfluidic devices have been used to mimic occlusion and thrombosis in microvasculature.[435,436] Additionally, tumor angiogenesis has been modeled. One study investigated how wall shear stress impacts paracrine signaling associated with angiogenesis in a tumor vascular model[178] and other work used a microfluidic system to create a perfusable vascularized bone-mimicking microenvironment to study breast cancer cell extravasation.[179]

7.4. Cardiac

Cardiac muscle tissue is composed of organized CMs that form the myocardium. CMs contain bundles of myofibrils that are made up of proteins in repeating units called sarcomeres – the functional contractile unit of myocytes. Pacemaker cells produce the electrical signals to stimulate CMs and their contractile function occurs via mechanical, chemical, and electrical stimuli.[437] Cardiac tissue is also comprised of fibroblasts. Furthermore, microvessels exist throughout the heart tissue and these are comprised of ECs and vascular smooth muscle cells.

There is a high demand for new drugs to prevent or treat cardiovascular diseases (CVDs), which are the leading cause of death globally,[438] but drug development for CVDs is hindered by the lack of adequate models. Additionally, many drugs for treatment of other organs have adverse side effects on cardiac tissue,[439] and these drugs should be tested on cardiac tissue models.

Topographical and electrical cues can be used to achieve alignment and maturation of CMs in engineered cardiac tissues. Au et al. used polystyrene chips with microgrooves to align neonatal rat CMs.[440] With the application of electrical stimulation, maturation and elongation of CMs increased and gap junctions formed. A chip design using MTF technology was developed to model cardiac tissue.[180] For arrangement of CMs into an anisotropically organized layer, microcontact printing of fibronectin on PDMS films was performed. AP propagation and contractility of the MTFs were measured. This system could be used to evaluate effect of different drugs on contractile function of cardiac tissues. A similar system using MTF technology incorporated temperature control, electrical field stimulation through the use of electrodes, and a transparent top, which allowed analysis of contraction by optical measurement of cantilever deflection.[181] The system included a channel with fluidic control to allow washout after each drug dosage. Conductive NPs have also been integrated into biomaterials for cardiac TE,[97,441] and these materials may be beneficial for incorporation into heart-on-chip platforms. Furthermore, cutting-edge technologies, such as 3D printing have been developed to make multiple engineered cardiac tissues on a chip for drug testing applications in a high-throughput manner. For instance, Lind et al. designed a cardiac tissue platform for drug testing that was entirely 3D printed using various functional inks (**Figure 9**A).[182]

Several systems incorporate aspects of perfusion or vasculature into cardiac tissue. For example, Xiao et al. designed a microfabricated bioreactor to create perfusable 3D microtissues called Biowire (Figure 9B).[59] Biowires were created using a polytetrafluoroethylene (PTFE) tubing template, seeded with neonatal rat CMs and human ESC derived CMs that elongated and aligned along the tubing. This system was able to test pharmacological agents by perfusion through the lumen of the PTFE tubing. Mathur et al. developed a microphysiological system with aligned human iPSC-derived cardiac cells that included perfusion to mimic the human vasculature.[184] They tested the effects of two pharmacological chemicals and two clinically used drugs on beating rates of tissues, which were found to be in agreement with clinical observations.

Another highly important use of heart-on-a-chip models is disease modeling. McCain et al. used an MTF platform to test mechanical overload of cardiac tissue, which is caused by hypertension and can lead to hypertrophy and fibrosis in the body.[442] Mechanical cyclic stress was applied to the MTFs and changes in gene expression, myocyte architecture, and functional responses were tested. Results from this work indicated that this model effectively mimics the failing myocardium and its microenvironment. Another cardiac disease model was developed to mimic hypoxia-induced myocardial injury (Figure 9C).[183] It was comprised of a microfluidic device to mimic the interface between blood vessels and cardiac tissue. Hypoxia was created using a specific oxygen consumption blocking agent carbonyl cyanide *p*-trifluoromethoxyphenylhydrazone into channels. The hypoxic conditions resulted in morphological changes including cell shrinkage, cytoskeleton disintegration, loss of mitochondrial membrane potential, and signs of apoptosis. Finally, Wang et al. developed a model of Barth syndrome (BTHS) that used iPSCs from patients with the disease and differentiated them into patient specific iPSC-derived CMs.[185] These cells were seeded on an MTF platform and the pathophysiology of BTHS, including reduced contractile performance, was observed.

7.5. Skeletal Muscle

Skeletal muscle belongs to the group of striated muscle tissues, which are composed of long, thin, multinucleated structures called myotubes bundled together to form fibers. The myotube is comprised of several components including the plasma membrane, the cytoplasm filled by myofibrils, and multiple nuclei. Myofibrils are made up of myosin and actin proteins, which make up repeating units called sarcomeres. These are highly aligned, and sarcomeres in different myofibrils are also aligned with each other, achieving the striated appearance of

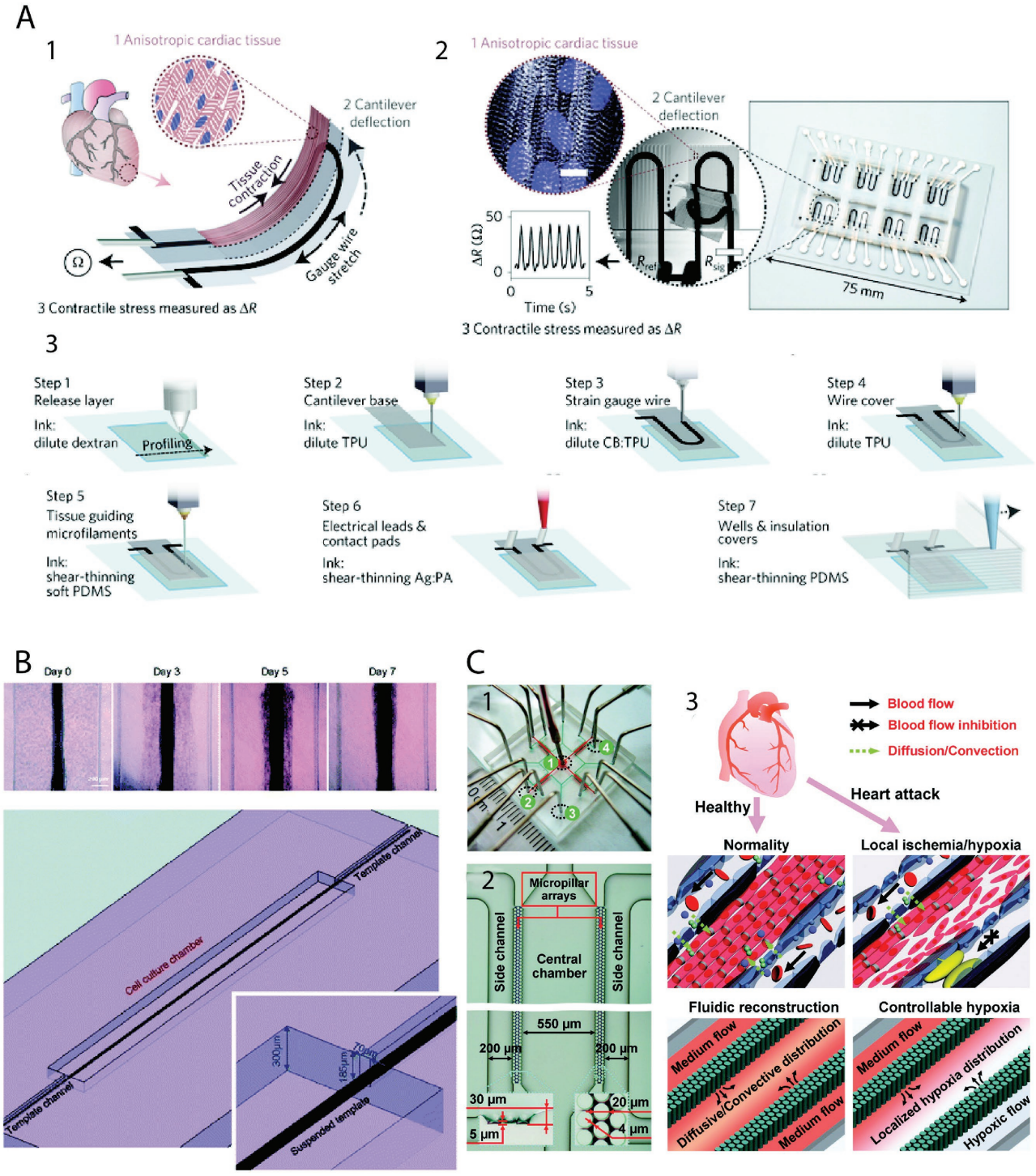

Figure 9. Cardiac-on-a-chip models. A) Multimaterial 3D-printed cardiac microphysiological device with functional readout of cardiac contractility. (1) Cardiac tissue contraction causes cantilever deflection that may be read as a resistance change proportional to the contractile stress of the tissue. (2) Schematic of the fully printed device, showing confocal microscopy image of immunostained cardiac tissue on the cantilever. (3) Automated printing of the device shown through seven steps.[182] Reproduced with permission.[182] Copyright 2016, Nature Publishing Group. B) CMs seeded in a custom bioreactor remodel the surrounding gel as they compact around the suture to form cardiac Biowires.[59] Reproduced with permission.[59] Copyright 2014, Royal Society of Chemistry. C) Microfluidic device for cardiac cell culture. (1) Device with four ports: 1 - central inlet, 2 - central outlet, 3 - side inlet, 4 - side outlet. (2) Microfluidic device uses micropillar arrays to create an interface between blood vessel and myocardial tissue. (3) Schematic shows how the microfluidic device may be used to study various microenvironmental states.[183] Reproduced with permission.[183] Copyright 2013, American Chemical Society.

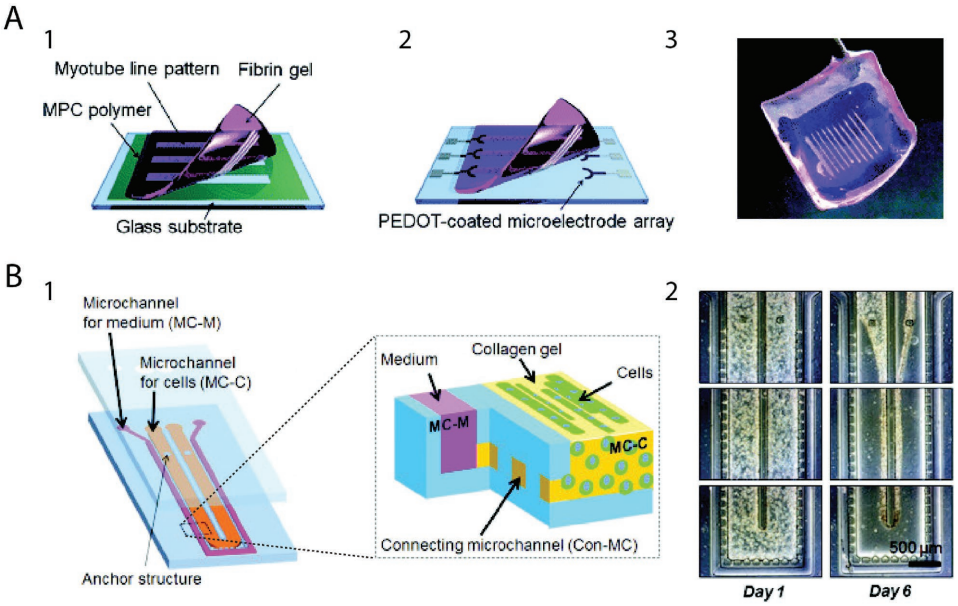

Figure 10. Skeletal muscle-on-a-chip models. A) Illustration of the myotube/fibrin gel sheet. (1) Myotubes are transferred from a glass substrate to fibrin gel. (2) The myotube/fibrin gel gets attached to the poly(3,4-ethylenedioxythiophene) microelectrode array chip. (3) Image of the fibrin gel with myotube pattern shown.[77] Reproduced with permission.[77] Copyright 2011, Royal Society of Chemistry. B) (1) Schematic of the microfluidic device for skeletal muscle microtissue culture. Microchannel for cells (MC-C), microchannel for medium (MC-M), connecting microchannels (Con-MCs). (2) Brightfield images show skeletal muscle microtissues in microchannel after 1 and 6 days of cultivation.[61] Reproduced with permission.[61] Copyright 2015, Elsevier.

skeletal muscle. The overlapping of myosin and actin filaments occurs during muscle contraction.[443] Myoblasts are the cells that differentiate into myotubes. C2C12, a mouse myoblast cell line, is commonly used to form contractile myotubes in skeletal-muscle-on-a-chip platforms.

One of the main features of the native skeletal muscle tissues is the alignment of muscle fibers. Specific topographical features act as a cue to control skeletal muscle cellular differentiation and alignment.[444] Alignment of skeletal myoblasts and myotubes has been achieved using microfibers,[445] nanofibers,[446] nanowhiskers,[447] microgrooves,[448] and microcantilevers.[449] Moreover, PDMS substrates were micropatterned with wavy features, to produce aligned myoblasts and myotubes.[450] Hume et al. demonstrated that although large topographical features do not facilitate skeletal muscle cell alignment well in two dimensions, they are able to do so in 3D,[451] highlighting the potential differences of topographical cues when moving from 2D to 3D models.

Surface patterning of cell repellant or adhesive molecules has been used to direct myoblast alignment. For instance, Nagamine et al. used this technique to obtain line-patterned myotubes in fibrin gel[452] and Huang et al. did so by transferring aligned myotubes into a type I collagen gel.[453] Another technique to achieve alignment of skeletal muscle cells involves the use of mechanical stimulation, and myotubes can be aligned parallel to the direction of continuous uniaxial strain.[454] Finally, electrical force[95,455] and magnetic fields[456] have also been used to achieve aligned myotubes.

Another important feature to mimic the native skeletal muscle is muscle contractility. It can be accomplished using electrical stimulation. Nagamine et al. stimulated myotubes using microelectrode arrays and controlled the contractile behavior of myotubes (**Figure 10**A).[77] Kaji et al. also controlled myotube contractility using electrodes placed above and below the cells on a PDMS layer.[186] Additionally, Shimizu et al. developed a microfluidic device to construct 3D skeletal muscle tissue in microchannels that is able to contract in response to applied electrical simulation (Figure 10B).[61] Another approach to electrically stimulate muscle cells is to use electrically conductive materials, including CNTs[187] and graphene oxide.[457] Ramón-Azcón et al. demonstrated the use of DEP to produce aligned CNTs in GelMA hydrogels. CNT alignment resulted in higher conductivity of hydrogels. Myoblasts cultured on this material exhibited more differentiation and contraction compared to those cultured on pure GelMA hydrogels and GelMA hydrogels with randomly dispersed CNTs.[188]

Contractility in skeletal muscle is accomplished by the contraction of aligned muscle fibers in response to neurotransmitters binding to acetylcholine receptions at neuromuscular junctions (NMJs). These NMJs, are therefore an important feature of the skeletal muscle and there have been attempts to promote NMJ formation in skeletal muscle tissue constructs. Morimoto et al. constructed aligned muscle fiber bundles using a PDMS stamp to form striped patterns of Matrigel containing muscle cells.[189] They added mouse neural SCs to the muscle fibers and differentiated them into motor neurons to achieve a neuron–muscle construct that could contract in response to neurotransmitter release. Skeletal muscle-on-a-chip platforms have also been used to model disease. Muscular dystrophy was modeled using contractile muscle tissue from dystrophic myoblasts in a 96-microwell plate and used for drug testing.[458]

7.6. Lung

The lung is composed of two zones: the conducting zone where the air enters and passes through pharynx, larynx, trachea, primary bronchi, bronchioles, and terminal bronchioles; and the respiratory zone (gas exchange zone), which includes alveolar ducts, bronchioles, and alveolar sacs. The alveoli provide a large surface area for gas exchange, which is the main function of the lung. The most basic unit of the lung is a layer of epithelial and ECs through which gas exchange between air and blood occurs. The epithelial layer faces the air and the endothelial layer faces the blood and the geometry of this layer is not particularly complex. Development of accurate in vitro lung tissue constructs is critical to study the effects of drugs, toxins, and pathogens that may enter through airways. Not only is it important for drug administration, but also for the study of infectious diseases or occupational pathology.

A main feature of the lung is its unique mechanical forces. A periodic mechanical force is exerted with each respiratory cycle, and this dynamic mechanical force makes the lung a challenging system to recreate in vitro. One of the most influential lung-on-a-chip models was introduced in Huh et al.[192] This work used a flexible PDMS membrane to act as an interface between human alveolar epithelial cells and human pulmonary microvascular ECs (**Figure 11**). This structure mimicked the alveolar–capillary interface. The lining of the alveolar air space was also mimicked with compartmentalized channels through which air and liquid could flow separately, creating an ALI. In this model, cyclic stretch was incorporated to mimic the effects of breathing on the alveolar epithelium and endothelium. Through this model, cellular immune response to pulmonary infection as well as response to NPs was tested. It was found that cyclic stretch affected experimental data, which reiterate the importance of having a physiologically relevant model for testing disease conditions and drugs.

A microfabricated alveolar model was developed by Douville et al. that recreated the solid mechanical stresses and surface-tension stresses, both independently and in combination.[190] Alveolar epithelial cell damage was studied under conditions similar to mechanical ventilation and cells that experienced a combination of fluid and solid mechanical stresses exhibited more cell death and detachment.

Lung-on-a-chip devices have been used to model specific lung pathologies. A platform was used to model pulmonary edema, which is characterized by an excessive accumulation of intravascular fluid in the alveolar air space and interstitial tissues and can result from treatment using IL-2.[194] Vascular leakage occurred and it resulted from intracellular gaps in the epithelium and endothelium. Furthermore, this work demonstrated that breathing motions increase vascular leakage leading to edema and unlike previous reports, the onset and progression of edema did not require circulating immune cells. The latter work also went on to identify potential new therapeutics for treatment of this disease. Tavana et al. used a

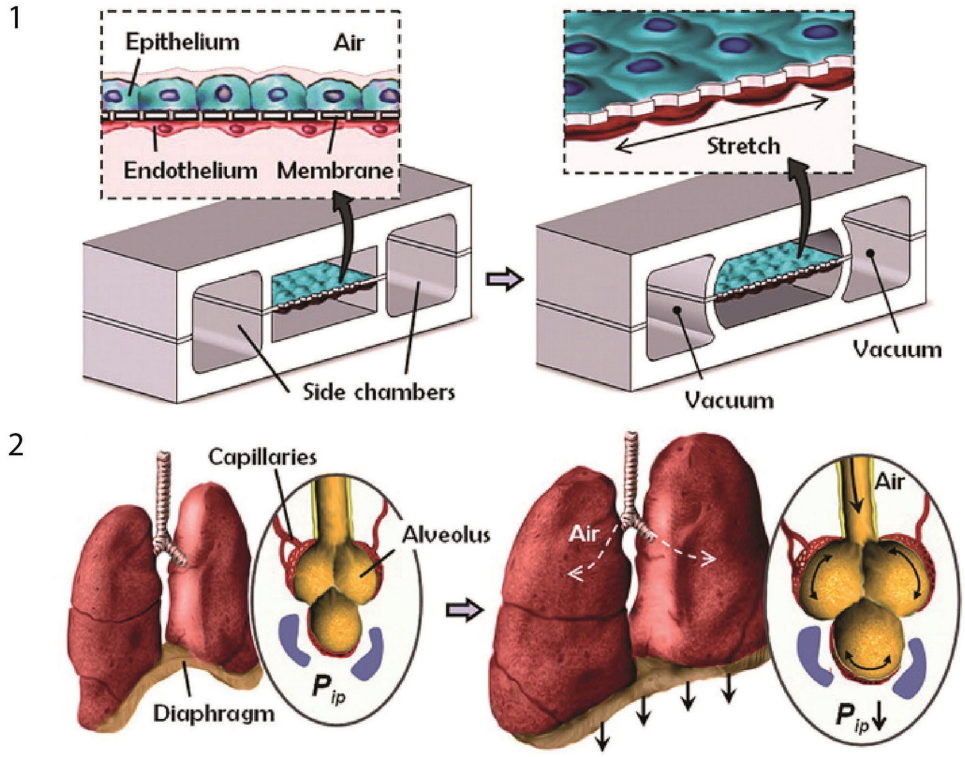

Figure 11. A lung-on-a-chip model. Breathing lung-on-a-chip microdevice. (1) A thin, porous, flexible PDMS membrane sandwiched between two microchannels and coated with the ECM serves as an alveolar–capillary barrier. Cyclic application of vacuum to the side chambers causes stretching of the PDMS membrane, imitating physiological breathing. (2) When the diaphragm contracts in the living lung, reduced intrapleural pressure leads to stretching of the alveolar–capillary interface.[192] Reproduced with permission.[192] Copyright 2010, American Association for the Advancement of Science.

microfluidic model to mimic lung airways and studied the cellular response to liquid plugs, which arise as a result of dysfunction or deficiency of pulmonary surfactant.[193] The propagation of occluding liquid plugs through the airway tubes occurred during airway reopening. They found that surfactant-free liquid plugs create gradients of shear stress and pressure that decrease cell viability and damage epithelium. This model was also used to study the effects of applying a clinically used surfactant. Other work used a microfluidic chip platform to mimic the microenvironment of lung cancer with cancer cell lines and primary cancer cells and tested different chemotherapeutic drugs.[191]

Another recent study mimicked asthma in a "small airway-on-a-chip" model.[195] The model consisted of an upper air channel and a lower fluid flow channel, between which a mucociliary bronchiolar epithelium layer was positioned. Asthma was modeled by exposing the epithelium to IL-13, and chronic obstructive pulmonary disease (COPD) was modeled by lining the airway with COPD epithelial cells and stimulating with viral mimic polyinosinic–polycytidylic acid or lipopolysaccharide endotoxin. With the models of human asthmatic and COPD airways, therapeutics were tested and the chip model recapitulated in vivo responses to a similar therapy.

7.7. Bone and Bone Marrow

Bone marrow refers to the soft, spongy, and flexible tissue found inside flat bones or within cancellous bones in long bones. This tissue is responsible for continuously producing blood cells in our bodies via hematopoietic SCs.[459] Hematopoietic SCs in bone marrow exist in a specific cell niche so that hematopoietic SCs maintain their phenotype and function.[260] The bone marrow niche has been shown to be critical for self-renewal and differentiation of hematopoietic SCs into blood cell lineage.[460]

It is difficult to recapitulate the complex hematopoietic microenvironment in vitro.[461] To tackle this problem, Torisawa et al.[196] developed a bone-on-a-chip by combining in vivo and in vitro conditions. A PDMS device, which had a cylindrical cavity in the middle, was microfabricated and then, type I collagen gel consisting of bone morphogenetic proteins (BMP2 and BMP4) and bone-inducing demineralized bone powder was used to fill the hollow part throughout the device. Finally, the device opening that faced the hypodermis was closed with solid PDMS in order to reduce adipocyte transfer to the marrow from adipocyte-rich area. After eight weeks, a cylindrical bone tissue was obtained. Another device possessed a distribution of hematopoietic SCs, progenitors, and differentiated blood cells (covering all cell lineages) closely resembling the natural bone marrow. The engineered bone marrow was placed inside a PDMS microfluidic device having a chamber with the same dimension as the marrow. The underlying and overlying microfluidic channels were separated from the chamber by a porous membrane. Cell viability and delivery of nutrients were maintained by microfluidic perfusion. This bone marrow-on-a-chip also resembled radiation toxicity only witnessed in vivo and as such, may be a promising alternative for preclinical investigation. Other research groups have also used scaffolds in vivo, but they have not utilized their models for in vitro studies.[196]

Bone-marrow-on-a-chip has also been utilized to study treatment efficiency of drugs on acute lymphoblastic leukemia (ALL). ALL is a type of cancer initiated by overproduction of lymphoblasts within the bone marrow. Inspired by the fact that previous 2D models failed to replicate the actual bone marrow,[462] Bruce et al. developed a 3D microfluidic model to study the effectiveness of an antimetabolite chemotherapeutic drug, Ara-C.[197] Triculture of leukemic cells, human bone marrow stromal cells, and human osteoblasts were cultured in the 3D microfluidic platform to comprehend the cell interactions and compare the effect of Ara-C on the 2D and 3D systems. The microfluidic platform was operated for 48 h under continuous 1×10^{-6} M stream of Ara-C in culture medium. It was noted that in comparison to a 2D model, 3D microfluidic platform exhibited less chemotherapeutic drug sensitivity by leukemic cells. In fact, the microenvironment supported the tumor cell survival. This study was a breakthrough toward understanding and devising more promising drugs with regards to the developed microenvironment, which is more consistent with in vivo studies.

In a recent study, Torisawa et al. developed a platform to investigate bone marrow response to radiation countermeasure drugs and showed persistent blood cell manufacturing in vitro.[198] The curing effects of two therapeutic proteins, bactericidal-/permeability-increasing protein (BPI) and granulocyte-colony stimulating factor (G-CSF), both of which have been known to recover the hematopoiesis in bone marrow after radiation, were investigated. In comparison to no therapy, the addition of G-CSF to the microfluidic device considerably enhanced hematopoietic SCs, progenitors, and myeloid cells. BPI addition to the microfluidic chip also considerably increased hematopoietic SCs and myeloid cells within 6 days period (nearly twice the amount of cells in comparison to no therapy). Accordingly, both drugs were successful in recovering blood cell production once the bone marrow-on-a-chip was injured in vitro by radiation.[198]

7.8. Brain

The brain is one of the most sophisticated parts of nervous system. The central nervous system (CNS) is highly compartmentalized and layered, comprising of a wide variety of cells with dendrite outgrowths and plastic connectivity via axons.[463] Research on the brain development from the earliest stages of embryo to final years of life is still limited. The use of animal-based CNS disease models have been associated with various limitations, such as low throughput, high cost, time consuming, labor-intensive procedures, and experimental variations.[463] To address these limitations, scientists have developed systematic platforms capable of imitating the in vivo neuronal environment. Microfluidics has helped to better simulate the in vivo conditions (chemical, electrical, and physical) of the brain.[464] There are extensive reviews on brain-on-a-chip systems and implementation of different stimuli.[465,466] We briefly present the latest developments of in vitro brain models.

The neuronal axons are important for the pathogenesis of CNS injuries and neurodegenerative diseases. Therefore, some

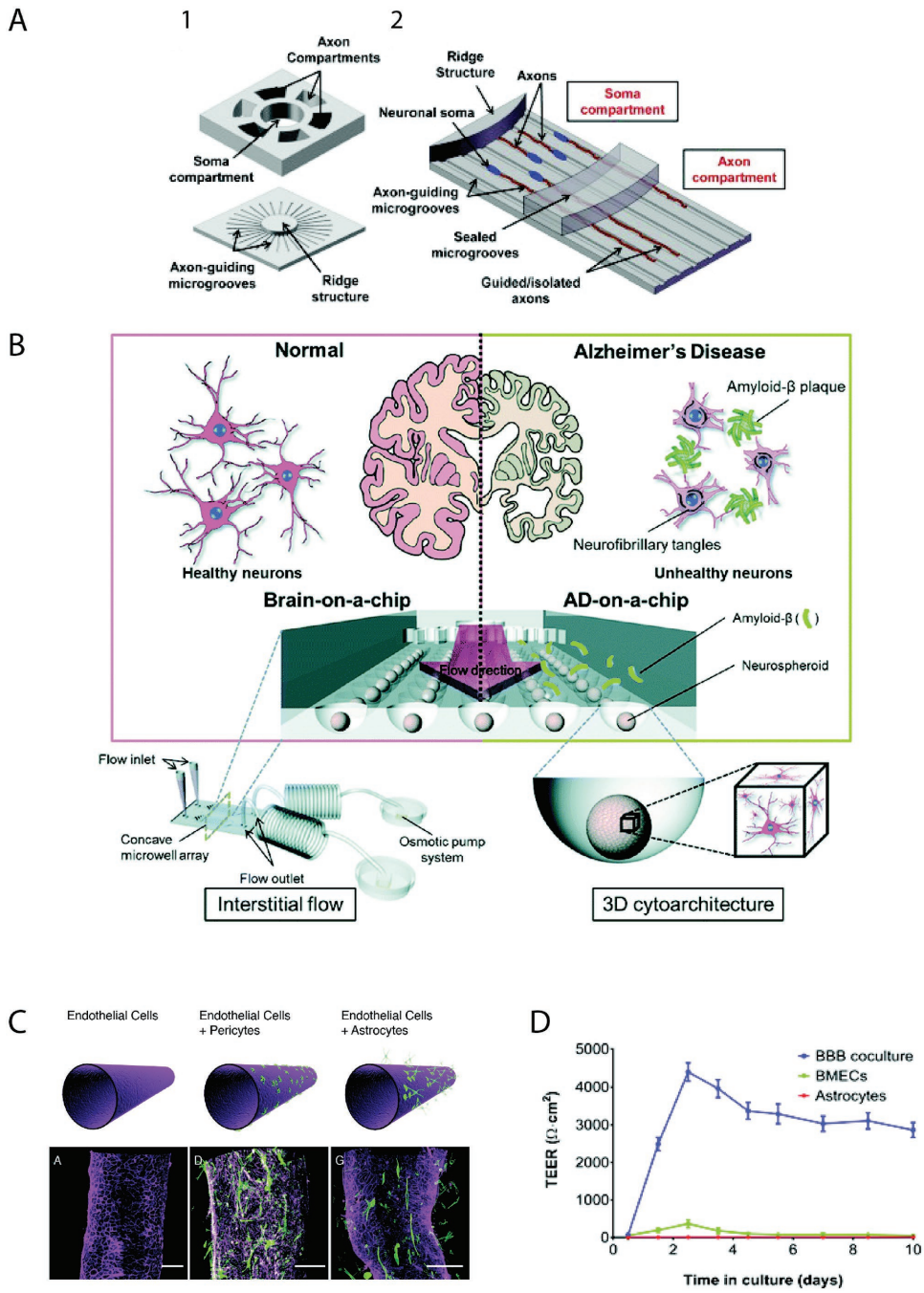

Figure 12. Brain-on-a-chip models. A) Schematic of microchip used for studying CNS axon growth. (1) Showing PDMS based top and bottom layers and (2) axon isolation using microgrooves.[203] Reproduced with permission.[203] Copyright 2014, Elsevier. B) Schematic for brain- and AD-on-a-chip using interstitial flow.[210] Reproduced with permission.[210] Copyright 2015, Royal Society of Chemistry. C) Top view of fluorescence confocal from brain engineered microvessels (scale bar, 200 µm).[215] Reproduced with permission.[215] Copyright 2016, PLOS ONE. D) Coculture of brain microvascular ECs and astrocytes, which showed noticeably higher TEER value compared to monoculturing of each cell type.[202] Reproduced with permission.[202] Copyright 2017, John Wiley & Sons.

studies have focused solely on axons.[199,203,467] For instance, Taylor et al. used a microfluidic system for high-resolution axonal transport that allowed the isolation and monitoring of axonal mitochondria and axonal growth.[199] The axon growth and isolation from somata or dendritic cells have several challenges including leakage,[468] short cell seeding period (usually less than 5 days),[469] time consuming isolation, and intensive axonal growth measurement.[470] To overcome this problem, Park et al. developed a circular microchip in which the soma compartment was located in the center and divided from the axonal compartment with sealed microgrooves (**Figure 12**A).[203] These microgrooves provided a straight pathway for axons to

grow from isolated neuronal somata/dendrites. To address the issue of invasive sampling to determine axonal growth, they fabricated an image processing method that was able to quantify the axonal growth. Furthermore, by separating axons and soma compartments, they investigated the effect of different biomolecules on each compartment and showed that chondroitin sulfate proteoglycan caused the axon retraction and growth when added to axon and somata sections, respectively.[203]

In addition to isolated neuronal studies, researchers have investigated the coculture of multiple CNS cells. For instance, the coculture of different CNS cells in a microfluidic platform provided the connection of different chambers and controllable perfusion of media.[204,471] In another study, Bianco et al. provided an approach for studying cell–cell communication using primary brain cells.[204] They plated different cells in separate chambers of a microfluidic system. Specific contribution of each cell type was measured by studying vitality, cellular morphology, calcium dynamics, and electrophysiological parameters. Microfluidic systems have enabled spatiotemporal control over specific brain slice regions and their communication, as well as enhanced oxygen penetration into the slice regions.[472] For example, Berdichevsky et al. fabricated a platform where brain slices were cultured and connected to each other by extending axons through microchannels.[209]

Aside from healthy CNS models, researchers have also utilized microfluidic devices to model various CNS diseases, including Alzheimer's disease (AD) and Parkisons's disease (PD). AD is the most common type of dementia that causes problems with thinking, memory, and behavior. Understanding the pathogenesis of AD is critical for the development of novel and effective pharmaceutical agents.[210,473] To create a more sophisticated model of AD, Park et al. designed a 3D brain-on-chip that mimics the in vivo brain microenvironment to investigate AD pathology (Figure 12B).[210] The constant fluid flow simulated the fluid in the interstitial space of brain. Furthermore, this system was also able to replicate toxic effects of amyloid-β, as the main contributor in AD. PD, the second most common neurodegenerative disorder, is a chronic and progressive movement disorder, caused by intense loss of nigrostriatal dopaminergic fibers.[474] To mimic the PD pathogenesis, Lu et al. created a microdevice platform for growth of sensitive neurons, such as those from the midbrain.[211] Using this approach, the authors were able to study the mechanism of axonal degeneration. Using these microfluidic systems, it may be possible to not only develop new treatments for human brain diseases but also more accurately predict the neurologic effects of drugs designed to treat other diseases.

The blood-brain barrier (BBB) is a highly selective semipermeable membrane barrier that separates the brain extracellular fluid from the circulating blood serving to protect the brain from harmful components in circulation by controlling the diffusion of molecules and ions.[475] The barrier is in part due to the formation of tight junctions between ECs from surrounding pericytes and astroycytes.[476] As a result of the BBB, therapeutic drug targets are limited as the most drugs cannot reach to disease neurons. Any dysfunction in the BBB may cause or intensify a variety of brain diseases including AD,[477] epilepsy,[478] PD,[479] and amyotrophic lateral sclerosis.[480] An ideal BBB model can be used to study the BBB transfer mechanism and diffusion of drug candidates through the BBB. One of the main barriers to develop a reliable microfluidic platform to recapitulate the human BBB function is the lack of suitable cell sources for human brain microvascular endothelial cells (BMECs). High sensitivity to agitation and poor viability[481] have been observed for human BMECs.[202] Due to low cost and facile harvesting, EC lines from humans[200,201] or rats[205–207] have been widely used in BBB microfluidic devices. However, these cell lines often have insufficient barrier properties.[482] Another approach is using primary human BMECs;[213,214] however, these cells may lose their function after a short period of time in culture.[483] Fortunately, differentiation of human iPSCs to human BMECs has paved the way for a reliable way to utilize human SCs as the cell source to mimic the BBB.[202] In most BBB-on-chip platforms, a semipermeable membrane is sandwiched between two microchannels. Polycarbonate,[200,205,207,213] PDMS,[484] PTFE,[208] and polyethylene terephthalate[201] have been utilized as a membrane in BBB-on-chip platforms. Booth and Kim developed a microfluidic BBB model and demonstrated the ability of device to be utilized for drug screening and optimization of drug permeability.[212]

TEER is the most common quantity to investigate the barrier tightness.[485] TEER value shows electrical resistance in tissue model. Tighter cells provide less room for ions and other charged molecules to pass through the cells resulting in higher resistance.[486] This characterization is noninvasive, label free, and quick for barrier tightness assessment and has the potential to be measured in real time using microfluidic platforms.[205,487] Flow type has significant effect on TEER measurement. In early BBB-on-chip studies, Griep et al. developed a BBB microfluidic model consisting of two PDMS channels. They utilized a platinum electrode to measure TEER. In the static flow condition, TEER value of 36 Ω cm^2 was reported, whereas in the dynamic flow and shear stress of 5.8×10^{-1} Pa, TEER value raised to 120 Ω cm^2.[200] A broad range of TEER values from 19 Ω cm^2[201] to 4400 Ω cm^2,[202] has been reported in BBB-on-chip platforms. Wang et al. reported the highest and in vivo-like TEER value with the coculture of BMECs and astrocytes.[202] However, each of monocultures did not reach over the value of 368 Ω cm^2, which shows how coculture is important for simulating in vivo function (Figure 12C). To overcome this problem, Herland et al. fabricated a cylindrical 3D hydrogel environment in which primary human brain ECs were located inside the lumen.[215] They explored coculture of astrocytes and pericytes with ECs to specify influence of cell types in neuroinflammatory responses (Figure 12D). To conclude, in order to compare and validate different BBB-on-chip devices, it is highly recommended to define standard experiments, such as permeability, TEER, and shear stress.[488] An ideal BBB-on-chip platform requires having several features, such as 3D multilayer scaffold containing ECs, astrocytes, pericytes, and muscle cells. Moreover, microfluidic platforms should provide suitable flow rate, pressure, and shear stress. The platform should also be equipped with biosensors to detect biophysical and biochemical parameters.[476]

7.9. Eye

Human eye has a complicated structure, composed of highly specialized tissue types, such as cornea and retina. Currently,

there are increasing demands to substitute these tissues, which may potentially be implemented by TE approaches.[489]

Cornea is composed of epithelium, stroma, and endothelium. The stroma layer is a thick, transparent layer including hundreds of sublayers of oriented collagen fibers.[490] Current research focuses on constructing the cornea architecture by culture of keratocytes on crosslinkable collagen,[491,492] fibrin hydrogels,[493] silk fibroin,[494] or decalcified fish scale,[495] all of which only achieve limited success in vitro. Autologous amniotic membranes[496] have been used in humans, however the long-term studies are still needed to access safety and benefits. Although current cornea TE cannot fulfill the requirements for cornea transplantation, development of physiologically relevant in vitro tissue models may help to explore the therapeutic strategies for nonterminal cornea diseases. Seo and Huh developed a cornea model called eye-on-a-chip including: artificial cornea with porous polystyrene scaffold filled with keratocytes, a 3D printed eye lid to mimic blinking activity, and a tear reservoir to simulate tear film dynamics. With further improvement, this model might potentially help to address some unanswered questions in cornea diseases related to limbal SC deficiency.[492]

Retina neuron loss was one of the major causes for blindness. Retina pigment epithelium replacement has partially restored the retina function.[497] With significant progress of SC technology, human SC differentiated retina pigment epithelium became available recently,[498] which may aid the exploration of therapeutic strategies. On the other hand, silicon and electronic-based chips have been implanted to either boost the electrical function of neuron for vision improvement or completely replace retina to pass signal to brain.[499] The former approach has gone through clinical trials and was proven to partially restore sight.[500] However, retina TE is still in its infancy, and hardly any approach has been shown to develop functional in vitro models.

7.10. Gut

There has been increasing interest in studying metabolism, mass transfer, and microenvironment of intestine mainly because inflammatory bowel diseases affect approximately one million people in the US[501] and therapeutic strategies are therefore urgently needed. As one of the major mass transfer and immune barriers for oral drug administration, intestine plays a critical role in drug pharmacokinetics including absorption, distribution, metabolism, elimination, and toxicity.[502] Therefore, in vitro intestine model can be a versatile tool to study pharmacokinetics.

Traditional 2D culture or culture in transwell inserts lack essential elements needed to recreate the physiologically relevant environment. For example, the intestinal epithelial cells (Caco-2 cells) in vivo require cyclic motion to differentiate into functional epithelium with villi for mucus secretion;[503,504] coculturing with bacteria in a static medium culture led to bacteria overgrowth and failed to establish stable symbiosis between epithelium and resident gut microbiome in the normal intestine.[501] Sato et al. have developed an in vitro model of 3D intestinal epithelial organoids (epithelial miniguts).[505] The formation of organoids recapitulates the complete SC differentiation hierarchy and allows for in vitro study of cell fate.[506] However, the process is relatively time consuming and the system cannot incorporate stimulus and design criteria other than biological cues.

Ingber and co-workers developed a human gut-on-a-chip to mimic normal intestinal environment.[217] The chip consists of two perfusable lumens separated by a porous PDMS membrane. Caco-2 cells were cultured on one side of membrane for 3 days with continuous media flow through both lumens. Cyclic stretch was applied to both lumens to mimic mechanically active environment of a small intestine. After Caco-2 cells reached confluency, they polarized rapidly and grew into folds with intestinal villi developing on the cellular surface. Multiple differentiated cell types in the intestine were found in this system, indicating that a more functionalized epithelium was developed.[503] Improved barrier function can also be verified by successfully coculturing intestinal microbes on the epithelium for over a week.[501] Using this in vitro model, the authors demonstrated the inflammation response at an organ level, as well as the effect of probiotics and antibiotics toward the intestinal epithelium.[217] Kimura et al.[218] developed a similar system with two lumens separated by a polyester-based porous membrane. The system was integrated with a stirring pump to control the flow patterns and an optical fiber for end-point observation. After Caco-2 cells were confluent on the membrane, rhodamine 123, considered as drug surrogate, was added into the system in order to study the permeability of epithelium. Although both systems were able to recapitulate parts of intestinal physiological and/or pathological behaviors, there are still limitations and challenges. First of all, both systems were made of PDMS, which is a highly hydrophobic material that has been approved in many drug loading or eluting devices.[54,507] The drug can be absorbed into the material and lead to unreliable results, which is not ideal for drug testing applications and not suitable for future human-on-a-chip design. On the other hand, both systems used nondegradable membrane to serve as a supporting scaffold for epithelium. However, these scaffolds were mostly over 10 μm in thickness, which is far from the commonly known basal membrane ≈400 nm in thickness. These differences can hinder the possibility of integrating other tissue types into the system, such as macrophages, and may not reproduce the actual drug transportation kinetics between intestine and blood stream.

7.11. Spleen

Spleen is a part of the immune system in the human body that helps to synthesize antibodies and remove pathogens from blood by filtration. The incentive of spleen-on-a-chip is to develop a blood filtration system that can aid existing immune system to fight sepsis.[508] Traditionally, donor spleen was sliced and implanted subcutaneously or intraperitoneally, which later connected with host vasculature for additional blood filtration.[508,509] Instead of creating hospitable in vitro or in vivo environment for spleen cells to function properly, Ingber and co-workers developed a microfluidic device to act as an external blood filtration system to mimic blood cleaning function of spleen with antibody coated NPs.[219] The device utilized a modified version of mannose-binding lectin, which is a

protein that binds to polysaccharides on the surfaces of more than 90 types of antigens and toxins in sepsis. The device significantly alleviated the survival of animals that were infected with *Escherichia coli*. This approach may potentially be applied in the clinical settings for severe systematic infections, such as human immunodeficiency virus and Ebola.[510]

7.12. Kidney

The kidney is a vital organ that performs blood filtration, waste removal, and hemodynamic regulation. However, the kidney is extremely susceptible to drug injury in the toxin removal process.[511] Despite its intrinsic regeneration capability, the kidney is still one of the most transplanted organs. There is a great interest to develop in vitro tissue models to emulate human kidney physiology and function.[512] The most widely modeled component of the kidney is the proximal tubule.[220–222,513] Recent development has also attempted to model the kidney glomerulus.[514] However, there has been no attempt to combine various components of kidney into a single OOC system. Nevertheless, kidney organoids with nephrons were created using human iPSCs.[515] This approach relied on the differentiation of SCs and self-assembly to reproduce intricate kidney-specific tubular and vascular structures. However, the internal tubular and vascular luminal space cannot be easily accessed and is not perfusable. In contrast, OOC devices based on membrane-based configuration provide both access to the luminal space and fluid perfusion.[220] The model used proximal tubular cells on a membrane within a microfluidic channel under perfusion and demonstrated glucose reabsorption, albumin transport, and alkaline phosphatase activity.

Some OOC devices were used to model the epithelial and vascular interface between podocytes and ECs in the kidney glomerulus.[514] Contrary to the proximal tubule, elevated shear stress and hydrodynamic pressure are detrimental to podocytes to simulate disease conditions, such as glomerular hypertension and leakage. In the latter model, the presence of key structural signatures of podocytes, such as the slit diaphragm, is still lacking and would be required to faithfully model the glomerular filtration function. Recent advances in 3D printing enabled the construction a 3D convoluted proximal tubule.[221] The 3D model demonstrated increased cell height and microvilli length, and albumin uptake compared to the 2D system, which are signs of mature proximal tubular cells. Similar fabrication techniques were applied with primary human kidney peritubular microvascular endothelial cells to engineer a kidney specific peritubular microvascular network.[222] The isolation and purification of patient-specific peritubular microvascular ECs and the establishment of fenestrated endothelium are key milestones. Future advances in this area could emerge from the combinatory use of existing technologies to move toward a kidney model with a more complete functionality.

7.13. Cancer

Despite the complexity, great successes have been made in understanding the basic cellular and molecular biology of cancer.[516] Many key events in the cancer metastatic cascade have been used as targets to develop anticancer therapeutics. However, major failure in cancer drug development is related to poor cancer models recapitulating the physiological tumor microenvironment.[517] Hence, better models are needed to study interaction between multiple tissues with cancer cells in a complex vascular network.[518]

Breast cancer is the most prevalent cancer type for women all over the world.[519] Breast cancer is mostly derived from the epithelium lining ducts or lobules, with the average width of duct channels ranging from 700 to 30 μm.[520] To model breast cancer disease, Grafton et al. developed a breast-on-chip platform using soft lithography.[223] They used a monolayer of non-neoplastic mammary epithelial cells to model ductal channels. The surface of PDMS hemichannels was coated with laminin and a PDMS membrane was utilized to close the channel. They guided superparamagnetic sub-micrometer particles, which have been shown previously to reach tumor cells inside the breast.[223] This study introduced a platform for future breast cancer modeling.

The most common in vitro model for studying cancer metastasis is the Boyden chamber/Transwell assay.[521] This assay utilizes a microporous membrane, which separates a well in a multiwell plate into upper and lower chambers. Cells will be seeded in the upper chamber and attracting molecules will be in the lower chamber. This assay fails to mimic the complexity of tumor microenvironment as it is performed in static condition and is unable to sustain chemotaxis gradients over time. As for in vivo models, direct tail-vein injection or xenograft of cancer cells in mice is performed for understanding the migration mechanism.[522] However, the metastatic cascade is hard to control and record. Moreover, animal models are inadequate to perform high-throughput studies. Therefore, new approaches are necessary for understanding the complex nature of tumor metastasis and evaluating the efficacy of novel therapeutics. Most of cancer-on-a-chip models can be divided into three general themes: (1) cancer cell and its microenvironment, (2) cancer cell adhesion and transendothelial migration, and (3) cancer-related angiogenesis as discussed below.

7.13.1. Modeling Tumor Microenvironment

Using a microfluidic 3D coculture model of human mammary fibroblasts with mammary epithelial cells[226] or an osteotropic prostate cancer cell line cocultured with bone marrow stromal cells,[225] it was demonstrated that soluble factors in the ECM as well as juxtacrine cell–cell signaling have accelerated the transition of cancer cells to their protrusive state. Moreover, it was reported that this invasive transition stimulated by stromal cells can be modulated spatially, as carcinoma cells remained rounded and dormant when the associated fibroblasts were further away from the cancer cell populations. Zervantonakis et al. also showed importance of stromal cells in remodeling the microenvironment in altering cancer cell fate.[227] They found that TNF-α can stimulate an impairment in the endothelial barrier, thereby increasing epithelial permeability, which facilitate a higher transmigration rate for the cancer cells. Similarly, Sobrino et al. recently proposed an advanced microfluidic

system that incorporates the roles played by the ECM, vasculature, and stromal perivascular cells to understand the tumor progression through angiogenesis.[523] Furthermore, Sobrino et al. used their vascularized microtumor systems to compare the effects of different receptor tyrosine kinase inhibitors on tumor and vascular network growth. Their results demonstrated that drugs targeting multiple receptor sites have the greatest effect in disrupting the vascular networks and limiting the cancer cells protrusion to the circulatory systems (**Figure 13**A).[523] These models further implicate that tumor metastatic behavior is greatly modulated by cell–cell interactions between cancer cells and stromal cells, and biochemical cytokine factors released into the tumor microenvironment. Thus, further studies that incorporate multiple cells to better mimic the in vivo environment are needed and can be the target of novel anticancer therapeutics.

7.13.2. Models of Cancer Cells Transendothelial Migration

Some cancer models have investigated the extravasation and adhesion of cancer cells. Takayama and co-workers fabricated a multilayered membrane-based microfluidic device with a physiological flow and demonstrated that breast cancer cell interaction with the endothelium was promoted through cancer cell receptors CXCR4 and CXCR7.[228] Moreover, the integration of breast cancer cell adhesion to the endothelium was manipulated when the CXCL12 chemokine was added to the basal side of endothelium. In a similar study, Jeon et al. analyzed the transmigration behavior of metastatic breast cancer cells MDA-MB-231 within a perfusable microvascularized microenvironment (Figure 13B).[230] They compared the migratory behavior of cells in device generated with either a muscle-mimicking or bone-mimicking microenvironment. Interestingly, the permeability of the vascular network was much higher in the muscle-mimicking microenvironment.[230,525] It further suggested that cancer migration is organ-specific. Recently, a more physiological model was proposed by Kong et al. to study the metastatic nature of cancer cells circulating in a multiple-organ platform (Figure 13C).[524] They revealed tumor cell adhesion and arrest on endothelium of liver and bone microenvironments were more prominent than in a muscle model. Due to the ease of recapitulating cancer cell adhesion to endothelium and monitoring biochemical molecules in guiding the extravasation of circulating cancer cells, these types of models are gaining interest to serve as a low-cost, time saving, and rapid alternative to assess antimetastatic compounds.

7.13.3. Models of Cancer-Related Angiogenesis

Some studies have demonstrated that solid tumor releases hypoxia-stimulated vascular endothelial growth factor (VEGF) to promote the extension of vasculature (**Figure 14**).[526]

The tumor angiogenesis is necessary for gas exchange and delivery of nutrients to the avascular regions of a tumor mass. It is therefore widely believed that blocking mechanisms, which modulate tumor angiogenesis, has a potential to attenuate the tumor growth and metastatic dissemination. In recent years, studies have pointed toward developing microfluidic devices to mimic the angiogenic events, especially through monitoring of EC migration as well as understanding factors that induce and stabilize the newly formed vascular beds. Using a 3D microfluidic system, Chung et al. were able to demonstrate the effect of different cancers on angiogenic sprouting in human adult dermal microvascular endothelial cells (HMVECs).[231] They quantified significant chemoattractant induced migration of HMVEC toward a channel seeded with MTLn3 breast cancer cells, while demonstrating minimal attraction to U87MG glioblastoma cells. In another study, Shin et al. have shown that although VEGF gradient alone can induce angiogenic sprouting, the tip ECs regress over time. It was shown to be reversed by the incorporation of angiopoietin-1 with the VEGF, as more of the tip cells formed a stable attachment to the stalk cells.[229] Kim et al. showed that interstitial flow has a critical regulatory role in pathological angiogenesis. They demonstrated that angiogenic sprouting occurred only in opposite direction of the interstitial flow, whereas vasculogenesis was unaffected by the direction of flow.[173] Theberge et al. were also able to identify the effect of soluble factor signaling on endothelial tubule formation (Figure 13D).[224] Interestingly, they showed that macrophages have a preventive effect in angiogenesis and this regulatory effect was alleviated when the matrix metalloproteinase-12 inhibitor was applied in the system. Of the systems discussed, angiogenesis can be modulated differently, depending on cocultured cell types, soluble factors in microenvironment, or direction of flow in microcirculation. Thus, a system that is representative to the physiological angiogenesis could have a significant impact on the development of potential antiangiogenic compounds.

7.14. Multi-Organ-On-A-Chip Platforms

Multi-OOC models have been developed to mimic the interplay between different organs, leading to further advancement in the development of an adequate in vitro model for drug testing and discovery.[528] The liver and kidney are critical organs in studying drug metabolism and excretion, respectively.[529] As such, incorporating these organs on a multi-OOC platform allows to more accurately examine drug-induced toxicity. For instance, Shintu et al. developed a liver and kidney coculture OOC platform to explore changes in metabolism as a result of drug addition.[232] They used a high-throughput metabolomics approach to screen the toxicity of a variety of small molecules. They utilized HepG2/C3A cells for liver tissue and cocultured them with kidney cells, which showed dose-dependent metabolic responses for ammonia. Another study reported a liver–kidney microfluidic device where it was shown that ifosfamide (an anticancer drug) was metabolized into a toxic metabolite (chloroacetaldehyde) by the liver.[530] However, they found that HepGA/C3A cells did not metabolized ifosfamide, which indicates the importance of cell type selection and tissue maturation to mimic the human body function. In other multi-OOC platforms, liver–heart systems were developed and tested.[233] Liver–heart interactions in such platforms could help in analyzing the toxicity and functionality of cardiovascular drugs (Figure 14A).[145] In a study conducted by Vunjak-Novakovic

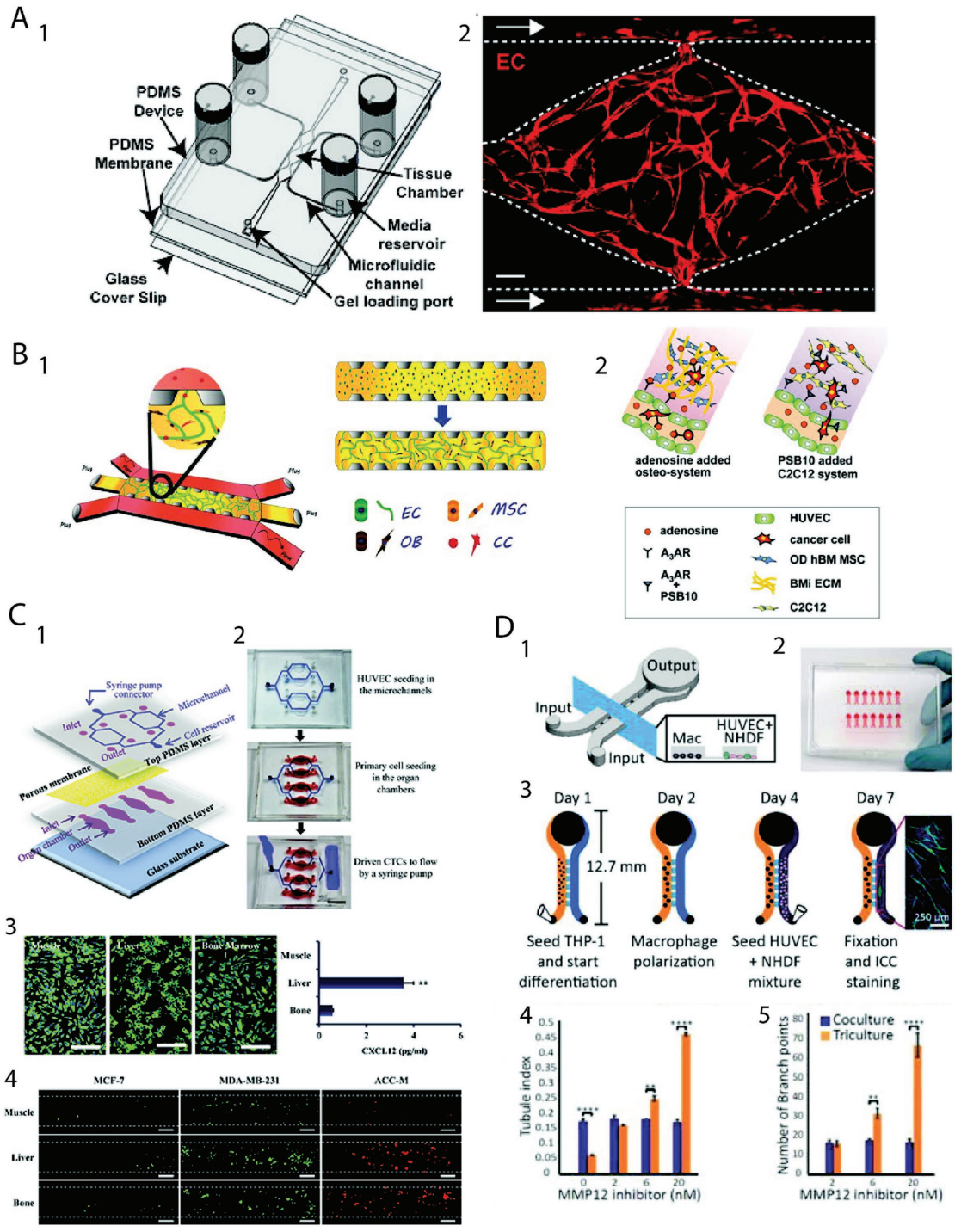

Figure 13. Tumor-on-a-chip models. A) (1) The three tissue chambers in the center are connected to two adjacent microfluidic channels, where cells may migrate outward. (2) Tissue chamber shows vascular network formation, and anastomoses of EC's to the adjacent microfluidic channels (scale bar, 100 μm). Reproduced with permission.[523] Copyright 2016, Nature Publishing Group. B) Extravasation model. (1) In the central tissue-mimicking gel channel, vasculature is able to form. Cells, biochemical factors, and media may flow across the central vasculature channel, from one side channel to the other. (2) Extravasation may be tracked as cancer cells introduced in the vessel channel travel through the central gel channel. Reproduced with permission.[230] Copyright 2015, National Academy of Science. C) (1) Schematic and (2) photograph, showing device design and construction. Branched microchannels mimic vascular microvessels (scale bar, 5 mm). (3 and 4) Device was used to study lung metastasis (scale bars, 250 μm in (3) and 200 μm in (4)). [524] D) Microfluidic device design. (1) Macrophages may be seeded in the left channel and HUVEC + normal human dermal fibroblast mixture on the right channel. Two channels may communicate through a series of small connecting channels. (2) Photograph showing 14 devices. (3) Schematic of device workflow. (4, 5) Quantification of the degree of tubular structure and number of branch points in different experimental conditions. Reproduced with permission.[224] Copyright 2015, American Chemical Society.

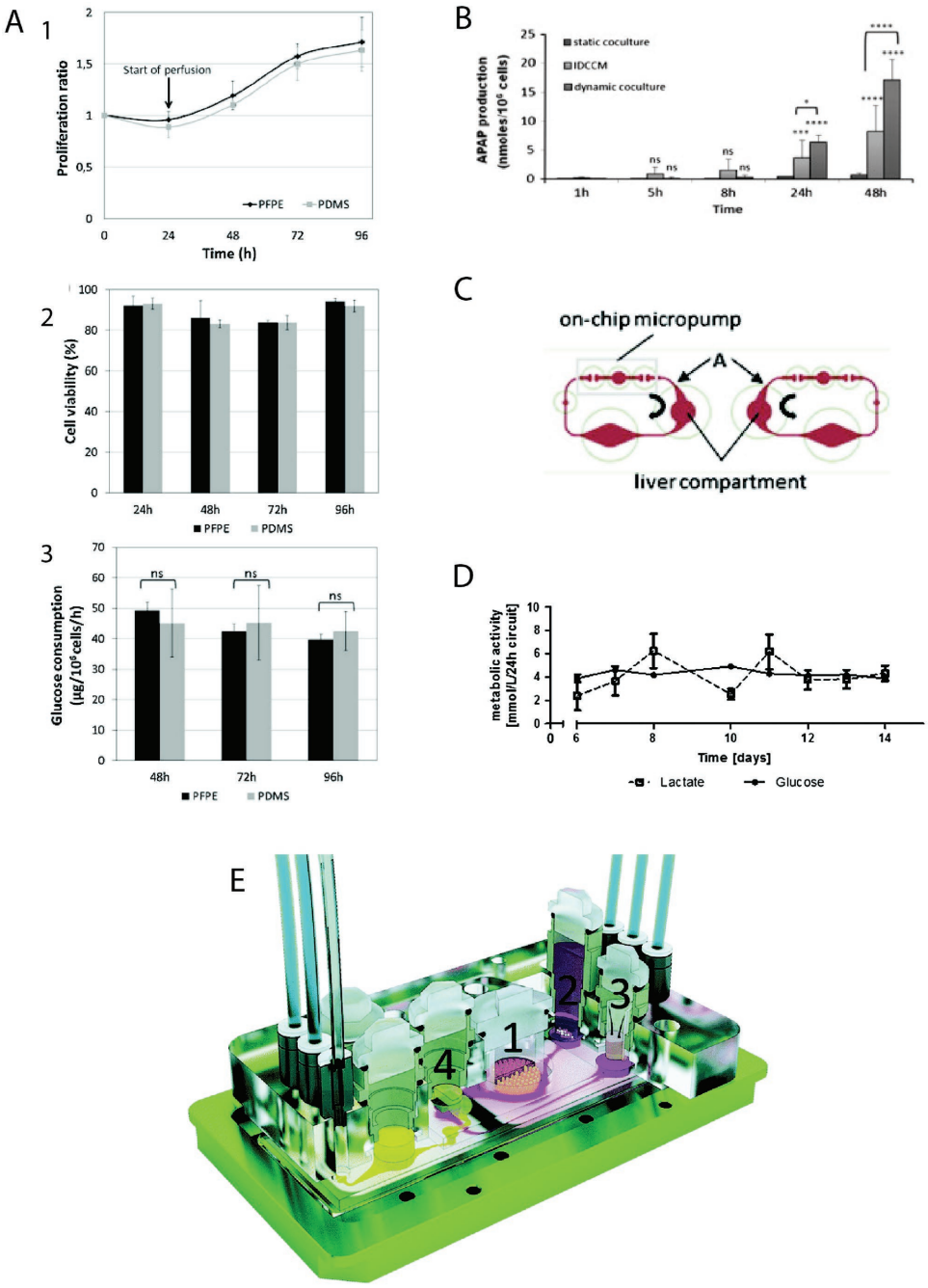

Figure 14. Multi-organ-on-a-chip models. A) Liver–kidney model: Madin–Darby canine kidney (MDCK) cells cultured in biochip and different parameters including (1) proliferation rate which increased after starting perfusion, (2) cell viability, (3) and glucose consumption were compared. Reproduced with permission.[233] Copyright 2016, Elsevier. B) Liver–intestine model: Acetaminophen production measured in 2 days to evaluate CYP1A2 activity in three different conditions including static coculture, dynamic coculture, and integrated dynamic cell cultures in microsystems. Reproduced with permission.[527] Copyright 2014, Elsevier. C) Schematic top view form liver–skin platform developed testing of drugs such as troglitazon. Reproduced with permission.[236] Copyright 2015, Elsevier. D) Liver, skin, and endothelial cells cultured in a microfluidic device and glucose and lactate consumptions compared for two weeks. Reproduced with permission.[236] Copyright 2015, Elsevier. E) (1–4) A schematic view for four organs-on-chip (liver, skin, intestine, and kidney) to study absorption, distribution, metabolism, and excretion. Reproduced with permission.[238] Copyright 2009, Royal Society of Chemistry.

et al., human iPSCs were differentiated into ECs, hepatocytes, and CMs.[264] to develop a platform called HeliVa which has a potential to be a high-throughput platform incorporating blood vessels, liver, and cardiac tissues.

The intestine plays a significant role in the absorption and excretion of orally administered drugs.[531] Esch et al. explored oral NP toxicity and utilized intestinal cells in coculture with liver cells.[234] They found that while the intestinal barrier was

able to prevent NP diffusion, NP might cause liver injury as measured by an enzyme released to injured liver cells. Furthermore, the intestinal microenvironment is critical for normal digestion and is particularly vulnerable to drug side effects. In another study, Bricks et al. developed an integrated coculture system using a microfluidic model to mimic the liver–intestine interaction.[527] The authors demonstrated a functional coculture system that could be utilized to examine intestinal absorption and liver metabolism of drugs, including acetaminophen (Figure 14B). Other studies have also been conducted using multi-OCC technology to mimic oral drug intake.[235] For example, Maschmeyer et al. utilized a coculture system to observe troglitazone intake, a drug that was withdrawn from the market as a result of liver toxicity in humans. Their results revealed that the liver-on-a-chip model was able to demonstrate liver toxicity in response to troglitazone, and there was no disruption in the polarization of intestine barrier.[236]

Another important pair for drug toxicity studies is the liver and skin, as skin is the main target for transdermal drugs.[532] In a study, a liver–skin model was exposed to troglitazone via an endothelialized microchannel over a period of 9 days (Figure 14C).[236] Glucose and lactate consumption were measured as metabolic activity of tissues and the result showed constant activity with minor fluctuations, indicating stable connection between tissues (Figure 14D). A similar model was designed and used by Wagner et al.[237] to study long-term cell cultivation. Liver–skin compartments were connected through a microchannel, with human biopsy tissue used for the skin compartment and microtissue aggregates for liver. The toxicity of troglitazone, which is normally prescribed to type 2 diabetes patients, was studied and the results showed a dose-dependent response to troglitazone. There are also other two organ-on-a-chip combinations including liver–tumor[533] and liver–neuron[534] platforms.

The complexity of human body and the ultimate goal of making a body-on-a-chip have persuaded researchers to connect more than two organs. Zhang et al. developed a microfluidic environment to study four-organ interactions including the liver, lung, kidney, and adipose tissues using human cell types (Figure 14E).[238] They made a "common medium" that incorporated essential components of each cell type. While the function of kidney compartment decreased by 10%, the rest of cell types retained their own specific function in this culture medium. The role of TGF-β1 was evaluated by varying the concentration from 10 to 50 ng mL^{-1} and it was shown that TGF-β1 induction enhanced the functions of lung and adipose tissues and inhibited the function of liver compartment. Besides their valuable discoveries, there are some limitations in mass transfer and metabolite exchange among chambers that did not enable longer operation periods.[535] In another study, a microfluidic device was designed to investigate absorption, distribution, metabolism, and excretion for human intestine, liver, skin, and kidney counterparts, respectively.[239] Their results revealed functional compartments, gene expression, and cell viability of tissues for 28 d. Other research groups also reported multiorgan microfluidic systems, such as liver–blood vessel–fat,[536] liver–tumor–bone marrow,[537] and liver–lung–fat tissues.[240]

8. Design Parameters in OOC Platforms

OOC platforms are typically used as a physical analogue to verify mathematical physiologically based pharmacokinetic (PBPK) models. PBPK models are typically used to study the absorption, distribution, metabolism, and excretion (ADME) of a drug. Parameters relating to the aforementioned drug characteristics can be estimated based on earlier drug studies using a single tissue construct. They can then be integrated in a PBPK model, which can be cross-referenced with an OOC platform consisting of multiple organs to validate the results. In addition, the PBPK model can be used to study spatial and temporal response of an organ to a drug and its interaction with additional organs. This review will not focus on developing the equations behind the PBPK model as there are many other reviews, which can be used to assist in model development.[1–3] Instead, the following section serves as an overview to the design parameters and considerations required to build a physiologically relevant OOC platform.

8.1. Estimation of ADME Parameters

There are several design parameters necessary to consider during OOC development. Some parameters, which can easily be attained from the literature include cardiac output of the desired organ (CO), blood flow rate in the organ (Q), number of cells per organ (n), and the residence time of each organ (τ). As an example, the kidney receives ≈20% of the cardiac output, has a flow rate of 1.2 L min^{-1}, $\approx 2 \times 10^9$ cells, and a residence time of 0.148 min.[4–8] However, there are additional parameters, which are desired when developing an OOC platform. These parameters can be estimated from in vitro experiments, and include drug partitioning into each organ (K), unbound fraction of a drug (f), intrinsic reaction rate per cell and per drug concentration in tissue (R), blood to plasma partitioning (B:P), and finally, intrinsic clearance rate (C).[9] Furthermore, a method known as in vitro to in vivo extrapolation (IVIVE) can be used to scale the in vitro results in vivo physiology. This approach depends on using a mathematical model to appropriately scale the result based on in vivo organ parameters.[10] As a result, the in vitro values can be used as an estimate for the whole body. These unknown parameters are closely related to the ADME parameters of a drug, which PBPK studies seek to answer. Therefore, there is a clear relationship between the need to develop a PBPK model before designing an OOC platform. These parameters, which are specific to some model molecules such as glucose, O_2, or albumin, are typically determined using in vitro assays or mathematical models. The OOC device is then formulated either based on the parameters from a single model molecule, or the average of multiple ADME parameters.

Absorption of a molecule defines its solubility (S) and permeability (P) to various barriers within the human body. Typically, the absorption profile of a molecule through the skin, gut, or lungs is desired. Prediction of absorption can be done through animal or human cultures, or human cadavers; however, these methods are not completely reliable.[9] A more reliable method consists of using single OOC devices to estimate the solubility and permeability of a drug.[11,12] Alternatively,

Table 4. Overview of parametric criteria for the development of an OOC platform. Equations were derived by Abaci et al.[9] CO is the cardiac output, Q is the blood flow rate, R is intrinsic reaction rate per cell and per drug concentration in the tissue, n is the number of cells per organ, τ is the residence time, K is the drug partitioning into each organ, $B{:}P$ is the blood to plasma partitioning ($B{:}P$), and f is the unbound fraction of a drug. The superscript, human or chip refers to parameters found in the human organ, or the scaled parameters for the OOC platform.

Parametric criteria	Unknown parameters	Known parameters (from literature)	Parameter definition
$\varnothing^{\text{chip}} = \varnothing^{\text{human}}$	$\varnothing^{\text{chip}}$	$\varnothing^{\text{human}}$	Cardiac output of the desired organ
$\frac{Q^{\text{chip}}}{R^{\text{chip}} n^{\text{chip}}} = \frac{Q^{\text{human}}}{R^{\text{human}} n^{\text{human}}}$	Q^{chip}	Q^{human}	Blood flow rate of the desired organ
	R^{chip}	R^{human}	Intrinsic reaction rate per cell and per drug concentration in the tissue
	n^{chip}	n^{human}	Number of cells in the organ
$\tau^{\text{chip}}_{\text{organ}} = \tau^{\text{human}}_{\text{organ}}$	$\tau^{\text{chip}}_{\text{organ}}$	$\tau^{\text{human}}_{\text{organ}}$	Residence time of each organ
$\tau^{\text{chip}}_{\text{body}} = \tau^{\text{human}}_{\text{body}}$	$\tau^{\text{chip}}_{\text{body}}$	$\tau^{\text{human}}_{\text{body}}$	Residence time of the body
$\frac{K^{\text{chip}}}{B{:}P^{\text{chip}}} = \frac{K^{\text{human}}}{B{:}P^{\text{human}}}$	K^{chip}	K^{human}	Drug partitioning into each
	$B{:}P^{\text{chip}}$	$B{:}P^{\text{human}}$	Blood to plasma partitioning
$f^{\text{chip}} = f^{\text{human}}$	f^{chip}	f^{human}	Unbound fraction of the drug on the OOC platform

there are models available, such as GastroPlus, SimCYP Ltd., PK-Sim, or ChloePK, which are able to predict the oral absorption of a drug.[13] The above models are based on a compartmental absorption and transit model.

Once a drug is absorbed, it distributes throughout the body. The unbound fraction of drug and the blood to plasma ratio are important for describing the distribution. Using a common media or blood source, and a single OOC, the distribution profile can be determined.[1,9] Furthermore, mathematic models exist to determine the distribution profile. Briefly, the equations work under a set of assumptions being that a drug distributes homogeneously through passive diffusion, and both nonspecific and reversible binding are possible.[13]

Metabolism of a drug is crucial in maintaining multiorgan interaction. Since the liver is largely responsible for the metabolism of drugs, single liver-on-a-chip devices can be used to derive this parameter.[15] Since it is difficult to model it or perform tests on animal models, IVIVE can be done to estimate the metabolism of a molecule for the whole body.

The final parameter required is excretion, which is typically determined through studies based on the kidney. Using a kidney-on-a-chip device, the renal clearance of the model molecule can be calculated and extrapolated to determine total kidney clearance of the whole body using the IVIVE method.[16]

8.2. OOC Design Principles

Once the ADME parameters have been estimated, they can be used in a model proposed by Abaci et al. The group derived a simplified set of design criteria useful for developing an OOC platform.[9] Using this model, parameters pertaining to the OOC platform can be calculated based on the ADME parameters. The equations were developed from a set of three criteria. Briefly, they proposed that concentrations of unbound nutrients in the OOC should be equal to that of the human body when at steady state. Additionally, the time dependent concentration of the desired drug in the OOC should be equal to that of the human body. Finally, they state that within each organ, the time dependent concentration of the unbound drug should be equal to that in the body. They developed one general parametric criterion, which they further simplified into a set of five equations; three pertaining to OOC development, and two drug specific equations. **Table 4** serves as an overview of the equations and parameter definition.

8.3. Mutli-OOC Design Considerations

While the above parameters will certainly aid in device design, it is important to consider other criteria such as device scaling, cell source, and culture media. In addition, combination of organs, and multiorgan devices are additional design considerations. If the organs do not directly interact with the drug of interest or its resulting metabolites, it is possible to simplify the model by combining the organs into one compartment, to study them implicitly. It is clear that the process of simplification can have a profound effect on decreasing the cost of device fabrication, and required materials and reagents. A final design parameter consists of controlling the fluid flow and shear rates within an organ. These parameters are available in literature for the human body and by controlling the diameter of the channels leading to the tissue, the flow rate can be scaled and adjusted accordingly.[9,17] It is important in ensuring physiological conditions, following organ scaling. Finally, the OOC platform should be tested and the results should be compared to the PBPK platform. Since there are many assumptions and simplifications, the OOC platform should be validated and the design should be iterated to ensure an adequate model.

9. Future Perspectives and Challenges

9.1. Physiological Relevance of OOC Platforms

While several OOC platforms have already been developed, these platforms should be able to reliably replicate the human physiology and metabolism to benefit pharmaceutical industry in drug discovery and development. The performance of current OOC platforms should be improved to further mimic the physiology and function of organs in the body. In what follows, we discuss challenges that need to be addressed to develop physiologically relevant OOC platforms.

9.1.1. Device Design and Material

OOC devices should be designed in physiologically relevant sizes. Otherwise, organ compartments may lead to underproduction or overproduction of metabolites, which can affect other organs in the device. An approach to properly scale the organ size is to construct the organ size according to fluid residence time in each organ. The blood residence time within an organ in the body has a correlation with the organ size, the perfusion rate, and the tissue composition.[538] The metabolic activity of native tissues and blood flow within them are also different from corresponding disease tissues, which should be considered as a design criterion. Minimizing the organ chamber volume has some advantages as to decrease the use of precious cell sources, culture medium, and soluble factors. However, a minimum cell number should be recruited to have meaningful metabolites in the device. Another consideration is that some culture media may be taken from the device at different time points to analyze metabolic profiles. This medium removal should not cause any significant perturbation in the system.

A potential challenge in OOC devices is scaffolds or materials used in chips. Roth and Singer[539] described a case study in which a microfluidic system was used to evaluate the drug clearance from liver tissues. Some known drugs were used to establish a protocol for the drug clearance assessment. Unexpectedly, the liver tissue has low sensitivity to the drugs because the plastic material used in the device absorbed high amount of drugs. There, nonspecific binding of drugs to chip materials should be checked. Chip materials and scaffolds should be inert to the absorption of drug candidates and thereby not affect the actual exposure of drug to cells. To solve this problem, Schimek et al. proposed that microchannels can fully be covered using human dermal microvascular ECs and thereby drug absorption on plastic material is avoided.[540] In another study, Zhang et al. coated the interior of PDMS tubes with HUVECs to develop biomimetic blood vessels with high transparency, tunable elasticity, and gas permeability.[541] However, fabrication of microfluidic channels with the ECM materials (e.g., basement membrane, glycosaminoglycans, and elastin) having an in vivo-like porosity and stiffness is desirable.

Some OOC models utilize biomaterials with unknown biological moieties in engineering tissues and organs. It may be hard to reproduce these biomaterials in a defined composition and they may release/degrade over culture time. As a result, it is difficult to decouple the effect of their biological factors on cellular behavior, molecular signaling, and tissue morphogenesis in an OOC platform. Therefore, biomaterials with well-defined composition and degradation/release profile and low lot-to-lot variability are required to construct OOC devices.

9.1.2. Cell Culture Medium

Cell culture media in OOC platforms should not only provide a saline solution to preserve tissues but should also include complex compositions to maintain tissue viability and function for an extended period of time. Here, a major challenge is that different tissues often require different cell culture media. Moreover, some reagents in media may have opposite effects on different tissues. For example, TGF-β1 supports the growth of A549 lung cells,[542] while it inhibits the growth of hepatocellular carcinoma cells.[543] Such problems make it difficult to find a universal cell culture medium that is in the favor of all cell types. This challenge should be overcome for the development of multiple OOC platforms.

Animal or human sera (e.g., fetal bovine serum) have often been employed as the supplement in common cell culture medium because they have similar transport properties to blood and possess essential compounds for the maintenance and growth of cells. Serum may have a wide variation in the composition, which can affect tissue culture conditions and subsequent resulting experimental data.[544] Therefore, development of a serum-free medium has been a subject of intensive research[545] because such media offer a defined and consistent culture medium. Schaffner et al. introduced the first serum-free media for hippocampal neurons.[546] Following that, serum-free media were proposed for different cell types. A serum-free media can be made by adding supplements and cell-specific growth factors to a common base medium.[547] However, the optimization is needed to make standard serum-free medium for a specific OOC platform having multiple cell types. Such media should be able to preserve morphology and function of different cells.

9.1.3. Cell Sources

iPSCs and ESCs have generally become attractive cellular options in human tissue modeling in vitro.[548] However, the efficiency of SC reprograming or differentiation protocols needs to be improved. In particular, highly efficient gene delivery without using viruses is desirable for iPSC production. Moreover, the use of iPSCs from patients makes it possible to construct personalized and disease-specific OOC platforms.[549] For instance, iPSCs have been used to model type 1 long QT syndrome in vitro using CMs derived from a patient.[550] Similar studies have been reported using iPSCs derived from patients having AD,[551] PD,[552] and other diseases[553] to evaluate the physiology and cellular responses of these genotypes. However, iPSC differentiation protocols may vary for different patients. Safety, reproducibility, and efficiency of differentiated iPSC should be evaluated prior to clinical studies. Highly efficient and successful differentiation of iPSCs into specific cell

types is still a major challenge. These SCs are largely susceptible to their physicochemical microenvironment, which has implications for the reproducibility of results by different labs. Therefore, a more complete deciphering of SC microenvironment, behavior, and fate is necessary to achieve highly efficient and reliable iPSC-derived cell lineages for OOC platforms. In addition, production of a large number of differentiated cells in a well-defined environment is still a major obstacle.

Genetic manipulation of some cell lines enables researchers to produce modified cell types with a fluorescent probe, which facilitates the optical assessment of their metabolic responses to therapeutic treatments.[554] Fu et al. recently showed that smart nanosensors are able to track viability and development of SC organoids in a noninvasive and real-time manner.[555] In addition, epigenetic identification of SCs using microplatforms (e.g., chromatic immunoprecipitation assays and antibody arrays[556]) provides great tools in monitoring SC behavior and function.

9.2. Tissue Assessment

Evaluating tissue behavior and function in OOC devices requires accurate, noninvasive, and real-time measurement of function and metabolites of different cell types.[557] Tissue characterization approaches should be scaled up for high-throughput measurements in drug screening and development. Microelectrode arrays can record the physiological activity of cells and tissues in a high-throughput manner.[558] In addition, such microelectrodes can measure some biological analytes (e.g., lactate[559] and superoxide radicals[560]) in a wide range of concentrations. Ion mobility spectrometry and mass spectrometry can also provide further insights into molecular compositions of culture media or waste products.[561] Further development of suitable analytical techniques for OOC devices is needed to assess drug effects on the physiology and function of organs in a real-time, high-throughput, and reliable manner. An ideal OOC device should be able to monitor various biological and physicochemical parameters of organ compartments and correlate them with drug type and concentration.

9.3. Commercialization

Commercialization of OOC platforms ensures their success in industrial settings. Some efforts have already led to the commercialization of tissue or OOC platforms, while others are still underway. Some model examples include Transwell-based system (RegeneMed, Inc.),[562] coculture model (Ascendance Biotechnology, Inc.),[563] spheroid model (InSphero, Inc.),[564] and Biowire system (TARA).[565] Large pharmaceutical and biotechnological companies have increased their partnership with start-up companies to use their novel OOC models in research and development. For example, Merck, Johnson & Johnson, and Pfizer have collaborated with Emulate (a biotech spinout from the Wyss Institute at the Harvard University, USA). These companies aim to use latest OOC technologies and discoveries in industry. In another example, Pfizer, GlaxoSmithKline, Sanofi, and Roche worked with Mimetas to develop brain-on-a-chip and kidney-on-a-chip models for toxicity assessment.[566]

Adaptation of new devices to pharmaceutical industry requires showing an affordable price and profit compared to conventional approaches.[567] OOC platforms should be user-friendly and compatible with commonly used biotechnological backbone and laboratory setups. Low price of OOC devices can be achieved by fabricating valveless or pumpless devices, which operate in an automatic and controllable manner.[568] The standardization of evaluation and validation methods in OOC platforms is also required for industrial applications of such platforms.

The longevity of OOC platforms is a critical issue that needs to be shown prior to their widespread applications in industry. OOC models should be maintained over a long time period to predict chronic effects of drug candidates.[297] However, some waste products and metabolites within organ compartments may limit the lifetime of device. Furthermore, some drugs may induce apoptotic pathways in cells, which can affect toxicological studies. A careful consideration of tissue culture variables, such as scaffold topography and chemistry, exogenous stimuli, and medium, is a key parameter to elongate tissue cultures.

There has been a long way starting from an exploratory method to a widely used and acceptable tool in pharmaceutical industry. Regulatory authorities approve a novel cellular model only after providing a substantial amount of scientific data and cross-pharma validations and assuring its reliability, robustness, and reproducibility. A good example is the ESC test validated by the European Centre for the Validation of Alternative Methods.[569] Therefore, OOC devices need to be validated by experimenting with a wide range of reference and well-documented drugs on them. Both sensitivity and specificity of OOC platforms should be documented. The automation and miniaturization of OOC platforms also help in their regulatory approval as to enhance cost-effectiveness by decreasing labor costs and biological reagents.

9.4. OOC Platforms to Assess Substances Other than Drugs

Number of chemicals registered at the Chemical Abstract Service has significantly been increased from 1965 (≈212 000 chemicals) to 2006 (≈88.7 million chemicals)[570] and this trend has been going on in recent years. As a result, the human exposure to chemicals has grown rapidly. Moreover, the National Research Council requested a paradigm shift in chemical risk assessment and regulatory toxicity testing from whole-animal testing.[571] As a result, the USA Environmental Protection Agency (USEPA) conducted the ToxCast program, while the FDA, the National Institute for Environmental Health Sciences, the USEPA, and the National Institutes of Health establish the Tox21 program to evaluate toxicity of chemicals.[572] These programs aim to understand effect of chemical hazards to humans and reveal corresponding molecular pathways using in vitro cell-based assays in a high-throughput manner.[573] In this perspective, it would be a great opportunity for OOC platforms to play an important role in chemical toxicology experiments and thereby help in risk assessments and regulatory decision-making. Such platforms would be able to accelerate

the movement from traditional toxicity models to more physiologically relevant, cost-effective, and high-throughput models.

10. Conclusions

The complex nature of the human body and the physiological processes required for tissue and organ structure and function is a major obstacle for studying human development and disease in a facile and systematic manner. While 2D cell cultures have been used as the model system to study physiological responses to drug candidates, OOC models have clearly increased the physiological relevance of cell and tissue models in drug screening and discovery. OOC models can be integrated with animal models in drug screening to increase the efficiency and biological relevance of drug screening models.[465,574] Fabrication of biomimetic, sophisticated, and reliable OOC platforms seeks a close and intensive collaboration among bioengineers, pharmacologists, biologists, and toxicologists. Owing to great advances in biomaterial science and engineering, SC biology, microfabrication techniques, and biosensors, the fabrication of functional OOC platforms is now a reality. Currently developed OOC platforms have shown great applicability for repetitive, quantitative, and systematic study of drugs. These platforms have also been used for disease modeling and thereby can be used to evaluate novel drug candidates and therapies in a controlled, low cost, and high-throughput manner. Here, we discussed synthetic or natural biomaterials and biological factors as the key elements in TE, providing different biological, structural, and mechanical cues in tissue morphogenesis and function. Novel cell sources derived from human iPSCs and ESCs were mentioned to fabricate personalized OOC platforms. Microscale technologies were described as the extremely powerful tools in making the biomimetic tissue structures. Sensory systems were also discussed to analyze metabolites and other OOC outputs in a high-throughput manner. We highlight the advances made in currently developed OOC platforms as functional tools in simulating human physiology and metabolism. Still, major challenges exist in the development of OOC platforms before they can be used systematically as drug screening platforms.

Acknowledgements

R.C., D.B., and M.H.M. contributed equally to this work. All authors contributed in writing the paper. M.R. supervised the paper preparation. All authors read the paper, commented on it, and approved its content.

Conflict of Interest

The authors declare no conflict of interest.

Keywords

biomaterials, cells, drug discovery, organ-on-a-chip, tissue engineering

Received: April 19, 2017
Revised: June 15, 2017
Published online:

[1] a) J. A. DiMasi, L. Feldman, A. Seckler, A. Wilson, *Clin. Pharmacol. Ther.* **2010**, *87*, 272.
[2] D. C. Harrison, R. Winkle, M. Sami, J. Mason, *Am. Heart J.* **1980**, *100*, 1046.
[3] D. S. Echt, P. R. Liebson, L. B. Mitchell, R. W. Peters, D. Obias-Manno, A. H. Barker, D. Arensberg, A. Baker, L. Friedman, H. L. Greene, *N. Engl. J. Med.* **1991**, *324*, 781.
[4] R. M. Plenge, *Sci. Transl. Med.* **2016**, *8*, 349ps15.
[5] A. K. Capulli, K. Tian, N. Mehandru, A. Bukhta, S. F. Choudhury, M. Suchyta, K. K. Parker, *Lab Chip* **2014**, *14*, 3181.
[6] C. Moraes, G. Mehta, S. C. Lesher-Perez, S. Takayama, *Ann. Biomed. Eng.* **2012**, *40*, 1211.
[7] C. R. Hooijmans, M. Ritskes-Hoitinga, *PLoS Med.* **2013**, *10*, e1001482.
[8] R. Greek, A. Menache, *Int. J. Med. Sci.10*, 206.
[9] R. Skalak, C. F. Fox, Eds., *Tissue Engineering*, New York, USA **1988**.
[10] U. Meyer, The History of Tissue Engineering and Regenerative Medicine in Perspective, *Fundamentals of Tissue Engineering and Regenerative Medicine*, Edited by U. Meyer, T. Meyer, J. Handschel, H. P. Wiesmann, Springer, New York, **2009**, p. 5.
[11] R. Langer, J. P. Vacanti, *Science* **1993**, *260*, 920.
[12] R. Obregón, J. Ramón-Azcón, S. Ahadian, H. Shiku, H. Bae, M. Ramalingam, T. Matsue, *J. Nanosci. Nanotechnol.* **2014**, *14*, 487.
[13] a) J. Vanderburgh, J. A. Sterling, S. A. Guelcher, *Ann. Biomed. Eng.* **2016**, *45*, 1; b) Y. Xiao, S. Ahadian, M. Radisic, *Tissue Eng., Part B* **2016**, *23*, 9.
[14] J. J. Marler, J. Upton, R. Langer, J. P. Vacanti, *Adv. Drug Delivery Rev.* **1998**, *33*, 165.
[15] N. T. Feric, M. Radisic, *Adv. Drug Delivery Rev.* **2016**, *96*, 110.
[16] S. Ostrovidov, V. Hosseini, S. Ahadian, T. Fujie, S. P. Parthiban, M. Ramalingam, H. Bae, H. Kaji, A. Khademhosseini, *Tissue Eng., Part B* **2014**, *20*, 403.
[17] K. L. Fujimoto, K. Tobita, W. D. Merryman, J. Guan, N. Momoi, D. B. Stolz, M. S. Sacks, B. B. Keller, W. R. Wagner, *J. Am. Coll. Cardiol.* **2007**, *49*, 2292.
[18] D.-A. Wang, S. Varghese, B. Sharma, I. Strehin, S. Fermanian, J. Gorham, D. H. Fairbrother, B. Cascio, J. H. Elisseeff, *Nat. Mater.* **2007**, *6*, 385.
[19] a) L. G. Griffith, G. Naughton, *Science* **2002**, *295*, 1009; b) A. Hansen, A. Eder, M. Bönstrup, M. Flato, M. Mewe, S. Schaaf, B. Aksehirlioglu, A. Schwörer, J. Uebeler, T. Eschenhagen, *Circ. Res.* **2010**, *107*, 35; c) F. Xu, J. Wu, S. Wang, N. G. Durmus, U. A. Gurkan, U. Demirci, *Biofabrication* **2011**, *3*, 034101.
[20] M. Gumbleton, K. L. Audus, *J. Pharm. Sci.* **2001**, *90*, 1681.
[21] K. A. Foster, C. G. Oster, M. M. Mayer, M. L. Avery, K. L. Audus, *Exp. Cell Res.* **1998**, *243*, 359.
[22] S. Anthérieu, C. Chesné, R. Li, C. Guguen-Guillouzo, A. Guillouzo, *Toxicol. In Vitro* **2012**, *26*, 1278.
[23] a) D. D. Allen, R. Caviedes, A. M. Cárdenas, T. Shimahara, J. Segura-Aguilar, P. A. Caviedes, *Drug Dev. Ind. Pharm.* **2005**, *31*, 757; b) A. Astashkina, B. Mann, D. W. Grainger, *Pharmacol. Ther.* **2012**, *134*, 82.
[24] E. S. Kostewicz, B. Abrahamsson, M. Brewster, J. Brouwers, J. Butler, S. Carlert, P. A. Dickinson, J. Dressman, R. Holm, S. Klein, *Eur. J. Pharm. Sci.* **2014**, *57*, 342.
[25] D. Huh, H. J. Kim, J. P. Fraser, D. E. Shea, M. Khan, A. Bahinski, G. A. Hamilton, D. E. Ingber, *Nat. Protoc.* **2013**, *8*, 2135.
[26] J. H. Sung, M. L. Shuler, *Bioprocess Biosyst. Eng.* **2010**, *33*, 5.
[27] J. H. Sung, B. Srinivasan, M. B. Esch, W. T. McLamb, C. Bernabini, M. L. Shuler, J. J. Hickman, *Exp. Biol. Med.* **2014**, *239*, 1225.
[28] P. Zhao, L. Zhang, J. A. Grillo, Q. Liu, J. M. Bullock, Y. J. Moon, P. Song, S. S. Brar, R. Madabushi, T. C. Wu, *Clin. Pharmacol. Ther.* **2011**, *89*, 259.
[29] S. N. Bhatia, D. E. Ingber, *Nat. Biotechnol.* **2014**, *32*, 760.

[30] X. Yin, B. E. Mead, H. Safaee, R. Langer, J. M. Karp, O. Levy, *Cell Stem Cell* **2016**, *18*, 25.
[31] O. Kilic, D. Pamies, E. Lavell, P. Schiapparelli, Y. Feng, T. Hartung, A. Bal- Price, H. T. Hogberg, A. Quinones-Hinojosa, H. Guerrero-Cazares, A. Levchenko, *Lab Chip* **2016**, *16*, 4152.
[32] L.-S. Liu, A. Y. Thompson, M. A. Heidaran, J. W. Poser, R. C. Spiro, *Biomaterials* **1999**, *20*, 1097.
[33] D. Huh, D. C. Leslie, B. D. Matthews, J. P. Fraser, S. Jurek, G. A. Hamilton, K. S. Thorneloe, M. A. McAlexander, D. E. Ingber, *Sci. Transl. Med.* **2012**, *4*, 159ra147.
[34] M. S. Sakar, D. Neal, T. Boudou, M. A. Borochin, Y. Li, R. Weiss, R. D. Kamm, C. S. Chen, H. H. Asada, *Lab Chip* **2012**, *12*, 4976.
[35] B. Zhang, M. Montgomery, M. D. Chamberlain, S. Ogawa, A. Korolj, A. Pahnke, L. A. Wells, S. Masse, J. Kim, L. Reis, A. Momen, S. S. Nunes, A. R. Wheeler, K. Nanthakumar, G. Keller, M. V. Sefton, M. Radisic, *Nat. Mater.* **2016**, *15*, 669.
[36] M. Wufuer, G. Lee, W. Hur, B. Jeon, B. J. Kim, T. H. Choi, S. Lee, *Sci. Rep.* **2016**, *6*, 37471.
[37] K. J. Jang, K. Y. Suh, *Lab Chip* **2010**, *10*, 36.
[38] S. A. Mousavi Shaegh, F. De Ferrari, Y. S. Zhang, M. Nabavinia, N. Binth Mohammad, J. Ryan, A. Pourmand, E. Laukaitis, R. Banan Sadeghian, A. Nadhman, *Biomicrofluidics* **2016**, *10*, 044111.
[39] P. J. Lee, P. J. Hung, L. P. Lee, *Biotechnol. Bioeng.* **2007**, *97*, 1340.
[40] H. J. Kim, D. Huh, G. Hamilton, D. E. Ingber, *Lab Chip* **2012**, *12*, 2165.
[41] N. Jusoh, S. Oh, S. Kim, J. Kim, N. L. Jeon, *Lab Chip* **2015**, *15*, 3984.
[42] L. G. Griffith, *Acta Mater.* **2000**, *48*, 263.
[43] J. A. Hubbell, *Curr. Opin. Biotechnol.* **1999**, *10*, 123.
[44] a) N. Beißner, T. Lorenz, S. Reichl, **2016**, 299; b) D. Huh, Y. S. Torisawa, G. A. Hamilton, H. J. Kim, D. E. Ingber, *Lab Chip* **2012**, *12*, 2156.
[45] S. N. Bhatia, D. E. Ingber, *Nat. Biotechnol.* **2014**, *32*, 760.
[46] a) G. T. Vladisavljevic, N. Khalid, M. A. Neves, T. Kuroiwa, M. Nakajima, K. Uemura, S. Ichikawa, I. Kobayashi, *Adv. Drug Delivery Rev.* **2013**, *65*, 1626; b) J. Wu, N. Y. Lee, *Lab Chip* **2014**, *14*, 1564.
[47] L. Davenport Huyer, B. Zhang, A. Korolj, M. Montgomery, S. Drecun, G. Conant, Y. Zhao, L. Reis, M. Radisic, *ACS Biomater. Sci. Eng.* **2016**, *2*, 780.
[48] K. H. K. Wong, J. M. Chan, R. D. Kamm, J. Tien, *Annu. Rev. Biomed. Eng.* **2012**, *14*, 205.
[49] B. Harink, S. Le Gac, R. Truckenmuller, C. van Blitterswijk, P. Habibovic, *Lab Chip* **2013**, *13*, 3512.
[50] K. Ren, J. Zhou, H. Wu, *Acc. Chem. Res.* **2013**, *46*, 2396.
[51] E. Berthier, E. W. Young, D. Beebe, *Lab Chip* **2012**, *12*, 1224.
[52] M. W. Laschke, M. D. Menger, *Biotechnol. Adv.* **2016**, *34*, 112.
[53] K. Sato, N. Sasaki, H. A. Svahn, K. Sato, *Adv. Drug Delivery Rev.* **2014**, *74*, 115.
[54] M. W. Toepke, D. J. Beebe, *Lab Chip* **2006**, *6*, 1484.
[55] M. Grellier, L. Bordenave, J. Amédée, *Trends Biotechnol.* **2009**, *27*, 562.
[56] L. D. Huyer, M. Montgomery, Y. Zhao, Y. Xiao, G. Conant, A. Korolj, M. Radisic, *Biomed. Mater.* **2015**, *10*, 034004.
[57] W. J. McCarty, L. Prodanov, S. S. Bale, A. Bhushan, R. Jindal, M. L. Yarmush, O. B. Usta, *J. Visualized Exp.* **2015**, *103*, e53078.
[58] X. Che, J. Nuhn, I. Schneider, L. Que, *Micromachines* **2016**, *7*, 84.
[59] Y. Xiao, B. Zhang, H. Liu, J. W. Miklas, M. Gagliardi, A. Pahnke, N. Thavandiran, Y. Sun, C. Simmons, G. Keller, M. Radisic, *Lab Chip* **2014**, *14*, 869.
[60] S. S. Verbridge, A. Chakrabarti, P. DelNero, B. Kwee, J. D. Varner, A. D. Stroock, C. Fischbach, *J. Biomed. Mater. Res., Part A* **2013**, *101*, 2948.
[61] K. Shimizu, H. Araki, K. Sakata, W. Tonomura, M. Hashida, S. Konishi, *J. Biosci. Bioeng.* **2015**, *119*, 212.
[62] R. Sudo, S. Chung, I. K. Zervantonakis, V. Vickerman, Y. Toshimitsu, L. G. Griffith, R. D. Kamm, *FASEB J.* **2009**, *23*, 2155.
[63] A. Odawara, M. Gotoh, I. Suzuki, *RSC Adv.* **2013**, *3*, 23620.
[64] L. Marinucci, C. Lilli, M. Guerra, S. Belcastro, E. Becchetti, G. Stabellini, E. M. Calvi, P. Locci, *J. Biomed. Mater. Res., Part A* **2003**, *67*, 504.
[65] W. R. Legant, A. Pathak, M. T. Yang, V. S. Deshpande, R. M. McMeeking, C. S. Chen, *Proc. Natl. Acad. Sci. USA* **2009**, *106*, 10097.
[66] S. S. Nunes, J. W. Miklas, J. Liu, R. Aschar-Sobbi, Y. Xiao, B. Zhang, J. Jiang, S. Masse, M. Gagliardi, A. Hsieh, N. Thavandiran, M. A. Laflamme, K. Nanthakumar, G. J. Gross, P. H. Backx, G. Keller, M. Radisic, *Nat. Methods* **2013**, *10*, 781.
[67] L. A. Vernetti, N. Senutovitch, R. Boltz, R. DeBiasio, T. Ying Shun, A. Gough, D. L. Taylor, *Exp. Biol. Med.* **2015**, *241*, 101.
[68] J. Fukuda, Y. Sakai, K. Nakazawa, *Biomaterials* **2006**, *27*, 1061.
[69] A. D. van der Meer, V. V. Orlova, P. ten Dijke, A. van den Berg, C. L. Mummery, *Lab Chip* **2013**, *13*, 3562.
[70] H.-C. Huang, Y.-J. Chang, W.-C. Chen, H. I. C. Harn, M.-J. Tang, C.-C. Wu, *Tissue Eng., Part A* **2013**, *19*, 2024.
[71] A. Odawara, M. Gotoh, I. Suzuki, *Lab Chip* **2013**, *13*, 2040.
[72] J. W. Lee, S.-Y. Jeong, J.-H. Lee, Y. Shin, S. Chung, H.-J. Kuh, *PloS One* **2016**, *11*, e0159013.
[73] J. Kang, D. W. Lee, H. J. Hwang, S.-E. Yeon, M.-Y. Lee, H.-J. Kuh, *Lab Chip* **2016**, *16*, 2265.
[74] Y. Zheng, J. Chen, M. Craven, N. W. Choi, S. Totorica, A. Diaz-Santana, P. Kermani, B. Hempstead, C. Fischbach-Teschl, J. A. Lopez, A. D. Stroock, *Proc. Natl. Acad. Sci. USA* **2012**, *109*, 9342.
[75] J. W. Gibble, P. M. Ness, *Transfusion* **1990**, *30*, 741.
[76] Van Susante, L. C. Job, P. Buma, L. Schuman, G. N. Homminga, W. B. van den Berg, R. P. Veth, *Biomaterials* **1999**, *20*, 1167.
[77] K. Nagamine, T. Kawashima, S. Sekine, Y. Ido, M. Kanzaki, M. Nishizawa, *Lab Chip* **2011**, *11*, 513.
[78] D. B. Kolesky, K. A. Homan, M. A. Skylar-Scott, J. A. Lewis, *Proc. Natl. Acad. Sci. USA* **2016**, *113*, 3179.
[79] A. Skardal, M. Devarasetty, S. Forsythe, A. Atala, S. Soker, *Biotechnol. Bioeng.* **2016**, *113*, 2020.
[80] D. T. Eddington, V. V. Abhyankar, M. Wu, C.-Y. Koh, A. V. Hatch, *PLoS One* **2016**, *11*, e0156341.
[81] A. Di Martino, M. Sittinger, M. V. Risbud, *Biomaterials* **2005**, *26*, 5983.
[82] N. Bhattarai, D. Edmondson, O. Veiseh, F. A. Matsen, M. Zhang, *Biomaterials* **2005**, *26*, 6176.
[83] A. Anitha, S. Sowmya, P. T. S. Kumar, S. Deepthi, K. P. Chennazhi, H. Ehrlich, M. Tsurkan, R. Jayakumar, *Prog. Polym. Sci.* **2014**, *39*, 1644.
[84] L. L. Chiu, M. Montgomery, Y. Liang, H. Liu, M. Radisic, *Proc. Natl. Acad. Sci. USA* **2012**, *109*, E3414.
[85] Y. S. Zhang, A. Arneri, S. Bersini, S.-R. Shin, K. Zhu, Z. Goli-Malekabadi, J. Aleman, C. Colosi, F. Busignani, V. Dell'Erba, C. Bishop, T. Shupe, D. Demarchi, M. Moretti, M. Rasponi, M. R. Dokmeci, A. Atala, A. Khademhosseini, *Biomaterials* **2016**, *110*, 45.
[86] X.-Y. Wang, Z.-H. Jin, B.-W. Gan, S.-W. Lv, M. Xie, W.-H. Huang, *Lab Chip* **2014**, *14*, 2709.
[87] K. Y. Lee, D. J. Mooney, *Prog. Polym. Sci.* **2012**, *37*, 106.
[88] J. H. Sung, C. Kam, M. L. Shuler, *Lab Chip* **2010**, *10*, 446.
[89] K. Alessandri, B. R. Sarangi, V. V. Gurchenkov, B. Sinha, T. R. Kiessling, L. Fetler, F. Rico, S. Scheuring, C. Lamaze, A. Simon, S. Geraldo, D. Vignjevic, H. Domejean, L. Rolland, A. Funfak, J. Bibette, N. Bremond, P. Nassoy, *Proc. Natl. Acad. Sci. USA* **2013**, *110*, 14843.
[90] H. F. Chan, Y. Zhang, K. W. Leong, *Small* **2016**, *12*, 2720.

[91] M. L. McCain, A. Agarwal, H. W. Nesmith, A. P. Nesmith, K. K. Parker, *Biomaterials* **2014**, *35*, 5462.
[92] C. Mummery, *Eur. J. Endocrinol.* **2004**, *151*, U7.
[93] L. Yang, M. H. Soonpaa, E. D. Adler, T. K. Roepke, S. J. Kattman, M. Kennedy, E. Henckaerts, K. Bonham, G. W. Abbott, R. M. Linden, L. J. Field, G. M. Keller, *Nature* **2008**, *453*, 524.
[94] L. Yang, S. V. Shridhar, M. Gerwitz, P. Soman, *Biofabrication* **2016**, *8*, 035015.
[95] J. Ramon-Azcon, S. Ahadian, R. Obregon, G. Camci-Unal, S. Ostrovidov, V. Hosseini, H. Kaji, K. Ino, H. Shiku, A. Khademhosseini, T. Matsue, *Lab Chip* **2012**, *12*, 2959.
[96] a) G. T. Christopherson, H. Song, H.-Q. Mao, *Biomaterials* **2009**, *30*, 556; b) Douezan, J. Dumond, F. Brochard-Wyart, *Soft Matter* **2012**, *8*, 4578; c) M. C. Cushing, K. S. Anseth, *Science* **2007**, *316*, 1133.
[97] S. Ahadian, L. Davenport Huyer, M. Estili, B. Yee, N. Smith, Z. Xu, Y. Sun, M. Radisic, *Acta Biomater.* **2016**, *52*, 81.
[98] B. Zhang, M. Montgomery, M. D. Chamberlain, S. Ogawa, A. Korolj, A. Pahnke, L. A. Wells, S. Masse, J. Kim, L. Reis, A. Momen, S. S. Nunes, A. R. Wheeler, K. Nanthakumar, G. Keller, M. V. Sefton, M. Radisic, *Nat. Mater.* **2016**, *15*, 669.
[99] L. A. Reis, L. L. Chiu, N. Feric, L. Fu, M. Radisic, *J. Tissue Eng. Regener. Med.* **2016**, *10*, 11.
[100] L. Cen, W. Liu, L. Cui, W. Zhang, Y. Cao, *Pediatr. Res.* **2008**, *63*, 492.
[101] L. Marinucci, C. Lilli, M. Guerra, S. Belcastro, E. Becchetti, G. Stabellini, E. M. Calvi, P. Locci, *J. Biomed. Mater. Res., Part A* **2003**, *67*, 504.
[102] K. Y. Lee, D. J. Mooney, *Prog. Polym. Sci.* **2012**, *37*, 106.
[103] L. L. Chiu, M. Montgomery, Y. Liang, H. Liu, M. Radisic, *Proc. Natl. Acad. Sci. USA* **2012**, *109*, E3414.
[104] Y. Cheng, Y. Yu, F. Fu, J. Wang, L. Shang, Z. Gu, Y. Zhao, *ACS Appl. Mater. Interfaces* **2016**, *8*, 1080.
[105] A. G. Ward, A. Courts, *The Science and Technology of Gelatin*, Academic Press, New York, **1977**.
[106] E. Gevaert, T. Billiet, H. Declercq, P. Dubruel, R. Cornelissen, *Macromol. Biosci.* **2014**, *14*, 419.
[107] A. Al-Abboodi, R. Tjeung, P. M. Doran, L. Y. Yeo, J. Friend, P. P. Yik Chan, *Adv. Healthcare Mater.* **2014**, *3*, 1655.
[108] a) G. Imparato, F. Urciuolo, C. Casale, P. A. Netti, *Biomaterials* **2013**, *34*, 7851; b) F. Urciuolo, A. Garziano, G. Imparato, V. Panzetta, S. Fusco, C. Casale, P. A. Netti, *Biofabrication* **2016**, *8*, 015010.
[109] Y. Xu, X. Wang, *Biotechnol. Bioeng.* **2015**, *112*, 1683.
[110] K. Yue, G. Trujillo-de Santiago, M. M. Alvarez, A. Tamayol, N. Annabi, A. Khademhosseini, *Biomaterials* **2015**, *73*, 254.
[111] a) A. Aung, I. S. Bhullar, J. Theprungsirikul, S. K. Davey, H. L. Lim, Y.-J. Chiu, X. Ma, S. Dewan, Y.-H. Lo, A. McCulloch, S. Varghese, *Lab Chip* **2016**, *16*, 153; b) N. Annabi, Š. Selimović, J. P. A. Cox, J. Ribas, M. A. Bakooshli, D. Heintze, A. S. Weiss, D. Cropek, A. Khademhosseini, *Lab Chip* **2013**, *13*, 3569.
[112] M. Kaminski, J. McDonagh, *J. Biol. Chem.* **1983**, *258*, 10530.
[113] A. Getgood, R. Brooks, L. Fortier, N. Rushton, *Bone Joint J.* **2009**, *91*, 565.
[114] S. A. Bencherif, *Synthesis, Characterization, and Evaluation of Biodegradable Polymers and Biomimetic Hydrogel Scaffolds for Biomedical Applications*, ProQuest, Michigan, **2009**.
[115] J. W. Gibble, P. M. Ness, *Transfusion* **1990**, *30*, 741.
[116] a) K. A. Ahmann, J. S. Weinbaum, S. L. Johnson, R. T. Tranquillo, *Tissue Eng., Part A* **2010**, *16*, 3261; b) H. Bruns, U. Kneser, S. Holzhüter, B. Roth, J. Kluth, P. M. Kaufmann, D. Kluth, H. C. Fiegel, *Tissue Eng.* **2005**, *11*, 1718; c) J. Meinhart, M. Fussenegger, W. Höbling, *Ann. Plast. Surg.* **1999**, *42*, 673.
[117] D. Huh, B. D. Matthews, A. Mammoto, M. Montoya-Zavala, H. Y. Hsin, D. E. Ingber, *Science* **2010**, *328*, 1662.
[118] G. Kogan, L. Šoltés, R. Stern, P. Gemeiner, *Biotechnol. Lett.* **2007**, *29*, 17.
[119] D. Jiang, J. Liang, P. W. Noble, *Annu. Rev. Cell Dev. Biol.* **2007**, *23*, 435.
[120] J. E. Rayahin, J. S. Buhrman, Y. Zhang, T. J. Koh, R. A. Gemeinhart, *ACS Biomater. Sci. Eng.* **2015**, *1*, 481.
[121] Y. D. Park, N. Tirelli, J. A. Hubbell, *Biomaterials* **2003**, *24*, 893.
[122] M. N. Collins, C. Birkinshaw, *Carbohydr. Polym.* **2013**, *92*, 1262.
[123] L.-S. Liu, A. Y. Thompson, M. A. Heidaran, J. W. Poser, R. C. Spiro, *Biomaterials* **1999**, *20*, 1097.
[124] R. M. Schek, J. M. Taboas, S. J. Segvich, S. J. Hollister, P. H. Krebsbach, *Tissue Eng.* **2004**, *10*, 1376.
[125] a) N. Bhattarai, J. Gunn, M. Zhang, *Adv. Drug Delivery Rev.* **2010**, *62*, 83; b) T. Kean, M. Thanou, *Adv. Drug Delivery Rev.* **2010**, *62*, 3.
[126] A. Di Martino, M. Sittinger, M. V. Risbud, *Biomaterials* **2005**, *26*, 5983.
[127] T. Jiang, M. Deng, R. James, L. S. Nair, C. T. Laurencin, *Acta Biomater.* **2014**, *10*, 1632.
[128] J. A. Rowley, G. Madlambayan, D. J. Mooney, *Biomaterials* **1999**, *20*, 45.
[129] M. S. Izydorczyk, S. W. Cui, Q. Wang, in *Food Carbohydrates: Chemistry, Physical Properties, and Applications*, (Eds.: C. G. Biliaderis, M. S. Izydorczyk), CRC Press, New York, **2005**, p. 293.
[130] J. Yu, Y. Gu, K. T. Du, S. Mihardja, R. E. Sievers, R. J. Lee, *Biomaterials* **2009**, *30*, 751.
[131] G. Dai, W. Wan, Y. Zhao, Z. Wang, W. Li, P. Shi, Y. Shen, *Biofabrication* **2016**, *8*, 025004.
[132] G. T. Christopherson, H. Song, H.-Q. Mao, *Biomaterials* **2009**, *30*, 556.
[133] S. Douezan, J. Dumond, F. Brochard-Wyart, *Soft Matter* **2012**, *8*, 4578.
[134] M. C. Cushing, K. S. Anseth, *Science* **2007**, *316*, 1133.
[135] a) E. J. Lee, F. K. Kasper, A. G. Mikos, *Ann. Biomed. Eng.* **2014**, *42*, 323; b) D. Shi, *Biomaterials and Tissue Engineering*, Springer Science & Business Media, **2013**; c) Z. Zhang, O. Ortiz, R. Goyal, J. Kohn, in *Principles of Tissue Engineering* (Eds: R. Langer, J. Vacanti), 4th ed., Academic Press, Boston **2014**, p. 441.
[136] D. L. Elbert, in *Biologically-Responsive Hybrid Biomaterials: A Reference for Material Scientists and Bioengineers*, Edited by E. Jabbari and A. Khademhosseini, World Scientific, Singapore, **2010**, p. 68.
[137] a) C. Fuoco, E. Sangalli, R. Vono, S. Testa, B. Sacchetti, M. V. Latronico, S. Bernardini, P. Madeddu, G. Cesareni, D. Seliktar, *Front. Physiol.* **2014**, *5*, 203; b) D. R. Albrecht, G. H. Underhill, A. Mendelson, S. N. Bhatia, *Lab Chip* **2007**, *7*, 702; c) G. D. Nicodemus, I. Villanueva, S. J. Bryant, *J. Biomed. Mater. Res., Part A* **2007**, *83*, 323.
[138] T. Billiet, M. Vandenhaute, J. Schelfhout, S. Van Vlierberghe, P. Dubruel, *Biomaterials* **2012**, *33*, 6020.
[139] J. M. Anderson, M. S. Shive, *Adv. Drug Delivery Rev.* **2012**, *64*, 72.
[140] R. T. Tran, P. Thevenot, D. Gyawali, J. C. Chiao, L. Tang, J. Yang, *Soft Matter* **2010**, *6*, 2449.
[141] G. Chen, T. Ushida, T. Tateishi, *Adv. Mater.* **2000**, *12*, 455.
[142] D. Dikovsky, H. Bianco-Peled, D. Seliktar, *Biomaterials* **2006**, *27*, 1496.
[143] Y. Mohammadi, H. Mirzadeh, F. Moztarzadeh, M. Soleimani, E. Jabbari, *Iran. Polym. J.* **2007**, *16*, 57.
[144] Y. Shirosaki, M. Hirai, S. Hayakawa, E. Fujii, M. A. Lopes, J. D. Santos, A. Osaka, *J. Biomed. Mater. Res., Part A* **2015**, *103*, 289.
[145] A. Rezaei Kolahchi, N. Khadem Mohtaram, H. Pezeshgi Modarres, M. H. Mohammadi, A. Geraili, P. Jafari, M. Akbari, A. Sanati-Nezhad, *Micromachines* **2016**, *7*, 162.
[146] F. Zheng, F. Fu, Y. Cheng, C. Wang, Y. Zhao, Z. Gu, *Small* **2016**, *12*, 2253.

[147] D. Huh, G. A. Hamilton, D. E. Ingber, *Trends Cell Biol.* **2011**, *21*, 745.
[148] M. J. Powers, K. Domansky, M. R. Kaazempur-Mofrad, A. Kalezi, A. Capitano, A. Upadhyaya, P. Kurzawski, K. E. Wack, D. B. Stolz, R. Kamm, L. G. Griffith, *Biotechnol. Bioeng.* **2002**, *78*, 257.
[149] S. Ostrovidov, J. Jiang, Y. Sakai, T. Fujii, *Biomed. Microdevices* **2004**, *6*, 279.
[150] K. Domansky, W. Inman, J. Serdy, A. Dash, M. H. Lim, L. G. Griffith, *Lab Chip* **2010**, *10*, 51.
[151] P. J. Lee, P. J. Hung, L. P. Lee, *Biotechnol. Bioeng.* **2007**, *97*, 1340.
[152] a) Z. Q. Feng, X. H. Chu, N. P. Huang, M. K. Leach, G. Wang, Y. C. Wang, Y. T. Ding, Z. Z. Gu, *Biomaterials* **2010**, *31*, 3604; b) Z. Q. Feng, X. Chu, N. P. Huang, T. Wang, Y. Wang, X. Shi, Y. Ding, Z. Z. Gu, *Biomaterials* **2009**, *30*, 2753; c) X. H. Chu, X. L. Shi, Z. Q. Feng, J. Y. Gu, H. Y. Xu, Y. Zhang, Z. Z. Gu, Y. T. Ding, *Biomaterials* **2009**, *30*, 4533.
[153] C. T. Ho, R. Z. Lin, R. J. Chen, C. K. Chin, S. E. Gong, H. Y. Chang, H. L. Peng, L. Hsu, T. R. Yew, S. F. Chang, C. H. Liu, *Lab Chip* **2013**, *13*, 3578.
[154] C. Du, K. Narayanan, M. F. Leong, A. C. Wan, *Biomaterials* **2014**, *35*, 6006.
[155] B. J. Kane, M. J. Zinner, M. L. Yarmush, M. Toner, *Anal. Chem* **2006**, *78*, 4291.
[156] C. H. Cho, J. Park, A. W. Tilles, F. Berthiaume, M. Toner, M. L. Yarmush, *BioTechniques* **2010**, *48*, 47.
[157] J. Schutte, B. Hagmeyer, F. Holzner, M. Kubon, S. Werner, C. Freudigmann, K. Benz, J. Bottger, R. Gebhardt, H. Becker, M. Stelzle, *Biomed. Microdevices* **2011**, *13*, 493.
[158] V. N. Goral, Y. C. Hsieh, O. N. Petzold, J. S. Clark, P. K. Yuen, R. A. Faris, *Lab Chip* **2010**, *10*, 3380.
[159] S. R. Khetani, S. N. Bhatia, *Nat. Biotechnol.* **2008**, *26*, 120.
[160] S. F. Wong, Y. No da, Y. Y. Choi, D. S. Kim, B. G. Chung, S. H. Lee, *Biomaterials* **2011**, *32*, 8087.
[161] S. A. Lee, Y. No da, E. Kang, J. Ju, D. S. Kim, S. H. Lee, *Lab Chip* **2013**, *13*, 3529.
[162] E. Holt, P. K. Lunde, O. M. Sejersted, G. Christensen, *Basic Res. Cardiol.* **1997**, *92*, 289.
[163] Y. B. (A.) Kang, T. R. Sodunke, J. Lamontagne, J. Cirillo, C. Rajiv, M. J. Bouchard, M. Noh, *Biotechnol. Bioeng.* **2015**, *112*, 2571.
[164] L. Prodanov, R. Jindal, S. S. Bale, M. Hegde, W. J. McCarty, I. Golberg, A. Bhushan, M. L. Yarmush, O. B. Usta, *Biotechnol. Bioeng.* **2016**, *113*, 241.
[165] Y. B. (A.) Kang, T. R. Sodunke, J. Lamontagne, J. Cirillo, C. Rajiv, M. J. Bouchard, M. Noh, *Biotechnol. Bioeng.* **2015**, *112*, 2571.
[166] Q. Zhou, D. Patel, T. Kwa, A. Haque, Z. Matharu, G. Stybayeva, Y. Gao, A. M. Diehl, A. Revzin, *Lab Chip* **2015**, *15*, 4467.
[167] N. Mori, Y. Morimoto, S. Takeuchi, *Biomaterials* **2017**, *116*, 48.
[168] B. Ataç, I. Wagner, R. Horland, R. Lauster, U. Marx, A. G. Tonevitsky, R. P. Azar, G. Lindner, *Lab Chip* **2013**, *13*, 3555.
[169] Q. Ramadan, F. C. W. Ting, *Lab Chip* **2016**, *16*, 1899.
[170] H. E. Abaci, K. Gledhill, Z. Guo, A. M. Christiano, M. L. Shuler, *Lab Chip* **2015**, *15*, 882.
[171] K. Schimek, M. Busek, S. Brincker, B. Groth, S. Hoffmann, R. Lauster, G. Lindner, A. Lorenz, U. Menzel, F. Sonntag, H. Walles, U. Marx, R. Horland, *Lab Chip* **2013**, *13*, 3588.
[172] D. Kim, S. Finkenstaedt-Quinn, K. R. Hurley, J. T. Buchman, C. L. Haynes, *Analyst* **2014**, *139*, 906.
[173] S. Kim, H. Lee, M. Chung, N. L. Jeon, *Lab Chip* **2013**, *13*, 1489.
[174] K. Namdee, A. J. Thompson, P. Charoenphol, O. Eniola-Adefeso, *Langmuir* **2013**, *29*, 2530.
[175] J. Kusunose, H. Zhang, M. K. Gagnon, T. Pan, S. I. Simon, K. W. Ferrara, *Ann. Biomed. Eng.* **2013**, *41*, 89.
[176] G. Lamberti, Y. Tang, B. Prabhakarpandian, Y. Wang, K. Pant, M. F. Kiani, B. Wang, *Microvasc. Res.* **2013**, *89*, 107.
[177] J. P. Morgan, P. F. Delnero, Y. Zheng, S. S. Verbridge, J. Chen, M. Craven, N. W. Choi, A. Diaz-Santana, P. Kermani, B. Hempstead, J. A. Lopez, T. N. Corso, C. Fischbach, A. D. Stroock, *Nat. Protoc.* **2013**, *8*, 1820.
[178] C. F. Buchanan, S. S. Verbridge, P. P. Vlachos, M. N. Rylander, *Cell Adhes. Migr.* **2014**, *8*, 517.
[179] J. S. Jeon, S. Bersini, M. Gilardi, G. Dubini, J. L. Charest, M. Moretti, R. D. Kamm, *Proc. Natl. Acad. Sci. USA* **2015**, *112*, 6.
[180] A. Grosberg, P. W. Alford, M. L. McCain, K. K. Parker, *Lab Chip* **2011**, *11*, 4165.
[181] A. Agarwal, J. A. Goss, A. Cho, M. L. McCain, K. K. Parker, *Lab Chip* **2013**, *13*, 3599.
[182] J. U. Lind, T. A. Busbee, A. D. Valentine, F. S. Pasqualini, H. Yuan, M. Yadid, S.-J. Park, A. Kotikian, A. P. Nesmith, P. H. Campbell, J. J. Vlassak, J. A. Lewis, K. K. Parker, *Nat. Mater.* **2016**, *16*, 303.
[183] L. Ren, W. Liu, Y. Wang, J. C. Wang, Q. Tu, J. Xu, R. Liu, S. F. Shen, J. Wang, *Anal. Chem.* **2013**, *85*, 235.
[184] A. Mathur, P. Loskill, K. Shao, N. Huebsch, S. Hong, S. G. Marcus, N. Marks, M. Mandegar, B. R. Conklin, L. P. Lee, K. E. Healy, *Sci. Rep.* **2015**, *5*, 8883.
[185] G. Wang, M. L. McCain, L. Yang, A. He, F. S. Pasqualini, A. Agarwal, H. Yuan, D. Jiang, D. Zhang, L. Zangi, J. Geva, A. E. Roberts, Q. Ma, J. Ding, J. Chen, D. Z. Wang, K. Li, J. Wang, R. J. Wanders, W. Kulik, F. M. Vaz, M. A. Laflamme, C. E. Murry, K. R. Chien, R. I. Kelley, G. M. Church, K. K. Parker, W. T. Pu, *Nat. Med.* **2014**, *20*, 616.
[186] H. Kaji, T. Ishibashi, K. Nagamine, M. Kanzaki, M. Nishizawa, *Biomaterials* **2010**, *31*, 6981.
[187] S. Sirivisoot, B. S. Harrison, *Int. J. Nanomed.* **2011**, *6*, 2483.
[188] J. Ramón-Azcón, S. Ahadian, M. Estili, X. Liang, S. Ostrovidov, H. Kaji, H. Shiku, M. Ramalingam, K. Nakajima, Y. Sakka, A. Khademhosseini, T. Matsue, *Adv. Mater.* **2013**, *25*, 4028.
[189] Y. Morimoto, M. Kato-Negishi, H. Onoe, S. Takeuchi, *Biomaterials* **2013**, *34*, 9413.
[190] N. J. Douville, P. Zamankhan, Y. C. Tung, R. Li, B. L. Vaughan, C. F. Tai, J. White, P. J. Christensen, J. B. Grotberg, S. Takayama, *Lab Chip* **2011**, *11*, 609.
[191] Z. Xu, Y. Gao, Y. Hao, E. Li, Y. Wang, J. Zhang, W. Wang, Z. Gao, Q. Wang, *Biomaterials* **2013**, *34*, 4109.
[192] D. Huh, B. D. Matthews, A. Mammoto, M. Montoya-Zavala, H. Y. Hsin, D. E. Ingber, *Science* **2010**, *328*, 1662.
[193] H. Tavana, P. Zamankhan, P. J. Christensen, J. B. Grotberg, S. Takayama, *Biomed. Microdevices* **2011**, *13*, 731.
[194] I. B. Gontcharov, I. V. Kovachevich, S. L. Pool, O. L. Navinkov, M. R. Barratt, V. V. Bogomolov, N. House, *Aviat., Space Environ. Med.* **2005**, *76*, 692.
[195] K. H. Benam, R. Villenave, C. Lucchesi, A. Varone, C. Hubeau, H. H. Lee, S. E. Alves, M. Salmon, T. C. Ferrante, J. C. Weaver, A. Bahinski, G. A. Hamilton, D. E. Ingber, *Nat. Methods* **2016**, *13*, 151.
[196] Y.-s. Torisawa, C. S. Spina, T. Mammoto, A. Mammoto, J. C. Weaver, T. Tat, J. J. Collins, D. E. Ingber, *Nat. Methods* **2014**, *11*, 663.
[197] A. Bruce, R. Evans, R. Mezan, L. Shi, B. S. Moses, K. H. Martin, L. F. Gibson, Y. Yang, *PloS One* **2015**, *10*, e0140506.
[198] Y.-S. Torisawa, T. Mammoto, E. Jiang, A. Jiang, A. Mammoto, A. L. Watters, A. Bahinski, D. E. Ingber, *Tissue Eng., Part C* **2016**, *22*, 509.
[199] A. M. Taylor, M. Blurton-Jones, S. W. Rhee, D. H. Cribbs, C. W. Cotman, N. L. Jeon, *Nat. Methods* **2005**, *2*, 599.
[200] L. Griep, F. Wolbers, B. De Wagenaar, P. Ter Braak, B. Weksler, I. A. Romero, P. Couraud, I. Vermes, A. Van Der Meer, A. Van den Berg, *Biomed. Microdevices* **2013**, *15*, 145.

[201] F. R. Walter, S. Valkai, A. Kincses, A. Petneházi, T. Czeller, S. Veszelka, P. Ormos, M. A. Deli, A. Dér, *Sens. Actuators, B* **2016**, *222*, 1209.
[202] Y. I. Wang, H. E. Abaci, M. L. Shuler, *Biotechnol. Bioeng.* **2017**, *114*, 184.
[203] J. Park, S. Kim, S. I. Park, Y. Choe, J. Li, A. Han, *J. Neurosci. Methods* **2014**, *221*, 166.
[204] F. Bianco, N. Tonna, R. D. Lovchik, R. Mastrangelo, R. Morini, A. Ruiz, E. Delamarche, M. Matteoli, *Anal. Chem.* **2012**, *84*, 9833.
[205] R. Booth, H. Kim, *Lab Chip* **2012**, *12*, 1784.
[206] a) J. A. Kim, H. N. Kim, S.-K. Im, S. Chung, J. Y. Kang, N. Choi, *Biomicrofluidics* **2015**, *9*, 024115; b) H. Cho, J. H. Seo, K. H. Wong, Y. Terasaki, J. Park, K. Bong, K. Arai, E. H. Lo, D. Irimia, *Sci. Rep.* **2015**, *5*, 15222.
[207] A. K. H. Achyuta, A. J. Conway, R. B. Crouse, E. C. Bannister, R. N. Lee, C. P. Katnik, A. A. Behensky, J. Cuevas, S. S. Sundaram, *Lab Chip* **2013**, *13*, 542.
[208] K. L. Sellgren, B. T. Hawkins, S. Grego, *Biomicrofluidics* **2015**, *9*, 061102.
[209] Y. Berdichevsky, K. J. Staley, M. L. Yarmush, *Lab Chip* **2010**, *10*, 999.
[210] J. Park, B. K. Lee, G. S. Jeong, J. K. Hyun, C. J. Lee, S.-H. Lee, *Lab Chip* **2015**, *15*, 141.
[211] X. Lu, J. S. Kim-Han, K. L. O'Malley, S. E. Sakiyama-Elbert, *J. Neurosci. Methods* **2012**, *209*, 35.
[212] R. Booth, H. Kim, *Ann. Biomed. Eng.* **2014**, *42*, 2379.
[213] J. A. Brown, V. Pensabene, D. A. Markov, V. Allwardt, M. D. Neely, M. Shi, C. M. Britt, O. S. Hoilett, Q. Yang, B. M. Brewer, *Biomicrofluidics* **2015**, *9*, 054124.
[214] L. Cucullo, N. Marchi, M. Hossain, D. Janigro, *J. Cereb. Blood Flow Metab.* **2011**, *31*, 767.
[215] A. Herland, A. D. van der Meer, E. A. FitzGerald, T.-E. Park, J. J. Sleeboom, D. E. Ingber, *PloS One* **2016**, *11*, e0150360.
[216] J. Seo, D. Huh, **2015**.
[217] H. J. Kim, H. Li, J. J. Collins, D. E. Ingber, *Proc. Natl. Acad. Sci. USA* **2016**, *113*, E7.
[218] H. Kimura, T. Yamamoto, H. Sakai, Y. Sakai, T. Fujii, *Lab Chip* **2008**, *8*, 741.
[219] J. H. Kang, M. Super, C. W. Yung, R. M. Cooper, K. Domansky, A. R. Graveline, T. Mammoto, J. B. Berthet, H. Tobin, M. J. Cartwright, A. L. Watters, M. Rottman, A. Waterhouse, A. Mammoto, N. Gamini, M. J. Rodas, A. Kole, A. Jiang, T. M. Valentin, A. Diaz, K. Takahashi, D. E. Ingber, *Nat. Med.* **2014**, *20*, 1211.
[220] K.-J. Jang, A. P. Mehr, G. A. Hamilton, L. A. McPartlin, S. Chung, K.-Y. Suh, D. E. Ingber, *Integr. Biol.* **2013**, *5*, 1119.
[221] K. A. Homan, D. B. Kolesky, M. A. Skylar-Scott, J. Herrmann, H. Obuobi, A. Moisan, J. A. Lewis, *Sci. Rep.* **2016**, *6*, 34845.
[222] G. Ligresti, R. J. Nagao, J. Xue, Y. J. Choi, J. Xu, S. Ren, T. Aburatani, S. K. Anderson, J. W. MacDonald, T. K. Bammler, *J. Am. Soc. Nephrol.* **2015**, *27*, 2370.
[223] M. M. Grafton, L. Wang, P.-A. Vidi, J. Leary, S. A. Lelievre, *Integr. Biol.* **2011**, *3*, 451.
[224] A. B. Theberge, J. Yu, E. W. Young, W. A. Ricke, W. Bushman, D. J. Beebe, *Anal. Chem.* **2015**, *87*, 3239.
[225] L. L. Bischel, B. P. Casavant, P. A. Young, K. W. Eliceiri, H. S. Basu, D. J. Beebe, *Integr. Biol.* **2014**, *6*, 627.
[226] K. E. Sung, G. Su, C. Pehlke, S. M. Trier, K. W. Eliceiri, P. J. Keely, A. Friedl, D. J. Beebe, *Biomaterials* **2009**, *30*, 4833.
[227] I. K. Zervantonakis, S. K. Hughes-Alford, J. L. Charest, J. S. Condeelis, F. B. Gertler, R. D. Kamm, *Proc. Natl. Acad. Sci. USA* **2012**, *109*, 13515.
[228] J. W. Song, S. P. Cavnar, A. C. Walker, K. E. Luker, M. Gupta, Y.-C. Tung, G. D. Luker, S. Takayama, *PLoS One* **2009**, *4*, e5756.
[229] Y. Shin, J. S. Jeon, S. Han, G. S. Jung, S. Shin, S. H. Lee, R. Sudo, R. D. Kamm, S. Chung, *Lab Chip* **2011**, *11*, 2175.
[230] J. S. Jeon, S. Bersini, M. Gilardi, G. Dubini, J. L. Charest, M. Moretti, R. D. Kamm, *Proc. Natl. Acad. Sci. USA* **2015**, *112*, 214.
[231] S. Chung, R. Sudo, P. J. Mack, C. R. Wan, V. Vickerman, R. D. Kamm, *Lab Chip* **2009**, *9*, 269.
[232] L. Shintu, R. G. Baudoin, V. Navratil, J.-M. Prot, C. m. Pontoizeau, M. Defernez, B. J. Blaise, C. l. Domange, A. R. Péry, P. Toulhoat, *Anal. Chem.* **2012**, *84*, 1840.
[233] R. Jellali, P. Paullier, M.-J. Fleury, E. Leclerc, *Sens. Actuators, B* **2016**, *229*, 396.
[234] M. B. Esch, G. J. Mahler, T. Stokol, M. L. Shuler, *Lab Chip* **2014**, *14*, 3081.
[235] T. Bricks, J. Hamon, M. J. Fleury, R. Jellali, F. Merlier, Y. E. Herpe, A. Seyer, J. M. Regimbeau, F. Bois, E. Leclerc, *Biopharm. Drug Dispos.* **2015**, *36*, 275.
[236] I. Maschmeyer, T. Hasenberg, A. Jaenicke, M. Lindner, A. K. Lorenz, J. Zech, L.-A. Garbe, F. Sonntag, P. Hayden, S. Ayehunie, *Eur. J. Pharm. Biopharm.* **2015**, *95*, 77.
[237] I. Wagner, E.-M. Materne, S. Brincker, U. Süßbier, C. Frädrich, M. Busek, F. Sonntag, D. A. Sakharov, E. V. Trushkin, A. G. Tonevitsky, *Lab Chip* **2013**, *13*, 3538.
[238] C. Zhang, Z. Zhao, N. A. A. Rahim, D. Noort, H. Yu, *Lab Chip* **2009**, *9*, 3185.
[239] I. Maschmeyer, A. K. Lorenz, K. Schimek, T. Hasenberg, A. P. Ramme, J. Hübner, M. Lindner, C. Drewell, S. Bauer, A. Thomas, *Lab Chip* **2015**, *15*, 2688.
[240] K. Viravaidya, M. L. Shuler, *Biotechnol. Prog.* **2004**, *20*, 590.
[241] J. M. Polak, A. E. Bishop, *Ann. N. Y. Acad. Sci.* **2006**, *1068*, 352.
[242] G. Stacey, *Primary Cell Cultures and Immortal Cell Lines, eLS*, Wiley, **2001**.
[243] P. Gangatirkar, S. Paquet-Fifield, A. Li, R. Rossi, P. Kaur, *Nat. Protoc.* **2007**, *2*, 178.
[244] Y.-C. Toh, T. C. Lim, D. Tai, G. Xiao, D. van Noort, H. Yu, *Lab Chip* **2009**, *9*, 2026.
[245] A. Rossini, A. Zacheo, D. Mocini, P. Totta, A. Facchiano, R. Castoldi, P. Sordini, G. Pompilio, D. Abeni, M. C. Capogrossi, *J. Mol. Cell. Cardiol.* **2008**, *44*, 683.
[246] P. Scherp, N. Putluri, G. J. LeBlanc, Z. Q. Wang, X. H. Zhang, Y. Yu, D. Ribnicky, W. T. Cefalu, I. Kheterpal, *J. Proteomics* **2012**, *75*, 3199.
[247] H. A. Golpon, V. A. Fadok, L. Taraseviciene-Stewart, R. Scerbavicius, C. Sauer, T. Welte, P. M. Henson, N. F. Voelkel, *FASEB J.* **2004**, *18*, 1716.
[248] J. Beigel, K. Fella, P.-J. Kramer, M. Kroeger, P. Hewitt, *Toxicol. In Vitro* **2008**, *22*, 171.
[249] D. Howard, L. D. Buttery, K. M. Shakesheff, S. J. Roberts, *J. Anat.* **2008**, *213*, 66.
[250] D. Hare, S. Collins, B. Cuddington, K. Mossman, *Viruses* **2016**, *8*, 297.
[251] M. A. Blasco, E. Maunsell, C. Diorio, *Cancer Epidemiol., Biomarkers Prev.* **2016**.
[252] C. Pan, C. Kumar, S. Bohl, U. Klingmueller, M. Mann, *Mol. Cell. Proteomics* **2009**, *8*, 443.
[253] K. Takahashi, S. Yamanaka, *Cell* **2006**, *126*, 663.
[254] J. Yu, M. A. Vodyanik, K. Smuga-Otto, J. Antosiewicz-Bourget, J. L. Frane, S. Tian, J. Nie, G. A. Jonsdottir, V. Ruotti, R. Stewart, I. I. Slukvin, J. A. Thomson, *Science* **2007**, *318*, 1917.
[255] Z. Ye, H. Zhan, P. Mali, S. Dowey, D. M. Williams, Y.-Y. Jang, C. V. Dang, J. L. Spivak, A. R. Moliterno, L. Cheng, *Blood* **2009**, *114*, 5473.
[256] S. Conrad, M. Renninger, J. Hennenlotter, T. Wiesner, L. Just, M. Bonin, W. Aicher, H.-J. Bühring, U. Mattheus, A. Mack, *Nature* **2008**, *456*, 344.
[257] T. Aasen, A. Raya, M. J. Barrero, E. Garreta, A. Consiglio, F. Gonzalez, R. Vassena, J. Bilić, V. Pekarik, G. Tiscornia, *Nat. Biotechnol.* **2008**, *26*, 1276.

[258] M. Stadtfeld, K. Brennand, K. Hochedlinger, *Curr. Biol.* **2008**, *18*, 890.
[259] E. Matsa, J. H. Ahrens, J. C. Wu, *Physiol. Rev.* **2016**, *96*, 1093.
[260] J. Kim, H. Lee, Š. Selimović, R. Gauvin, H. Bae, *Drug Saf.* **2015**, *38*, 409.
[261] J. Xu, Y. Du, H. Deng, *Cell Stem Cell* **2015**, *16*, 119.
[262] V. K. Bajpai, S. T. Andreadis, *Tissue Eng., Part B* **2012**, *18*, 405.
[263] G. G. Giobbe, F. Michielin, C. Luni, S. Giulitti, S. Martewicz, S. Dupont, A. Floreani, N. Elvassore, *Nat. Methods* **2015**, *12*, 637.
[264] G. Vunjak-Novakovic, S. Bhatia, C. Chen, K. Hirschi, *Stem Cell Res. Ther.* **2013**, *4*, 1.
[265] K. K. Parker, D. E. Ingber, *Philos. Trans. R. Soc. London, Ser. B* **2007**, *362*, 1267.
[266] W. P. Daley, S. B. Peters, M. Larsen, *J. Cell Sci.* **2008**, *121*, 255.
[267] T. Dvir, B. P. Timko, D. S. Kohane, R. Langer, *Nat. Nanotechnol.* **2011**, *6*, 13.
[268] A. H. Li, P. P. Liu, F. J. Villarreal, R. A. Garcia, *Circ. Res.* **2014**, *114*, 916.
[269] T. K. Borg, K. Rubin, W. Carver, A. Samarel, L. Terracio, *Trends Cardiovasc. Med.* **1996**, *6*, 65.
[270] R. G. Wells, *Biochim. Biophys. Acta* **2013**, *1832*, 884.
[271] J. Diez, R. Querejeta, B. Lopez, A. Gonzalez, M. Larman, J. L. Martinez Ubago, *Circulation* **2002**, *105*, 2512.
[272] a) Q. Y. Zhang, Y. Y. Zhang, J. Xie, C. X. Li, W. Y. Chen, B. L. Liu, X. A. Wu, S. N. Li, B. Huo, L. H. Jiang, H. C. Zhao, *Sci. Rep.* **2014**, *4*, 6215; b) Y. Gu, Y. Ji, Y. Zhao, Y. Liu, F. Ding, X. Gu, Y. Yang, *Biomaterials* **2012**, *33*, 6672.
[273] A. J. Engler, M. A. Griffin, S. Sen, C. G. Bönnemann, H. L. Sweeney, D. E. Discher, *J. Cell Biol.* **2004**, *166*, 877.
[274] A. Khademhosseini, R. Langer, *Biomaterials* **2007**, *28*, 5087.
[275] H. Geckil, F. Xu, X. Zhang, S. Moon, U. Demirci, *Nanomedicine* **2010***5*, 469.
[276] N. Zaari, P. Rajagopalan, S. K. Kim, A. J. Engler, J. Y. Wong, *Adv. Mater.* **2004**, *16*, 2133.
[277] J. A. Burdick, A. Khademhosseini, R. Langer, *Langmuir* **2004**, *20*, 5153.
[278] S. Ahadian, L. D. Huyer, M. Estili, B. Yee, N. Smith, Z. Xu, Y. Sun, M. Radisic, *Acta Biomater.* **2016**, *52*, 81.
[279] G. Vunjak-Novakovic, N. Tandon, A. Godier, R. Maidhof, A. Marsano, T. P. Martens, M. Radisic, *Tissue Eng., Part B* **2009**, *16*, 169.
[280] W. L. Stoppel, D. L. Kaplan, L. D. Black III, *Adv. Drug Delivery Rev.* **2016**, *96*, 135.
[281] B. Liau, D. Zhang, N. Bursac, *Regener. Med.* **2012**, *7*, 187.
[282] L. Ghasemi-Mobarakeh, M. P. Prabhakaran, M. Morshed, M. H. Nasr-Esfahani, S. Ramakrishna, *Tissue Eng., Part A* **2009**, *15*, 3605.
[283] A. Subramanian, U. M. Krishnan, S. Sethuraman, *J. Biomed. Sci.* **2009**, *16*, 108.
[284] H. Fujita, T. Nedachi, M. Kanzaki, *Exp. Cell Res.* **2007**, *313*, 1853.
[285] S. S. Nunes, J. W. Miklas, J. Liu, R. Aschar-Sobbi, Y. Xiao, B. Zhang, J. Jiang, S. Massé, M. Gagliardi, A. Hsieh, N. Thavandiran, M. A. Laflamme, K. Nanthakumar, G. J. Gross, P. H. Backx, G. Keller, M. Radisic, *Nat. Methods* **2013**, *10*, 781.
[286] J. W. Miklas, S. S. Nunes, A. Sofla, L. Reis, A. Pahnke, Y. Xiao, C. Laschinger, M. Radisic, *Biofabrication* **2014**, *6*, 024113.
[287] S. Rangarajan, L. Madden, N. Bursac, *Ann. Biomed. Eng.* **2014**, *42*, 1391.
[288] K. Donnelly, A. Khodabukus, A. Philp, L. Deldicque, R. G. Dennis, K. Baar, *Tissue Eng., Part C* **2010**, *16*, 711.
[289] G. Kaur, R. Adhikari, P. Cass, M. Bown, P. Gunatillake, *RSC Adv.* **2015**, *5*, 37553.
[290] X. Jia, F. Wei, *Top. Curr. Chem.* **2017**, *375*, 18.
[291] Y. S. Ahadian, S. Yamada, J. Ramón-Azcón, M. Estili, X. Liang, K. Nakajima, H. Shiku, A. Khademhosseini, T. Matsue, *Acta Biomater.* **2016**, *31*, 134.
[292] C. E. Schmidt, V. R. Shastri, J. P. Vacanti, R. Langer, *Proc. Natl. Acad. Sci. USA* **1997**, *94*, 8948.
[293] S. Paulose, R. Raghavan, B. K. George, *J. Colloid Interface Sci.* **2017**, *494*, 64.
[294] I.-C. Liao, J. B. Liu, N. Bursac, K. W. Leong, *Cell. Mol. Bioeng.* **2008**, *1*, 133.
[295] C. Fink, S. Ergün, D. Kralisch, U. Remmers, J. Weil, T. Eschenhagen, *FASEB J.* **2000**, *14*, 669.
[296] W. H. Zimmermann, C. Fink, D. Kralisch, U. Remmers, J. Weil, T. Eschenhagen, *Biotechnol. Bioeng.* **2000**, *68*, 106.
[297] R. D. Abbott, D. L. Kaplan, *Trends Biotechnol.* **2015**, *33*, 401.
[298] S. R. Peyton, C. M. Ghajar, C. B. Khatiwala, A. J. Putnam, *Cell Biochem. Biophys.* **2007**, *47*, 300.
[299] a) F. Kurth, K. Eyer, A. Franco-Obregón, P. S. Dittrich, *Curr. Opin. Chem. Biol.* **2012**, *16*, 400; b) W. J. Polacheck, R. Li, S. G. M. Uzel, R. D. Kamm, *Lab Chip* **2013**, *13*, 2252.
[300] P. A. Galie, D.-H. T. Nguyen, C. K. Choi, D. M. Cohen, P. A. Janmey, C. S. Chen, *Proc. Natl. Acad. Sci. USA* **2014**, *111*, 7968.
[301] J. Zhu, *Biomaterials* **2010**, *31*, 4639.
[302] R. H. W. Lam, Y. Sun, W. Chen, J. Fu, *Lab Chip* **2012**, *12*, 1865.
[303] B. Tian, J. Liu, T. Dvir, L. Jin, J. H. Tsui, Q. Qing, Z. Suo, R. Langer, D. S. Kohane, C. M. Lieber, *Nat. Mater.* **2012**, *11*, 986.
[304] R. Feiner, L. Engel, S. Fleischer, M. Malki, I. Gal, A. Shapira, Y. Shacham-Diamand, T. Dvir, *Nat. Mater.* **2016**, *15*, 679.
[305] X. Dai, W. Zhou, T. Gao, J. Liu, C. M. Lieber, *Nat. Nanotechnol.* **2016**, *11*, 776.
[306] a) R. A. Civitarese, A. Kapus, C. A. McCulloch, K. A. Connelly, *Basic Res. Cardiol.* **2017**, *112*, 6; b) R. A. Civitarese, I. Talior-Volodarsky, J. F. Desjardins, G. Kabir, J. Switzer, M. Mitchell, A. Kapus, C. A. McCulloch, D. Gullberg, K. A. Connelly, *Am. J. Physiol.: Heart Circ. Physiol.* **2016**, *311*, H96.
[307] C. M. Puleo, W. McIntosh Ambrose, T. Takezawa, J. Elisseeff, T.-H. Wang, *Lab Chip* **2009**, *9*, 3221.
[308] K. Maedler, K. S. Sankar, B. J. Green, A. R. Crocker, J. E. Verity, S. M. Altamentova, J. V. Rocheleau, *PLoS One* **2011**, *6*, e24904.
[309] R. Derda, A. Laromaine, A. Mammoto, S. K. Y. Tang, T. Mammoto, D. E. Ingber, G. M. Whitesides, *Proc. Natl. Acad. Sci. USA* **2009**, *106*, 18457.
[310] Y. Lu, A. A. Aimetti, R. Langer, Z. Gu, *Nat. Rev. Mater.* **2016**, *2*, 16075.
[311] M. E. Kolewe, H. Park, C. Gray, X. Ye, R. Langer, L. E. Freed, *Adv. Mater.* **2013**, *25*, 4459.
[312] H. Bae, H. Chu, F. Edalat, J. M. Cha, S. Sant, A. Kashyap, A. F. Ahari, C. H. Kwon, J. W. Nichol, S. Manoucheri, B. Zamanian, Y. Wang, A. Khademhosseini, *J. Tissue Eng. Regener. Med.* **2014**, *8*, 1.
[313] S. S. Nunes, N. Feric, A. Pahnke, J. W. Miklas, M. Li, J. Coles, M. Gagliardi, G. Keller, M. Radisic, *ACS Biomater. Sci. Eng.* **2016**.
[314] B. Mohanraj, A. J. Farran, R. L. Mauck, G. R. Dodge, *J. Biomech.* **2014**, *47*, 2137.
[315] K. Lee, E. A. Silva, D. J. Mooney, *J. R. Soc., Interface* **2010**, *8*, 153.
[316] N. L. Ward, P. Van Slyke, C. Sturk, M. Cruz, D. J. Dumont, *Dev. Dyn.* **2004**, *229*, 500.
[317] M. Ehrbar, *Circ. Res.* **2004**, *94*, 1124.
[318] R. Chapanian, B. G. Amsden, *J. Controlled Release* **2010**, *143*, 53.
[319] A. Marui, A. Kanematsu, K. Yamahara, K. Doi, T. Kushibiki, M. Yamamoto, H. Itoh, T. Ikeda, Y. Tabata, M. Komeda, *J. Vasc. Surg.* **2005**, *41*, 82.
[320] L. L. Y. Chiu, M. Radisic, *J. Controlled Release* **2011**, *155*, 376.
[321] B. Li, J. M. Davidson, S. A. Guelcher, *Biomaterials* **2009**, *30*, 3486.
[322] L. Meinel, E. Zoidis, J. Zapf, P. Hassa, M. O. Hottiger, J. A. Auer, R. Schneider, B. Gander, V. Luginbuehl, R. Bettschart-Wolfisberger, O. E. Illi, H. P. Merkle, B. v. Rechenberg, *Bone* **2003**, *33*, 660.
[323] H. Park, J. S. Temenoff, T. A. Holland, Y. Tabata, A. G. Mikos, *Biomaterials* **2005**, *26*, 7095.

[324] J. H. Kim, K. Kushiro, N. A. Graham, A. R. Asthagiri, *Proc. Natl. Acad. Sci. USA* **2009**, *106*, 11149.
[325] P. Yilgor, N. Hasirci, V. Hasirci, *J. Biomed. Mater. Res., Part A* **2010**, *93A*, 528.
[326] Y. Huang, D. Cai, P. Chen, *Anal. Chem.* **2011**, *83*, 4393.
[327] N. G. Rim, C. S. Shin, H. Shin, *Biomed. Mater.* **2013**, *8*, 014102.
[328] D. Huh, D. C. Leslie, B. D. Matthews, J. P. Fraser, S. Jurek, G. A. Hamilton, K. S. Thorneloe, M. A. McAlexander, D. E. Ingber, *Sci. Transl. Med.* **2012**, *4*, 159ra147.
[329] T. R. Polte, G. S. Eichler, N. Wang, D. E. Ingber, *Am. J. Physiol.: Cell Physiol.* **2004**, *286*, C518.
[330] a) Y. Kikuchi, K. Sato, Y. Mizuguchi, *Microvasc. Res.* **1994**, *47*, 126; b) Y. Kikuchi, K. Sato, H. Ohki, T. Kaneko, *Microvasc. Res.* **1992**, *44*, 226.
[331] J. Kim, M. Junkin, D.-H. Kim, S. Kwon, Y. S. Shin, P. K. Wong, B. K. Gale, *Microfluid. Nanofluid.* **2009**, *7*, 149.
[332] J. Tien, *Curr. Opin. Chem. Eng.* **2014**, *3*, 36.
[333] R. Y. Kwon, D. R. Meays, W. J. Tang, J. A. Frangos, *J. Bone Miner. Res.* **2010**, *25*, 1798.
[334] P. J. Lee, P. J. Hung, L. P. Lee, *Biotechnol. Bioeng.* **2007**, *97*, 1340.
[335] C.-C. Wang, K.-C. Yang, K.-H. Lin, H.-C. Liu, F.-H. Lin, *Biomaterials* **2011**, *32*, 7118.
[336] B. G. Chung, L. A. Flanagan, S. W. Rhee, P. H. Schwartz, A. P. Lee, E. S. Monuki, N. L. Jeon, *Lab Chip* **2005**, *5*, 401.
[337] H. Andersson, A. Van Den Berg, *Lab Chip* **2004**, *4*, 98.
[338] G. T. Vladisavljević, I. Kobayashi, M. Nakajima, *Microfluid. Nanofluid.* **2012**, *13*, 151.
[339] L. L. Bischel, E. W. K. Young, B. R. Mader, D. J. Beebe, *Biomaterials* **2013**, *34*, 1471.
[340] S. J. Trietsch, G. D. Israëls, J. Joore, T. Hankemeier, P. Vulto, *Lab Chip* **2013**, *13*, 3548.
[341] V. van Duinen, S. J. Trietsch, J. Joore, P. Vulto, T. Hankemeier, *Curr. Opin. Biotechnol.* **2015**, *35*, 118.
[342] S. Takayama, E. Ostuni, P. LeDuc, K. Naruse, D. E. Ingber, G. M. Whitesides, *Nature* **2001**, *411*, 1016.
[343] J. Pihl, J. Sinclair, E. Sahlin, M. Karlsson, F. Petterson, J. Olofsson, O. Orwar, *Anal. Chem.* **2005**, *77*, 3897.
[344] M. Junkin, S. Tay, *Lab Chip* **2014**, *14*, 1246.
[345] A. D. van der Meer, K. Vermeul, A. A. Poot, J. Feijen, I. Vermes, *Am. J. Physiol.: Heart Circ. Physiol.* **2010**, *298*, H719.
[346] S. Han, J.-J. Yan, Y. Shin, J. J. Jeon, J. Won, H. E. Jeong, R. D. Kamm, Y.-J. Kim, S. Chung, *Lab Chip* **2012**, *12*, 3861.
[347] T. Nisisako, T. Torii, *Lab Chip* **2008**, *8*, 287.
[348] Y. Wang, W.-Y. Lin, K. Liu, R. J. Lin, M. Selke, H. C. Kolb, N. Zhang, X.-Z. Zhao, M. E. Phelps, C. K. F. Shen, *Lab Chip* **2009**, *9*, 2281.
[349] V. Sivagnanam, M. A. M. Gijs, *Chem. Rev.* **2013**, *113*, 3214.
[350] C. Smith, *Nature* **2007**, *446*, 219.
[351] A. Chandresekaran, M. Abduljawad, C. Moraes, *Expert Opin. Drug Discovery* **2016**, *11*, 745.
[352] A. Khademhosseini, R. Langer, J. Borenstein, J. P. Vacanti, *Proc. Natl. Acad. Sci. USA* **2006**, *103*, 2480.
[353] a) Y. C. L. Chin Hock Kua, I. Rodriguez, C. Yang, K. Youcef-Toumi, *Anal. Chem.* **2008**, *80*, 5454; b) D. R. Albrecht, R. L. Sah, S. N. Bhatia, *Biophys. J.* **2004**, *87*, 2131.
[354] a) S. Ahadian, S. Yamada, J. Ramon-Azcon, M. Estili, X. Liang, K. Nakajima, H. Shiku, A. Khademhosseini, T. Matsue, *Acta Biomater.* **2016**, *31*, 134; b) P. Bajaj, D. Marchwiany, C. Duarte, R. Bashir, *Adv. Healthcare Mater.* **2013**, *2*, 450.
[355] C. T. Ho, R. Z. Lin, W. Y. Chang, H. Y. Chang, C. H. Liu, *Lab Chip* **2006**, *6*, 724.
[356] T. Sasagawa, T. Shimizu, S. Sekiya, Y. Haraguchi, M. Yamato, Y. Sawa, T. Okano, *Biomaterials* **2010**, *31*, 1646.
[357] T. Shimizu, H. Sekine, J. Yang, Y. Isoi, M. Yamato, A. Kikuchi, E. Kobayashi, T. Okano, *FASEB J.* **2006**, *20*, 708.
[358] Y. Tsuda, T. Shimizu, M. Yamato, A. Kikuchi, T. Sasagawa, S. Sekiya, J. Kobayashi, G. Chen, T. Okano, *Biomaterials* **2007**, *28*, 4939.
[359] a) K. Nagase, J. Kobayashi, T. Okano, *J. R. Soc., Interface* **2009**, *6*, S293; b) K. Matsuura, R. Utoh, K. Nagase, T. Okano, *J. Controlled Release* **2014**, *190*, 228.
[360] G. Kaushik, J. Leijten, A. Khademhosseini, *Stem Cells* **2017**, *35*, 51.
[361] N. L'Heureux, N. Dusserre, G. Konig, B. Victor, P. Keire, T. N. Wight, N. A. Chronos, A. E. Kyles, C. R. Gregory, G. Hoyt, R. C. Robbins, T. N. McAllister, *Nat. Med.* **2006**, *12*, 361.
[362] Y. Nahmias, R. E. Schwartz, C. M. Verfaillie, D. J. Odde, *Biotechnol. Bioeng.* **2005**, *92*, 129.
[363] X. Cui, T. Boland, D. D. D'Lima, M. K. Lotz, *Recent Pat. Drug Delivery Formulation* **2012**, *6*, 149.
[364] I. T. Ozbolat, M. Hospodiuk, *Biomaterials* **2016**, *76*, 321.
[365] T. J. Sill, H. A. von Recum, *Biomaterials* **2008**, *29*, 1989.
[366] Y. S. Zhang, J. Aleman, S. R. Shin, T. Kilic, D. Kim, S. A. M. Shaegh, S. Massa, R. Riahi, S. Chae, N. Hu, *Proc. Natl. Acad. Sci. USA* **2017**, E2293.
[367] D. M. Vykoukal, G. P. Stone, R. C. Gascoyne, E. U. Alt, J. Vykoukal, *Angew. Chem., Int. Ed.* **2009**, *48*, 7649.
[368] R. Baudoin, L. Griscom, J. M. Prot, C. Legallais, E. Leclerc, *Biochem. Eng. J.* **2011**, *53*, 172.
[369] A. Seidi, H. Kaji, N. Annabi, S. Ostrovidov, M. Ramalingam, A. Khademhosseini, *Biomicrofluidics* **2011**, *5*, 22214.
[370] S. A. M. Shaegh, F. D. Ferrari, Y. S. Zhang, M. Nabavinia, N. B. Mohammad, J. Ryan, A. Pourmand, E. Laukaitis, R. B. Sadeghian, A. Nadhman, S. R. Shin, A. S. Nezhad, A. Khademhosseini, M. R. Dokmeci, *Biomicrofluidics* **2016**, *10*, 044111.
[371] M. H. Wu, J. L. Lin, J. Wang, Z. Cui, Z. Cui, *Biomed. Microdevices* **2009**, *11*, 265.
[372] S. M. Grist, L. Chrostowski, K. C. Cheung, *Sensors* **2010**, *10*, 9286.
[373] a) C. Escobedo, Y. W. Chou, M. Rahman, X. Duan, R. Gordon, D. Sinton, A. Brolo, J. Ferreira, *Analyst* **2013**, *138*, 1450; b) Y. Uludag, I. E. Tothill, *Anal. Chem.* **2012**, *84*, 5898.
[374] S. H. Kim, W. Chegal, J. Doh, H. M. Cho, D. W. Moon, *Biophys. J.* **2011**, *100*, 1819.
[375] E. B. Magnusson, S. Halldorsson, R. M. T. Fleming, K. Leosson, *Biomed. Opt. Express* **2013**, *4*, 1749.
[376] F. X. Schmid, *Biological Macromolecules: UV-visible Spectrophotometry, eLS, Wiley*, **2001**.
[377] H. L. Lee, P. Boccazzi, R. J. Ram, A. J. Sinskey, *Lab Chip* **2006**, *6*, 1229.
[378] a) L. Wang, W. Liu, J. C. Wang, Q. Tu, R. Liu, J. Wang, *Lab Chip* **2013**, *13*, 695; b) D. Sud, G. Mehta, K. Mehta, J. Linderman, S. Takayama, M. A. Mycek, *J. Biomed. Opt.* **2006**, *11*, 050504; c) L. Wang, M. A. Acosta, J. B. Leach, R. L. Carrier, *Lab Chip* **2013**, *13*, 1586.
[379] Z. Lin, T. C. Wen, P. Roy, D. Trau, *Lab Chip* **2009**, *9*, 257.
[380] M. I. Mohammaed, M. P. Y. Desmulliez, *Lab Chip* **2010**, *11*, 569.
[381] C. McDonagh, C. S. Burke, B. D. MacCraith, *Chem. Rev.* **2008**, *108*, 400.
[382] S. A. Pfeiffer, S. Nagl, *Methods Appl. Fluoresc.* **2015**, *3*, 034003.
[383] X. D. Wang, O. S. Wolfbeis, *Chem. Soc. Rev.* **2014**, *43*, 3666.
[384] S. Sun, B. Ungerbock, T. Mayr, *Methods Appl. Fluoresc.* **2015**, *3*, 034002.
[385] J. Han, K. Burgess, *Chem. Rev.* **2010**, *110*, 2709.
[386] X. D. Wang, O. S. Wolfbeis, R. J. Meier, *Chem. Soc. Rev.* **2013**, *42*, 7834.
[387] a) X. D. Wang, O. S. Wolfbeis, *Anal. Chem.* **2013**, *85*, 487; b) A. L. Washburn, R. C. Bailey, *Analyst* **2011**, *136*, 227.
[388] B. Kuswandi, J. Huskens, W. Verboom, *Anal. Chim. Acta* **2007**, *601*, 141.
[389] H. Szmacinski, J. R. Lakowicz, *Sens. Actuators, B* **1995**, *29*, 16.

[390] A. D. Elder, S. M. Matthews, J. Swartling, J. Yunus, J. H. Frank, C. M. Brennan, A. C. Fisher, C. F. Kaminski, *Opt. Express* **2006**, *14*, 5456.
[391] a) K. Aoki, Y. Kamioka, M. Matsuda, *Dev., Growth Differ.* **2013**, *55*, 515; b) A. E. Albers, V. S. Okreglak, C. J. Chang, *J. Am. Chem. Soc.* **2006**, *128*, 9640.
[392] M. R. Tadross, S. A. Park, B. Veeramani, D. T. Yue, *J. Microsc.* **2009**, *233*, 192.
[393] a) S. M. Borisov, I. Klimant, *Microchim. Acta* **2009**, *164*, 7; b) Y. E. K. Lee, R. Kopelman, *Wiley Interdiscip. Rev.: Nanomed. Nanobiotechnol.* **2009**, *1*, 98.
[394] S. M. Borisov, C. Krause, S. Arain, O. S. Wolfbeis, *Adv. Mater.* **2006**, *18*, 1511.
[395] J. Ehgartner, H. Wiltsche, S. M. Borisov, T. Mayr, *Analyst* **2014**, *139*, 4924.
[396] a) M. I. J. Stich, S. Nagl, O. S. Wolfbeis, U. Henne, M. Schaferling, *Adv. Funct. Mater.* **2008**, *18*, 1399; b) S. Nagl, S. I. J. Matthias, M. Schaferling, O. S. Wolfbeis, *Anal. Bioanal. Chem.* **2009**, *393*, 1199; c) M. E. Kose, B. F. Carroll, K. S. Schanze, *Langmuir* **2005**, *21*, 9121.
[397] a) Z. Zhang, S. Zhang, X. Zhang, *Anal. Chim. Acta* **2005**, *541*, 37; b) I. H. Cho, E. H. Paek, Y. K. Kim, S. H. Peak, *Anal. Chim. Acta* **2009**, *632*, 247.
[398] J. Homola, *Chem. Rev.* **2008**, *108*, 462.
[399] S. Scarano, M. Mascini, A. P. F. Turner, M. Minunni, *Biosens. Bioelectron.* **2010**, *5*, 957.
[400] O. Krupin, H. Asiri, C. Wang, R. N. Tait, P. Berini, *Opt. Express* **2013**, *21*, 698.
[401] E. V. Dydek, M. Petersen, D. Nocera, K. F. Jensen, *J. Electrochem. Soc.* **2012**, *159*, 853.
[402] S. K. Arya, T. S. Pui, C. C. Wong, S. Kumar, A. R. Rahman, *Langmuir* **2013**, *29*, 6770.
[403] J. Patel, L. Radhakrishnan, B. Zhao, B. Uppalapati, R. C. Daniels, K. R. Ward, M. R. Collinson, *Anal. Chem.* **2013**, *85*, 11610.
[404] B. V. Chikkaveeraiah, A. A. Bhirde, N. Y. Morgan, H. S. Eden, X. Chen, *ACS Nano* **2012**, *6*, 6546.
[405] D. Grieshaber, R. MacKenzie, J. Voros, E. Reimhult, *Sensors* **2008**, *8*, 1400.
[406] S. Song, L. Wang, J. Li, C. Fan, J. Zhao, *Trends Anal. Chem.* **2008**, *27*, 108.
[407] E. Bakker, Y. Qin, *Anal. Chem.* **2006**, *78*, 3965.
[408] P. B. Luppa, L. J. Sokoll, D. W. Chan, *Clin. Chim. Acta* **2001**, *314*, 1.
[409] D. W. Kimmel, G. LeBlanc, M. E. Meschievitz, D. E. Cliffel, *Anal. Chem.* **2012**, *84*, 685.
[410] a) C. S. Lee, S. K. Kim, M. Kim, *Sensors* **2009**, *9*, 7111; b) M. J. Schoning, A. Poghossian, *Analyst* **2002**, *2002*, 1137; c) W. H. Baumann, M. Lehmann, A. Schwinde, R. Ehret, M. Brischwein, B. Wolf, *Sens. Actuators, B* **1999**, *55*, 77.
[411] E. E. Krommenhoek, M. van Leeuwen, H. Gardeniers, W. M. van Gulik, A. van den Berg, X. Li, M. Ottens, L. A. van der Wielen, J. J. Heijnen, *Biotechnol. Bioeng.* **2008**, *99*, 884.
[412] G. A. Messina, N. V. Panini, N. A. Martinez, J. Raba, *Anal. Biochem.* **2008**, *380*, 262.
[413] Y. Liu, T. Kwa, A. Revzin, *Biomaterials* **2012**, *33*, 7345.
[414] Z. Matharu, D. Patel, Y. Gao, A. Haque, Q. Zhou, A. Revzin, *Anal. Chem.* **2014**, *86*, 8865.
[415] C. Zhu, G. Yang, H. Li, D. Du, L. Yuehe, *Anal. Chem.* **2015**, *87*, 230.
[416] a) J. W. Choi, K. W. Oh, J. H. Thomas, W. R. Heineman, H. B. Halsall, J. H. Nevin, A. J. Helmicki, H. T. Henderson, C. H. Ahn, *Lab Chip* **2001**, *2*, 27; b) S. Centi, S. Tombelli, M. Minunni, M. Mascini, *Anal. Chem.* **2007**, *79*, 1466.
[417] R. Riahi, S. A. M. Shaegh, M. Ghaderi, Y. S. Zhang, S. R. Shin, J. Aleman, S. Massa, D. Kim, M. R. Dokmeci, A. Khademhosseini, *Sci. Rep.* **2016**, *6*, 24598.
[418] a) F. Patolsky, G. Zheng, C. M. Lieber, *Nanomedicine* **2006**, *1*, 51; b) F. Patolsky, B. P. Timko, G. Zheng, C. M. Lieber, *MRS Bull.* **2007**, *32*, 99; c) I. Lee, X. Luo, J. Huang, X. T. Cui, M. Yun, *Biosensors* **2012**, *2*, 205.
[419] a) B. Srinivasan, A. R. Kolli, M. B. Esch, H. E. Aaci, M. L. Sculer, J. J. Hickman, *J. Lab. Autom.* **2015**, *20*, 107; b) M. Odijk, A. D. van der Meer, D. Levner, H. J. Kim, M. W. van der Helm, L. I. Segerink, J. P. Frimat, G. A. Hamilton, D. E. Ingber, L. A. van der Wielen, *Lab Chip* **2014**, *15*, 745.
[420] a) T. A. Nguyen, T. I. Yin, D. Reyes, G. A. Urban, *Anal. Chem.* **2013**, *85*, 11068; b) N. Kramer, A. Walzl, C. Unger, M. Rosner, G. Krupitza, Hengstchlager, H. Dolznig, *Mutat. Res.* **2013**, *752*, 10.
[421] H. Yu, M. Li, W. Wang, X. Wang, *Acta Pharmacol. Sin.* **2016**, *37*, 107.
[422] R. Feiner, L. Engel, S. Fleischer, M. Malki, I. Gal, A. Shapira, Y. Shacham-Diamand, T. Dvir, *Nat. Mater.* **2016**, *15*, 679.
[423] N. D. T. Romil Saxena, J. M. Crawford, *Hepatology* **2015**, *30*, 8.
[424] A. Geerts, *Semin. Liver Dis.* **2001**, *21*, 311.
[425] J. M. Prot, C. Aninat, L. Griscom, F. Razan, C. Brochot, C. G. Guillouzo, C. Legallais, A. Corlu, E. Leclerc, *Biotechnol. Bioeng.* **2011**, *108*, 1704.
[426] Y. Morimoto, R. Tanaka, S. Takeuchi, *Adv. Healthcare Mater.* **2013**, *2*, 261.
[427] E. Bell, H. P. Ehrlich, D. J. Buttle, T. Nakatsuji, *Science* **1981**, *211*, 1052.
[428] T. Biedermann, A. S. Klar, S. Böttcher-Haberzeth, C. Schiestl, E. Reichmann, M. Meuli, *Pediatr. Surg. Int.* **2014**, *30*, 165.
[429] M. H. Mohammadi, B. Heidary Araghi, V. Beydaghi, A. Geraili, F. Moradi, P. Jafari, M. Janmaleki, K. P. Valente, M. Akbari, A. Sanati-Nezhad, *Adv. Healthcare Mater.* **2016**, *5*, 2459.
[430] S. Pappinen, E. Pryazhnikov, L. Khiroug, M. B. Ericson, M. Yliperttula, A. Urtti, *J. Controlled Release* **2012**, *161*, 656.
[431] a) J. H. Fentem, P. A. Botham, *ATLA, Altern. Lab. Anim.* **2002**, *30*, 61; b) N. Alépée, C. Tornier, C. Robert, C. Amsellem, M.-H. Roux, O. Doucet, J. Pachot, M. Méloni, A. D. B. de Fraissinette, *Toxicol. In Vitro* **2010**, *24*, 257.
[432] G. Bilousova, J. Chen, D. R. Roop, *J. Invest. Dermatol.* **2011**, *131*, 857.
[433] J. Ribas, H. Sadeghi, A. Manbachi, J. Leijten, K. Brinegar, Y. S. Zhang, L. Ferreira, A. Khademhosseini, *Appl. In Vitro Toxicol.* **2016**, *2*, 82.
[434] W. E. Lowry, L. Richter, R. Yachechko, A. D. Pyle, J. Tchieu, R. Sridharan, A. T. Clark, K. Plath, *Proc. Natl. Acad. Sci. USA* **2008**, *105*, 2883.
[435] N. Korin, M. Kanapathipillai, B. D. Matthews, M. Crescente, A. Brill, T. Mammoto, K. Ghosh, S. Jurek, S. A. Bencherif, D. Bhatta, A. U. Coskun, C. L. Feldman, D. D. Wagner, D. E. Ingber, *Science* **2012**, *337*, 738.
[436] a) M. Li, N. A. Hotaling, D. N. Ku, C. R. Forest, *PLoS One* **2014**, *9*, e82493; b) R. W. Muthard, S. L. Diamond, *Lab Chip* **2013**, *13*, 1883; c) M. Tsai, A. Kita, J. Leach, R. Rounsevell, J. N. Huang, J. Moake, R. E. Ware, D. A. Fletcher, W. A. Lam, *J. Clin. Invest.* **2012**, *122*, 408.
[437] P. Clark, P. Connolly, A. S. Curtis, J. A. Dow, C. D. Wilkinson, *J. Cell Sci.* **1991**, *99*, 73.
[438] S. Singare, Y. Liu, D. Li, B. Lu, J. Wang, S. He, *J. Prosthodontics* **2008**, *17*, 135.
[439] *G. Minotti, Cardiotoxicity of Non-Cardiovascular Drugs*, John Wiley & Sons, New York, **2010**.
[440] H. T. H. Au, B. Cui, Z. E. Chu, T. Veres, M. Radisic, *Lab Chip* **2009**, *9*, 564.
[441] a) P. Baei, S. Jalili-Firoozinezhad, S. Rajabi-Zeleti, M. Tafazzoli-Shadpour, H. Baharvand, N. Aghdami, *Mater. Sci. Eng., C* **2016**, *63*, 131; b) R. Ravichandran, R. Sridhar, J. R. Venugopal, S. Sundarrajan, S. Mukherjee, S. Ramakrishna, *Macromol. Biosci.* **2014**, *14*, 515.

[442] E. T. den Braber, J. E. de Ruijter, H. T. Smits, L. A. Ginsel, A. F. von Recum, J. A. Jansen, *J. Biomed. Mater. Res.* **1995**, *29*, 511.
[443] D. S. Julian Seifter, A. Ratner, *Concepts in Medical Physiology*, Lippincott Williams & Wilkins, Baltimore, **2005**.
[444] a) M. C. Wallis, H. Yeger, L. Cartwright, Z. Shou, M. Radisic, J. Haig, M. Suoub, R. Antoon, W. A. Farhat, *Tissue Eng., Part A* **2008**, *14*, 339; b) P. Clark, G. A. Dunn, A. Knibbs, M. Peckham, *Int. J. Biochem. Cell Biol.* **2002**, *34*, 816.
[445] a) B. D. Plouffe, D. N. Njoka, J. Harris, J. Liao, N. K. Horick, M. Radisic, S. K. Murthy, *Langmuir* **2007**, *23*, 5050; b) H. Kondoh, Y. Sawa, S. Miyagawa, S. Sakakida-Kitagawa, I. A. Memon, N. Kawaguchi, N. Matsuura, T. Shimizu, T. Okano, H. Matsuda, *Cardiovasc. Res.* **2006**, *69*, 466.
[446] a) S. Arnesen, S. Mosler, N. Larsen, N. Gadegaard, P. Purslow, M. Lawson, *Connect. Tissue Res.* **2004**, *45*, 238; b) B. Lanfer, F. P. Seib, U. Freudenberg, D. Stamov, T. Bley, M. Bornhäuser, C. Werner, *Biomaterials* **2009**, *30*, 5950.
[447] I. Kim, S. O. Moon, S. K. Park, S. W. Chae, G. Y. Koh, *Circ. Res.* **2001**, *89*, 477.
[448] a) J. L. Charest, A. J. Garcia, W. P. King, *Biomaterials* **2007**, *28*, 2202; b) H. T. Au, I. Cheng, M. F. Chowdhury, M. Radisic, *Biomaterials* **2007**, *28*, 4277.
[449] M. Das, K. Wilson, P. Molnar, J. J. Hickman, *Nat. Protoc.* **2007**, *2*, 1795.
[450] M. T. Lam, S. Sim, X. Zhu, S. Takayama, *Biomaterials* **2006**, *27*, 4340.
[451] S. L. Hume, S. M. Hoyt, J. S. Walker, B. V. Sridhar, J. F. Ashley, C. N. Bowman, S. J. Bryant, *Acta Biomater.* **2012**, *8*, 2193.
[452] K. Nagamine, T. Kawashima, T. Ishibashi, H. Kaji, M. Kanzaki, M. Nishizawa, *Biotechnol. Bioeng.* **2010**, *105*, 1161.
[453] Y.-C. Huang, R. G. Dennis, L. Larkin, K. Baar, *J. Appl. Physiol.* **2005**, *98*, 706.
[454] a) C. P. Pennisi, C. G. Olesen, M. de Zee, J. Rasmussen, V. Zachar, *Tissue Eng., Part A* **2011**, *17*, 2543; b) D. W. van der Schaft, A. C. van Spreeuwel, H. C. van Assen, F. P. Baaijens, *Tissue Eng., Part A* **2011**, *17*, 2857.
[455] S. Ahadian, J. Ramon-Azcon, S. Ostrovidov, G. Camci-Unal, V. Hosseini, H. Kaji, K. Ino, H. Shiku, A. Khademhosseini, T. Matsue, *Lab Chip* **2012**, *12*, 3491.
[456] D. Coletti, L. Teodori, M. C. Albertini, M. Rocchi, A. Pristera, M. Fini, M. Molinaro, S. Adamo, *Cytometry, Part A* **2007**, *71*, 846.
[457] B. Chaudhuri, D. Bhadra, L. Moroni, K. Pramanik, *Biofabrication* **2015**, *7*, 015009.
[458] H. Vandenburgh, J. Shansky, F. Benesch-Lee, K. Skelly, J. M. Spinazzola, Y. Saponjian, B. S. Tseng, *FASEB J.* **2009**, *23*, 3325.
[459] H.-G. Kopp, S. T. Avecilla, A. T. Hooper, S. Rafii, *Physiology* **2005**, *20*, 349.
[460] S. H. Orkin, L. I. Zon, *Cell* **2008**, *132*, 631.
[461] N. Di Maggio, E. Piccinini, M. Jaworski, A. Trumpp, D. J. Wendt, I. Martin, *Biomaterials* **2011**, *32*, 321.
[462] J. E. Nichols, J. Cortiella, J. Lee, J. A. Niles, M. Cuddihy, S. Wang, J. Bielitzki, A. Cantu, R. Mlcak, E. Valdivia, *Biomaterials* **2009**, *30*, 1071.
[463] Y. Yi, J. Park, J. Lim, C. J. Lee, S.-H. Lee, *Trends Biotechnol.* **2015**, *33*, 762.
[464] A. D. van der Meer, A. van den Berg, *Integr. Biol.* **2012**, *4*, 461.
[465] J. D. Caplin, N. G. Granados, M. R. James, R. Montazami, N. Hashemi, *Adv. Healthcare Mater.* **2015**, *4*, 1426.
[466] Y. Xiong, A. Mahmood, M. Chopp, *Nat. Rev. Neurosci.* **2013**, *14*, 128.
[467] R. Siddique, N. Thakor, *J. R. Soc., Interface* **2014**, *11*, 20130676.
[468] B. K. Ng, L. Chen, W. Mandemakers, J. M. Cosgaya, J. R. Chan, *J. Neurosci.* **2007**, *27*, 7597.
[469] J. L. Goldberg, M. P. Klassen, Y. Hua, B. A. Barres, *Science* **2002**, *296*, 1860.
[470] L. I. Benowitz, D. E. Goldberg, N. Irwin, *Prog. Brain Res.* **2002**, *137*, 389.
[471] a) D. Majumdar, Y. Gao, D. Li, D. J. Webb, *J. Neurosci. Methods* **2011**, *196*, 38; b) J. Park, H. Koito, J. Li, A. Han, *Biomed. Microdevices* **2009**, *11*, 1145; c) J. Park, H. Koito, J. Li, A. Han, *Lab Chip* **2012**, *12*, 3296.
[472] Y. Huang, J. C. Williams, S. M. Johnson, *Lab Chip* **2012**, *12*, 2103.
[473] A. Kunze, R. Meissner, S. Brando, P. Renaud, *Biotechnol. Bioeng.* **2011**, *108*, 2241.
[474] A. J. Lees, *Neurology* **2009**, *72*, S2.
[475] W. M. Pardridge, *NeuroRx* **2005**, *2*, 3.
[476] M. H. Mohammadi, R. Obregon, S. Ahadian, J. Ramon-Azcon, M. Radisic, *Curr. Pharm. Des.* **2017**, *23*, 2991.
[477] L. O. Soto-Rojas, F. de la Cruz-López, M. A. O. Torres, A. Viramontes-Pintos, M. D. C. Cárdenas-Aguayo, M. A. Meraz-Ríos, C. Salinas-Lara, B. Florán-Garduño, J. Luna-Muñoz, in *Alzheimer's Disease - Challenges for the Future*, (Ed. I. Zerr), InTech, Croatia, **2015**.
[478] E. Van Vliet, E. Aronica, J. Gorter, *Semin. Cell Dev. Biol.* **2015**, 38, 26.
[479] K. E. Ohlin, V. Francardo, H. S. Lindgren, S. E. Sillivan, S. S. O'Sullivan, A. S. Luksik, F. M. Vassoler, A. J. Lees, C. Konradi, M. A. Cenci, *Brain* **2011**, *134*, 2339.
[480] J. Henkel, D. Beers, S. Wen, R. Bowser, S. Appel, *Neurology* **2009**, *72*, 1614.
[481] E. W. Young, D. J. Beebe, *Chem. Soc. Rev.* **2010**, *39*, 1036.
[482] A. Wolff, M. Antfolk, B. Brodin, M. Tenje, *J. Pharm. Sci.* **2015**, *104*, 2727.
[483] R. Shawahna, X. Declèves, J.-M. Scherrmann, *Curr. Drug Metab.* **2013**, *14*, 120.
[484] a) J. H. Yeon, D. Na, K. Choi, S.-W. Ryu, C. Choi, J.-K. Park, *Biomed. Microdevices* **2012**, *14*, 1141; b) B. Prabhakarpandian, M.-C. Shen, J. B. Nichols, I. R. Mills, M. Sidoryk-Wegrzynowicz, M. Aschner, K. Pant, *Lab Chip* **2013**, *13*, 1093.
[485] N. J. Abbott, *J. Inherited Metab. Dis.* **2013**, *36*, 437.
[486] R. Thuenauer, E. Rodriguez-Boulan, W. Römer, *Analyst* **2014**, *139*, 3206.
[487] K. Benson, S. Cramer, H.-J. Galla, *Fluids Barriers CNS* **2013**, *10*, 5.
[488] M. W. van der Helm, A. D. van der Meer, J. C. Eijkel, A. van den Berg, L. I. Segerink, *Tissue Barriers* **2016**, *4*, e1142493.
[489] D. Karamichos, *J. Funct. Biomater.* **2015**, *6*, 77.
[490] Y. Komai, T. Ushiki, *Invest. Ophthalmol. Visual Sci.* **1991**, *32*, 2244.
[491] a) X. Hu, W. Lui, L. Cui, M. Wang, Y. Cao, *Tissue Eng.* **2005**, *11*, 1710; b) K. Merrett, P. Fagerholm, C. R. McLaughlin, S. Dravida, N. Lagali, N. Shinozaki, M. A. Watsky, R. Munger, Y. Kato, F. Li, C. J. Marmo, M. Griffith, *Invest. Ophthalmol. Visual Sci.* **2008**, *49*, 3887; c) W. Liu, K. Merrett, M. Griffith, P. Fagerholm, S. Dravida, B. Heyne, J. C. Scaiano, M. A. Watsky, N. Shinozaki, N. Lagali, R. Munger, F. Li, *Biomaterials* **2008**, *29*, 1147; d) A. Acun, V. Hasirci, *J. Biomater. Sci., Polym. Ed.* **2014**, *25*, 1110.
[492] H. J. Levis, A. K. Kureshi, I. Massie, L. Morgan, A. J. Vernon, J. T. Daniels, *J. Funct. Biomater.* **2015**, *6*, 50.
[493] B. Han, I. R. Schwab, T. K. Madsen, R. R. Isseroff, *Cornea* **2002**, *21*, 505.
[494] B. D. Lawrence, J. K. Marchant, M. A. Pindrus, F. G. Omenetto, D. L. Kaplan, *Biomaterials* **2009**, *30*, 1299.
[495] C. C. Lin, R. Ritch, S. M. Lin, M. H. Ni, Y. C. Chang, Y. L. Lu, H. J. Lai, F. H. Lin, *Eur. Cells Mater.* **2010**, *19*, 50.
[496] B. A. Schechter, W. J. Rand, R. S. Nagler, I. Estrin, S. S. Arnold, N. Villate, G. E. Velazquez, *Cornea* **2005**, *24*, 106.
[497] W. K. Song, K. M. Park, H. J. Kim, J. H. Lee, J. Choi, S. Y. Chong, S. H. Shim, L. V. Del Priore, R. Lanza, *Stem Cell Rep.* **2015**, *4*, 860.

[498] J. Maruotti, S. R. Sripathi, K. Bharti, J. Fuller, K. J. Wahlin, V. Ranganathan, V. M. Sluch, C. A. Berlinicke, J. Davis, C. Kim, L. Zhao, J. Wan, J. Qian, B. Corneo, S. Temple, R. Dubey, B. Z. Olenyuk, I. Bhutto, G. A. Lutty, D. J. Zack, *Proc. Natl. Acad. Sci. USA* **2015**, *112*, 10950.
[499] B. Thirion, E. Duchesnay, E. Hubbard, J. Dubois, J. B. Poline, D. Lebihan, S. Dehaene, *NeuroImage* **2006**, *33*, 1104.
[500] F. Gekeler, E. Zrenner, K. U. Bartz-Schmidt, *Ophthalmologe* **2015**, *112*, 712.
[501] H. J. Kim, D. Huh, G. Hamilton, D. E. Ingber, *Lab Chip* **2012**, *12*, 2165.
[502] P. Fasinu, V. Pillay, V. M. Ndesendo, L. C. du Toit, Y. E. Choonara, *Biopharm. Drug Dispos.* **2011**, *32*, 185.
[503] H. J. Kim, D. E. Ingber, *Integr. Biol.* **2013**, *5*, 1130.
[504] M. D. Basson, *Digestion* **2003**, *68*, 217.
[505] T. Sato, R. G. Vries, H. J. Snippert, M. van de Wetering, N. Barker, D. E. Stange, J. H. van Es, A. Abo, P. Kujala, P. J. Peters, H. Clevers, *Nature* **2009**, *459*, 262.
[506] T. Sato, H. Clevers, *Science* **2013**, *340*, 1190.
[507] J. H. Lee, R. M. Pidaparti, G. M. Atkinson, R. S. Moorthy, *J. Drug Delivery* **2012**, *2012*, 527516.
[508] T. C. Grikscheit, F. G. Sala, J. Ogilvie, K. A. Bower, E. R. Ochoa, E. Alsberg, D. Mooney, J. P. Vacanti, *J. Surg. Res.* **2008**, *149*, 214.
[509] R. J. Holdsworth, *Br. J. Surg.* **1991**, *78*, 270.
[510] T. F. Didar, M. J. Cartwright, M. Rottman, A. R. Graveline, N. Gamini, A. L. Watters, D. C. Leslie, T. Mammoto, M. J. Rodas, J. H. Kang, A. Waterhouse, B. T. Seiler, P. Lombardo, E. I. Qendro, M. Super, D. E. Ingber, *Biomaterials* **2015**, *67*, 382.
[511] N. Poornejad, L. B. Schaumann, E. M. Buckmiller, B. L. Roeder, A. D. Cook, *Tissue Eng., Part B* **2016**, *22*, 358.
[512] a) M. J. Wilmer, C. P. Ng, H. L. Lanz, P. Vulto, L. Suter-Dick, R. Masereeuw, *Trends Biotechnol.* **2016**, *34*, 156; b) S. Kim, S. Takayama, *Kidney Res. Clin. Pract.* **2015**, *34*, 165.
[513] E. J. Weber, A. Chapron, B. D. Chapron, J. L. Voellinger, K. A. Lidberg, C. K. Yeung, Z. Wang, Y. Yamaura, D. W. Hailey, T. Neumann, *Kidney Int.* **2016**, *90*, 627.
[514] M. Zhou, X. Zhang, X. Wen, T. Wu, W. Wang, M. Yang, J. Wang, M. Fang, B. Lin, H. Lin, *Sci. Rep.* **2016**, *6*, 31771.
[515] M. Takasato, X. E. Pei, H. S. Chiu, B. Maier, G. J. Baillie, C. Ferguson, R. G. Parton, E. J. Wolvetang, M. S. Roost, S. M. C. de Sousa Lopes, *Nature* **2015**, *526*, 564.
[516] W. Han, S. Chen, W. Yuan, Q. Fan, J. Tian, X. Wang, L. Chen, X. Zhang, W. Wei, R. Liu, *Proc. Natl. Acad. Sci. USA* **2016**, *113*, 11208.
[517] a) A. Kamb, *Nat. Rev. Drug Discovery* **2005**, *4*, 161; b) D. V. LaBarbera, B. G. Reid, B. H. Yoo, *Expert Opin. Drug Discovery* **2012**, *7*, 819; c) Y. Imamura, T. Mukohara, Y. Shimono, Y. Funakoshi, N. Chayahara, M. Toyoda, N. Kiyota, S. Takao, S. Kono, T. Nakatsura, H. Minami, *Oncol. Rep.* **2015**, *33*, 1837.
[518] a) N. Peela, D. Truong, H. Saini, H. Chu, S. Mashaghi, S. L. Ham, S. Singh, H. Tavana, B. Mosadegh, M. Nikkhah, *Biomaterials* **2017**, *133*, 176; b) D. Truong, J. Puleo, A. Llave, G. Mouneimne, R. D. Kamm, M. Nikkhah, *Sci. Rep.* **2016**, *6*, 34094; c) Q. Zhang, T. Liu, J. Qin, *Lab Chip* **2012**, *12*, 2837.
[519] J. Robijns, S. Censabella, P. Bulens, A. Maes, J. Mebis, *Lasers Med. Sci.* **2017**, *32*, 229.
[520] J. E. Rusby, E. F. Brachtel, J. S. Michaelson, F. C. Koerner, B. L. Smith, *Breast Cancer Res. Treat.* **2007**, *106*, 171.
[521] a) W. Saadi, S. J. Wang, F. Lin, N. L. Jeon, *Biomed. Microdevices* **2006**, *8*, 109; b) M. E. J. Doerr, J. I. Jones, *J. Biol. Chem.* **1996**, *271*, 2443.
[522] a) C. Kuperwasser, S. Dessain, B. E. Bierbaum, D. Garnet, K. Sperandio, G. P. Gauvin, S. P. Naber, R. A. Weinberg, M. Rosenblatt, *Cancer Res.* **2005**, *65*, 6130; b) T. W. Shibue, R. A. Weinberg, *Proc. Natl. Acad. Sci. USA* **2009**, *106*, 10290.
[523] A. Sobrino, D. T. Phan, R. Datta, X. Wang, S. J. Hachey, M. Romero-López, E. Gratton, A. P. Lee, S. C. George, C. C. Hughes, *Sci. Rep.* **2016**, *6*, 31589.
[524] J. Kong, Y. Luo, D. Jin, F. An, W. Zhang, L. Liu, J. Li, S. Fang, X. Li, X. Yang, *Oncotarget* **2016**, *7*, 78421.
[525] S. B. Bar-Yehuda, F. L. Volfsson, P. Fishman, *Neoplasia* **2001**, *3*, 125.
[526] P. Carmeliet, *Oncology* **2005**, *69*, 4.
[527] T. Bricks, P. Paullier, A. Legendre, M.-J. Fleury, P. Zeller, F. Merlier, P. M. Anton, E. Leclerc, *Toxicol. In Vitro* **2014**, *28*, 885.
[528] M. B. Esch, A. S. Smith, J.-M. Prot, C. Oleaga, J. J. Hickman, M. L. Shuler, *Adv. Drug Delivery Rev.* **2014**, *69*, 158.
[529] S. Wei, C. Yu-Qing, L. Guo-An, M. Zhang, H.-Y. Zhang, W. Yue-Rong, H. Ping, *Chin. J. Anal. Chem.* **2016**, *44*, 533.
[530] L. Choucha-Snouber, C. Aninat, L. Grsicom, G. Madalinski, C. Brochot, P. E. Poleni, F. Razan, C. G. Guillouzo, C. Legallais, A. Corlu, *Biotechnol. Bioeng.* **2013**, *110*, 597.
[531] a) P. G. Welling, *J. Pharmacokinet. Biopharm.* **1977**, *5*, 291; b) P. Macheras, P. Argyrakis, *Pharm. Res.* **1997**, *14*, 842; c) J. Bevernage, J. Brouwers, M. E. Brewster, P. Augustijns, *Int. J. Pharm.* **2013**, *453*, 25; d) L. M. Ensign, R. Cone, J. Hanes, *Adv. Drug Delivery Rev.* **2012**, *64*, 557.
[532] a) S. Küchler, K. Strüver, W. Friess, *Expert Opin. Drug Metab. Toxicol.* **2013**, *9*, 1255; b) S. Bagherifard, A. Tamayol, P. Mostafalu, M. Akbari, M. Comotto, N. Annabi, M. Ghaderi, S. Sonkusale, M. R. Dokmeci, A. Khademhosseini, *Adv. Healthcare Mater.* **2016**, *5*, 175.
[533] H. Lee, D. S. Kim, S. K. Ha, I. Choi, J. M. Lee, J. H. Sung, *Biotechnol. Bioeng.* **2017**, *114*, 432.
[534] E.-M. Materne, A. P. Ramme, A. P. Terrasso, M. Serra, P. M. Alves, C. Brito, D. A. Sakharov, A. G. Tonevitsky, R. Lauster, U. Marx, *J. Biotechnol.* **2015**, *205*, 36.
[535] M. Esch, T. King, M. Shuler, *Annu. Rev. Biomed. Eng.* **2011**, *13*, 55.
[536] E. Iori, B. Vinci, E. Murphy, M. C. Marescotti, A. Avogaro, A. Ahluwalia, *PLoS One* **2012**, *7*, e34704.
[537] J. H. Sung, M. L. Shuler, *Lab Chip* **2009**, *9*, 1385.
[538] D. A. Tatosian, M. L. Shuler, *Biotechnol. Bioeng.* **2009**, *103*, 187.
[539] A. Roth, T. Singer, *Adv. Drug Delivery Rev.* **2014**, *69*, 179.
[540] K. Schimek, M. Busek, S. Brincker, B. Groth, S. Hoffmann, R. Lauster, G. Lindner, A. Lorenz, U. Menzel, F. Sonntag, H. Walles, U. Marx, R. Horland, *Lab Chip* **2013**, *13*, 3588.
[541] W. Zhang, Y. S. Zhang, S. M. Bakht, J. Aleman, S. R. Shin, K. Yue, M. Sica, J. Ribas, M. Duchamp, J. Ju, R. B. Sadeghian, D. Kim, M. R. Dokmeci, A. Atala, A. Khademhosseini, *Lab Chip* **2016**, *16*, 1579.
[542] W. Ning, R. Song, C. Li, E. Park, A. Mohsenin, A. M. K. Choi, M. E. Choi, *Am. J. Physiol.: Lung Cell. Mol. Physiol.* **2002**, *283*, L1094.
[543] F. Dituri, A. Mazzocca, F. J. Peidrò, P. Papappicco, I. Fabregat, F. De Santis, A. Paradiso, C. Sabbà, G. Giannelli, *PLoS One* **2013**, *8*, e67109.
[544] J. Van der Valk, D. Brunner, K. De Smet, Å. F. Svenningsen, P. Honegger, L. E. Knudsen, T. Lindl, J. Noraberg, A. Price, M. L. Scarino, *Toxicol. In Vitro* **2010**, *24*, 1053.
[545] S. Gottipamula, M. S. Muttigi, U. Kolkundkar, R. N. Seetharam, *Cell Proliferation* **2013**, *46*, 608.
[546] A. E. Schaffner, J. L. Barker, D. A. Stenger, J. J. Hickman, *J. Neurosci. Methods* **1995**, *62*, 111.
[547] D. Edwards, M. Das, P. Molnar, J. J. Hickman, *J. Neurosci. Methods* **2010**, *190*, 155.
[548] J. Bilic, J. C. I. Belmonte, *Stem Cells* **2012**, *30*, 33.
[549] A. Williamson, S. Singh, U. Fernekorn, A. Schober, *Lab Chip* **2013**, *13*, 3471.

[550] I. Itzhaki, L. Maizels, I. Huber, L. Zwi-Dantsis, O. Caspi, A. Winterstern, O. Feldman, A. Gepstein, G. Arbel, H. Hammerman, *Nature* **2011**, *471*, 225.
[551] M. A. Israel, S. H. Yuan, C. Bardy, S. M. Reyna, Y. Mu, C. Herrera, M. P. Hefferan, S. Van Gorp, K. L. Nazor, F. S. Boscolo, *Nature* **2012**, *482*, 216.
[552] M. J. Devine, M. Ryten, P. Vodicka, A. J. Thomson, T. Burdon, H. Houlden, F. Cavaleri, M. Nagano, N. J. Drummond, J.-W. Taanman, *Nat. Commun.* **2011**, *2*, 440.
[553] Y. Avior, I. Sagi, N. Benvenisty, *Nat. Rev. Mol. Cell Biol.* **2016**, *17*, 170.
[554] H. Xu, W. L. Kraus, M. L. Shuler, *Biotechnol. Bioeng.* **2008**, *101*, 1276.
[555] J. Fu, C. Wiraja, R. Chong, C. Xu, D.-A. Wang, *Acta Biomater.* **2017**, *49*, 358.
[556] E. Phizicky, P. I. H. Bastiaens, H. Zhu, M. Snyder, S. Fields, *Nature* **2003**, *422*, 208.
[557] B. Harink, S. Le Gac, R. Truckenmüller, C. van Blitterswijk, P. Habibovic, *Lab Chip* **2013**, *13*, 3512.
[558] A. Natarajan, T. B. DeMarse, P. Molnar, J. J. Hickman, *J. Biotechnol. Biomater.* **2013**, *3*, 2.
[559] I. A. Ges, F. Baudenbacher, *Biosens. Bioelectron.* **2010**, *26*, 828.
[560] X. J. Chen, A. C. West, D. M. Cropek, S. Banta, *Anal. Chem.* **2008**, *80*, 9622.
[561] J. R. Enders, J. A. McLean, *Chirality* **2009**, *21*, E253.
[562] R. Kostadinova, F. Boess, D. Applegate, L. Suter, T. Weiser, T. Singer, B. Naughton, A. Roth, *Toxicol. Appl. Pharmacol.* **2013**, *268*, 1.
[563] S. R. Khetani, C. Kanchagar, O. Ukairo, S. Krzyzewski, A. Moore, J. Shi, S. Aoyama, M. Aleo, Y. Will, *Toxicol. Sci.* **2012**, *132*, 107.
[564] S. Messner, I. Agarkova, W. Moritz, J. M. Kelm, *Arch. Toxicol.* **2013**, *87*, 209.
[565] S. S. Nunes, J. W. Miklas, J. Liu, R. Aschar-Sobbi, Y. Xiao, B. Zhang, J. Jiang, S. Massé, M. Gagliardi, A. Hsieh, N. Thavandiran, M. A. Laflamme, K. Nanthakumar, G. J. Gross, P. H. Backx, G. Keller, M. Radisic, *Nat. Methods* **2013**, *10*, 781.
[566] K. Kingwell, *Nat. Rev. Drug Discovery* **2017**, *16*, 6.
[567] E. W. K. Young, *Integr. Biol.* **2013**, *5*, 1096.
[568] P. Neuži, S. Giselbrecht, K. Länge, T. J. Huang, A. Manz, *Nat. Rev. Drug Discovery* **2012**, *11*, 620.
[569] P. Marx-Stoelting, E. Adriaens, H.-J. Ahr, S. Bremer, B. Garthoff, H.-P. Gelbke, A. Piersma, C. Pellizzer, U. Reuter, V. Rogiers, *ATLA, Altern. Lab. Anim.* **2009**, *37*, 313.
[570] R. Binetti, F. M. Costamagna, I. Marcello, *Ann. Ist. Super. Sanita* **2008**, *44*, 13.
[571] D. Krewski, D. Acosta Jr., M. Andersen, H. Anderson, J. C. Bailar III, K. Boekelheide, R. Brent, G. Charnley, V. G. Cheung, S. Green Jr., *J. Toxicol. Environ. Health, Part B* **2010**, *13*, 51.
[572] a) R. S. Judson, K. A. Houck, R. J. Kavlock, T. B. Knudsen, M. T. Martin, H. M. Mortensen, D. M. Reif, D. M. Rotroff, I. Shah, A. M. Richard, *Environ. Health Perspect.* **2010**, *118*, 485; b) R. R. Tice, C. P. Austin, R. J. Kavlock, J. R. Bucher, *Environ. Health Perspect.* **2013**, *121*, 756.
[573] M. C. Warren, *Toxicol. Res.* **2016**, *32*, 9.
[574] E. L. Jackson, H. Lu, *Integr. Biol.* **2016**, *8*, 672.